TECHNISCHE UNIVERSITÄT MÜNCHEN
Lehrstuhl für Bauchemie

A Comprehensive Study on Multiple Phenomena Originating From Sulfate Ions Which Influence the Dispersing Mechanism of Polycarboxylate Based Superplasticizers in Cementitious Systems

Ahmad Habbaba

Vollständiger Abdruck der von der Fakultät für Chemie der Technischen Universität München zur Erlangung des akademischen Grades eines

Doktors der Naturwissenschaften (Dr. rer. nat.)

genehmigten Dissertation.

Vorsitzender: Univ.-Prof. Dr. Michael Schuster

Prüfer der Dissertation:
1. Univ.-Prof. Dr. Johann P. Plank
2. Univ.-Prof. Dr.-Ing. Detlef Heinz
3. apl. Prof. Dr. Anton Lerf

Die Dissertation wurde am 28.11.2012 bei der Technischen Universität München eingereicht und durch die Fakultät für Chemie am 11.02.2013 angenommen.

﴿ رَبِّ قَدۡ ءَاتَيۡتَنِي مِنَ ٱلۡمُلۡكِ وَعَلَّمۡتَنِي مِن تَأۡوِيلِ ٱلۡأَحَادِيثِۚ فَاطِرَ ٱلسَّمَٰوَٰتِ وَٱلۡأَرۡضِ أَنتَ وَلِيِّۦ فِي ٱلدُّنۡيَا وَٱلۡأٓخِرَةِۖ تَوَفَّنِي مُسۡلِمٗا وَأَلۡحِقۡنِي بِٱلصَّٰلِحِينَ ﴾ يوسف: ١٠١

"My Lord! Thou have given me something of sovereignty and taught me to interpret events. Creator of the heavens and the earth! Thou are my Guardian in this world and in the Everlasting Life. Make me to die submissive unto Thee, and join me to the righteous"

Yusuf 12:101

DEDICATION

This thesis is dedicated to my mother *Afaf Bawadkji*. Without her love, encouragement and support under all conditions, I would not have succeeded. Also, I would like to dedicate this work to my lovely wife *Alaa Ibrik* who always had an open and comforting ear for all problems I met. May I can dedicate this research to my wonderful and brilliant daughter *Afaf*, who brightens up our life.

Acknowledgement

Thanks and deep gratitude to my mentor and brilliant professor, who inculcated in me the love and passion for the science of construction chemicals, that by his supervision of my investigations with careful attention and positive enthusiasm*, Prof. Dr. Johann Plank*.

Gratitude is paid to *Dr. Roland Sieber* for his contribution to the first part of this project. Also, I would like to express my gratitude to *Dr. Oksana Storcheva* for her encouragement and support.

Special thanks go to *Al-Baath University* in Homs, Syria for a stipend to finance the major part of my study, and I warmly thank *TUM graduate school* for their encouragement.

I also would like to express my gratitude to our secretaries *Daniela Michler* and *Tim Dannemann* for their help to cope with bureaucracy in an uncomplicated way.

Special thanks go to my senior colleagues *Bernhard Sachsenhauser*, *Helena Keller*, *Vera Nilles*, *Christof Schröfl*, *Markus Gretz*, *Matthias Lesti*, *Nils Recalde Lummer*, *Fatima Dugonjić-Bilić*, *Hang Bian, Nadia Zouaoui* and *Tobias Kornprobst* for supporting me at the beginning of my study.

Furthermore, I would like to thank the junior colleagues for the nice collegial atmosphere; *Nan Zou*, *Daniel Bülichen*, *Salami Oyewole Taye*, *Constantin Tiemeyer*, *Alex Lange*, *Yu Jin*, *Markus Meier*, *Maike Müller*, *Julia Pickelmann*, *Michael Glanzer*, *Stefan Baueregger*, *Timon Echt*, *Somruedee Klaithong* and *Lei Lei*. I wish them all the best in the future.

My gratitude goes to all persons working at the Chair for Construction Chemicals, Technischen Universität München for helping me completing this Ph.D. thesis successfully. I sincerely appreciated all the advices and skills that I have picked up during residence in the group.

I would also like to warmly thank *Mirko Gruber* and *Friedrich von Hoessle* for their readiness to help and advise whenever I asked for.

In addition, I am grateful to *Elina Dubina* for her friendship and for the lovely scientific chats that we used to have. Moreover, I would like to express my heartfelt thanks to *Johanna de Reese* for her kindness and helping me during the practical course. I also wish to express my gratitude to *Thomas Pavlitschek* for helping me with all problems I met regarding the computer. Thanks go to *Richard Beiderbeck* and *Dagmar Lettrich* for the extra speed in analysis and helping me in my experiments.

Appreciation and gratitude is well paid to my friends *Abdussalam Qaroush*, *Marwan Radi*, *Ahmad Shahrori* and *Khalifa Salmiah* for their help and encouragement.

Special gratitude is paid to *Serina Ng* who has always been a good companion in all these years; thanks for her deep friendship, encouragement, great support, and respect for what I do represent and believe.

Last but not least, I would like to thank my mother, my sisters and extended family, for their love, faith, and unwavering support for me over all these years. I also want to express my very special and deep gratitude to my lovely wife *Alaa Ibrik*. Thanks for always being next to me.

Abstract

Optimization of superplasticizer (SP) performance and thus reducing the amount which has to be applied in order to reach a desired flow value of the slurries of cementitious systems, is a major target for the building materials industry. Therefore, it is important to gain sufficient information on the mechanisms involved in the superplasticizing process. Many parameters can significantly affect the dispersing performance of SP, such as cement composition (clinker phase content), blended with supplementary cementitious materials, type and chemical structure of the SP, the presence of sulfate ions in the pore solution, the addition time of SP to the cement slurry … *etc*. In this thesis, all of these parameters were studied individually by employing mainly polycarboxylate-based dispersants (PCEs) which present the most widely applied SPs in the construction industry. They can produce highly flowable and/or high strength concrete possessing a low water to cement ratio.

In general, the main topics discussed in this thesis include:

- Study of the surface chemistry of ground granulated blast furnace slag dispersed in water and synthetic cement pore solution employing zeta potential and ionic strength analysis.
- Determination of the adsorption mechanism of polycarboxylates on different cementitious materials (cement, slag and limestone) by investigation of their adsorption isotherms and zeta potential.
- Study of the impact of sulfate ions present in cement pore solution on the dispersing performance of different PCEs.
- Proof of the high compatibility of a novel PCE with difficult cements, and confirm its high tolerance for sulfate.
- Explanation for the high dispersing performance of most SPs at delayed addition to concrete.

In blended cements, most researchers focused on the interaction between SPs and the entire cement system including slag, but did not differentiate between the individual components. For this reason, we focused on the behavior of slag as a single component in water or cement pore solution, and determined the specific interactions occurring between PCEs and slag. It was found that competitive adsorption between PCEs and sulfate ions on the surface of slag occurs. The adsorbed amount of PCE mainly depends on the difference in anionic charge

amount between the copolymer and sulfate. Thus, the chemical structure of the polymer has a significant influence on its dispersing performance. Moreover, this study also revealed that slag is not inert toward SP, and higher or lower PCE dosages compared to pure Portland cement-based systems have to be considered when formulating concretes containing slag.

During cement hydration, sulfate ions are released into the pore solution in different amounts, depending on the specific composition of a cement sample. It is well established that the performance of PCEs can be severely impeded in the presence of sulfate ions in the cement pore solution. Contrary to previous researchers who focused on the negative impact of sulfate, it was found here that the addition of controlled amounts of sulfate to the cement paste can in fact significantly enhance the dispersing effectiveness of specific PCE polymers. The enhanced dispersing effectiveness of highly anionic PCEs by sulfate stems from concomitant adsorption of both PCE and sulfate. Contrary, sulfate can negatively impact the performance of PCEs possessing low anionic character, as a consequence of competitive adsorption between the PCE and sulfate.

Compatibility problems between certain cements and PCE superplasticizers present a big challenge for these dispersants. This effect can decrease the dispersing power of the polymer used and thus can adversely affect the workability of concrete. Specific modification of the polymer structure revealed that perfect compatibility of the polymer with any type of cement as well as high tolerance for sulfate ions can be achieved. Moreover, in contrast to other previous studies it was found that the APEG-type PCEs do not shrink or coil significantly in the presence of sulfate ions.

Delayed addition of most SPs to an already mixed concrete (delayed mode) reveals a significantly higher dispersing performance comparing to the early mode (addition of SP with the mixing water). Here, it was found that the different behavior at early and delayed addition is due to the content of alkali sulfates and C_3A present in the cement sample, which play the key role. In case of using cement with a low alkali sulfate/C_3A molar ratio (less than ~ 1.5), chemisorption (intercalation) of the SP into C_3A hydrates occurs resulting this difference. While at high alkali sulfate/C_3A molar ratios (~ 2), similar flow values are attained at early and delayed addition, because of predominant formation of AF_t (ettringite), and thus no SP intercalation into layered calcium aluminate hydrates from the hydrocalumite type can take place.

List of Papers

This thesis includes the following papers:

Peer reviewed SCI(E) journal manuscripts:

1. **Interaction between Polycarboxylate Superplasticizers and Amorphous Ground Granulated Blast Furnace Slag**

   Ahmad Habbaba and Johann Plank.

   Journal of the American Ceramic Society, 93 (2010) 2857 – 2863.

2. **Surface Chemistry of Ground Granulated Blast Furnace Slag in Cement Pore Solution and Its Impact on the Effectiveness of Polycarboxylate Superplasticizers**

   Ahmad Habbaba and Johann Plank.

   Journal of the American Ceramic Society, 95 (2012) 768 – 775.

3. **Synthesis and Performance of a Modified Polycarboxylate Dispersant for Concrete Possessing Enhanced Cement Compatibility**

   A. Habbaba, A. Lange and J. Plank.

   Journal of Applied Polymer Science, published online, DOI: 10.1002/app.38742

Manuscripts submitted to peer reviewed SCI(E) journals:

4. **SYNERGISTIC AND ANTAGONISTIC EFFECT OF SO_4^{2-} ON DISPERSING POWER OF PC**

   A. Habbaba, N. Zouaoui and J. Plank.

   ACI Materials Journal (accepted).

5. **Intercalation of Superplasticizers into AFm Phases: Can It Explain the Differences Occasionally Observed at Early and Delayed Addition of Admixtures?**

   Ahmad Habbaba, Zhimin Dai and Johann Plank.

   Journal of Cement and Concrete Research (under review).

Refereed conference paper:

6. **Surface chemistry of ground granulated blast furnace slag in cement pore solution: Understanding the behavior of slag in blended cements containing polycarboxylate superplasticizers**

   A. Habbaba, J. Plank. Proceedings of the XIII ICCC International Congress on the Chemistry of Cement, Abstract book p. 407, Madrid/Spain 2011.

Conference papers:

7. **Interaction between Polycarboxylate Superplasticizers and Amorphous Ground Granulated Blast Furnace Slag**

   A. Habbaba, J. Plank

   GDCh-Monographie, 42 (2010) 152 – 159.

8. **Wechselwirkung von Polycarboxylat-basierten Fließmitteln mit Hüttensandmehlen**

   J. Plank, A. Habbaba, R. Sieber

   17. ibausil, Tagungsband 1, Bauhaus-Universität Weimar (2009) 369-374.

Table of contents

List of figures

List of tables

List of Abbreviations

AAS	Atomic absorption spectroscopy
AF_m	Monosulfoaluminate, monosulfoaluminate ferrite
AF_t	Trisulfatealuminate, trisulfatealuminate ferrite
BET	Brunauer, S. – Emmett, P. – Teller, E. (inventors of the BET theory)
BNS	β-naphthalene sulfonate formaldehyde condensate
bwoc	By weight of cement
bwos	By weight of solid
C_3S	Tricalcium silicate, alite
CEM I	Portland cement with max. 5% of miner constituents
C-S-H	Calcium silicate hydrate
CVI	Colloid vibration current
d_{50}	Average particle size
DI water	Deionized water
DIN	The German national standards organization
EDL	Electrical double layer
EO	Ethylene oxide
eq/g	Equivalent amount per gram of polymer
g	Gram
GGBFS	Ground granulated blast furnace slag
GHG	Greenhouse gas
GPC	Gel permeation chromatography
h	Hour(s)
IC	Ionic chromatography
IEP	Isoelectric point
IHL	Inner Helmholtz layer
IHP	Inner Helmholtz plane
L	Liter
LDH	Layered double hydroxide
LOI	Loss on ignition
M	Molar (Mol per liter)
MA	Methacrylic acid
ME	Methacrylate ester
min	Minute(s)
M_n	Number average molecular weight
MPEG	Methoxy poly(ethylene glycol)
M_w	Weight average molecular weight
m. r.	Molar ratio
NDIR	Nondispersive infrared sensor
n_{EO}	Number of ethylene oxide units
OHL	Outer Helmholtz layer

OHP	Outer Helmholtz plane
OMP	Organo-mineral phase
OPC	Ordinary Portland cement
pH	Pondus hydrogenii
PC or PCE	Polycarboxylate (ether)
PDI	Polydispersity Index
PEG ME	Poly(ethylene glycol) methacrylate ester
PEO	Polyethylene oxide
Poly-DADMAC	Poly diallyl dimethylammonium chloride
PTFE	Polytetrafluoroethylene (Teflon)
R_h	Hydrodynamic radius
rpm	Rotations per minute
SCM	Supplementary cementitious material
SCPS	Synthetic cement pore solution
SEM	Scanning electron microscopy
SP	Superplasticizer
TOC	Total organic carbon
V	Volt
v %	Volume percent
wt. %	Weight percent
w/s ratio	Water to solid ratio
w/c ratio	Water to cement ratio
XRD	X-ray diffraction
XRF	X-ray fluorescence
β	Thickness of inner Helmholtz layer
σ	Charge density
μ	Micro
ψ	Potential
θ_A	Degree of adsorption
ζ potential	Zeta potential

1. INTRODUCTION

Superplasticizers (SP) are applied in the construction industry to allow producing a highly flowable concrete and/or to reduce the water/cement ratio (w/c) of concrete, resulting in higher compressive strength and improved durability. Generally, polycarboxylate (PCE) superplasticizers which are comb-shaped copolymers consist of a negatively charged backbone (owed to the carboxylate groups) and grafted side chains which are mainly composed of polyethylene oxide units (PEO). The negatively charged backbone adsorbs onto the surface of the hydrated cementitious particles (cement and supplementary cementitious materials (SCMs)), while the non-adsorbed graft chains extend away from the cement surface into the pore solution [1, 2]. The interaction between SPs and cement is generally well understood [3 - 6]. It was found that the mechanism behind the dispersing effect of PCEs is based on steric hindrance between cement particles as well as electrostatic repulsion forces between the cement grains. It essentially depends on the chemical structure of the PCE used [7 - 10]. Moreover, PCE adsorption has also a retardation effect on the cement hydration due to the change in growth kinetics and morphology of early hydrates [11, 12].

It was reported before that some SPs interact strongly with cement possessing a high C_3A content, consuming huge amounts of SPs to achieve the fluidity required [1, 2]. This behavior is owed to the intercalation of SPs into lamellar calcium aluminate hydrates. Formation of these organo-mineral phases (OMPs) was reported previously by using β-naphthalene sulfonate formaldehyde condensate (BNS) [13], or PCE [14]. Delayed addition of SPs to the cement paste can eliminate this behavior [15]. In our study we tried to find the actual factor which determines whether SP intercalation at early and delayed addition does occur or not.

In cementitious systems sulfate has a remarkable impact on the hydration process of cement and its properties [16, 17]. Moreover, the sulfate balance existing in a cement has a significant influence on the workability of most SPs [18, 19]. Several studies clearly

revealed that sulfate ions can adsorb onto the surface of cement particles immediately and in competition with PCE [20 - 22].

The main part of this work focused on studying the surface chemistry of ground granulated blast furnace slag (GGBFS) which belongs to the group of SCMs. GGBFS is commonly blended with Portland cement clinker to produce Portland composite cements which show a lower carbon footprint than ordinary Portland cement (OPC). Moreover, slag cements allow to build high strength and durable concrete structures similar to those achieved with OPC [23, 24]. Up till now, the interaction between slag and common concrete admixtures such as PCEs has been poorly investigated. Therefore, the dispersing effect of PCE polymers on different GGBFS samples in the absence and presence of sulfate was studied here. This research aimed at providing an overview on the competition between the surfaces of cement and slag for PCE adsorption. Additionally, occurrence of competitive adsorption between PCEs and sulfate ions for positively charged sites existing on the surface of slag particles was confirmed as well.

For better understanding of the complex working mechanism of SPs in cement, the impact of PCEs on an inert model system (hydraulically unreactive $CaCO_3$ powder) was investigated. The calcium carbonate (limestone) system is much simpler compared to cement, due to the absence of sulfate ions resulting from the dissolution of calcium sulfates present in cement. Moreover, no hydration process which can alter the surface chemistry of $CaCO_3$ takes place. This study was done to prove the hypothesis of competitive adsorption occurring between PCE polymers and sulfate ions. Moreover, and contrary to many previous studies [25, 26], the possibility of improving the dispersing performance of specific PCEs by the addition of controlled amounts of sulfate salts to the liquid admixture was confirmed here.

It was reported before that a compatibility problem between certain cements and comb-shaped SPs exists, which can adversely affect concrete workability [27]. Various explanations have been presented for this behavior, such as the variation in clinker composition of cement, contamination of the concrete with clay or silt, and perturbation of PCE by sulfate ions released from cement (“sulfate effect”) [28]. Therefore, to prove

the high compatibility of a newly synthesized APEG-type PCE polymer, its dispersing performance was studied using "difficult" cements in presence of high sulfate content. These results were compared with those from other conventional PCE polymers.

In general, investigations on the sorption behavior (adsorption and/or intercalation) of PCE based SPs on slag, limestone and cement were carried out in this thesis. The aim was to gain insights into the surface chemistry of their mineral surfaces and to determine the mechanism of interaction between PCE-based SPs and these cementitious materials. Moreover, this work focuses mainly on the influence of sulfate on the dispersing power of different PCEs.

2. THEORETICAL BACKGROUND

This chapter presents a brief background about the surface chemistry of colloids (such as cementitious materials), and how it can be affected by the presence of ions and/or polymers in the pore solution. This information is necessary to understand the discussions of the results obtained from the main two analytical methods used in this work (zeta potential and adsorption measurement).

2.1 ZETA POTENTIAL AND ELECTRICAL DOUBLE LAYER

In suspensions, the net charge at the particle's surface attracts ions present in the surrounding interfacial region, thus increasing the concentration of counter ions (ions possessing an opposite charge to the particle's surface) close to the surface. The ions in the medium form an electrical double layer (EDL) that surrounds a colloidal particle (see **Fig. 1**). Thus, the colloidal dispersion will be stabilized due to the electrostatic repulsion between the ion-coated particles.

The ionic strength of the suspension's pore solution has a significant impact on the thickness of the EDL. At low ionic strength (concentration of ions is less than 10^{-3} M), its thickness will be between 5 to 10 nm. Such a thick EDL can produce a considerable repulsive force at the solid-liquid interface which is strong enough to overcome the attractive Van de Waals inter-particle forces (Van der Waals attractive forces normally occur at inter-particle distances in the range of 5 to 7 nm). This way, the attractive force is balanced by the EDL, and the dispersion is stabilized. In case of very high ionic strengths (concentration of ions is more than 10^{-1} M, which is characteristic for cement systems), the thickness of the double layer will not exceed 1 nm. This thin EDL generates insufficient repulsion between colloidal particles which results in a short distance between the colloidal particles. Thus, the distances between particles are not large enough to overcome the Van der Waals attractive forces which hence will persist and cause agglomeration of the particles [29, 30].

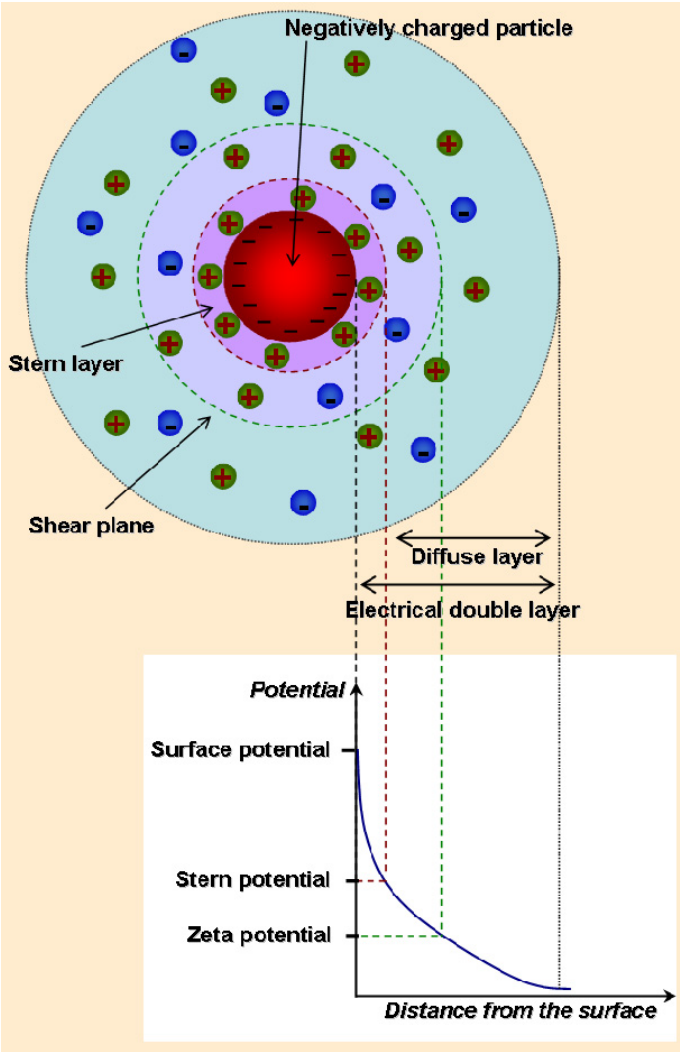

Fig. 1 Schematic illustration of an electric double layer around a negatively charged colloidal particle

The term *Stern* layer is normally used for the uncharged region between the surface and the location of hydrated counter-ions. This layer is followed by another region called *diffuse* layer or *Gouy* layer. Thus, the EDL consists of these two layers. The *Stern* layer can be subdivided into an *inner Helmholtz layer* (IHL), and an *outer Helmholtz layer* (OHL). IHL is located between the particle surface and the *inner Helmholtz plane* (IHP), while OHL is bounded by the IHP and the *outer Helmholtz plane* (OHP). The arrangement of these layers is shown schematically in **Fig. 2**. IHL consists of specifically adsorbed ions on the particle surface (possessing a chemical affinity for the surface),

whereas OHL contains the other ion types which interact with the surface charge only through electrostatic forces. The IHP is the site of the first ion layer, and the OHP determines the beginning of the diffuse layer. The fixed surface charge density, the charge density at the IHP and the charge density in the diffuse layer are denoted σ^0, σ^i and σ^d, respectively. The entire system is electro-neutral [31, 32].

$$\sigma^0 + \sigma^i + \sigma^d = 0$$

At the distance β from the surface, the potential is changed from ψ^o (the surface potential) to ψ^i (the IHP potential). While at distance *d* from the surface ($\beta \leq d$), the potential of OHP is called the diffuse-layer potential, or *Stern* potential. ψ^d is the potential at the beginning of the diffuse part of the double layer. All potentials are defined with respect to the potential in bulk solution.

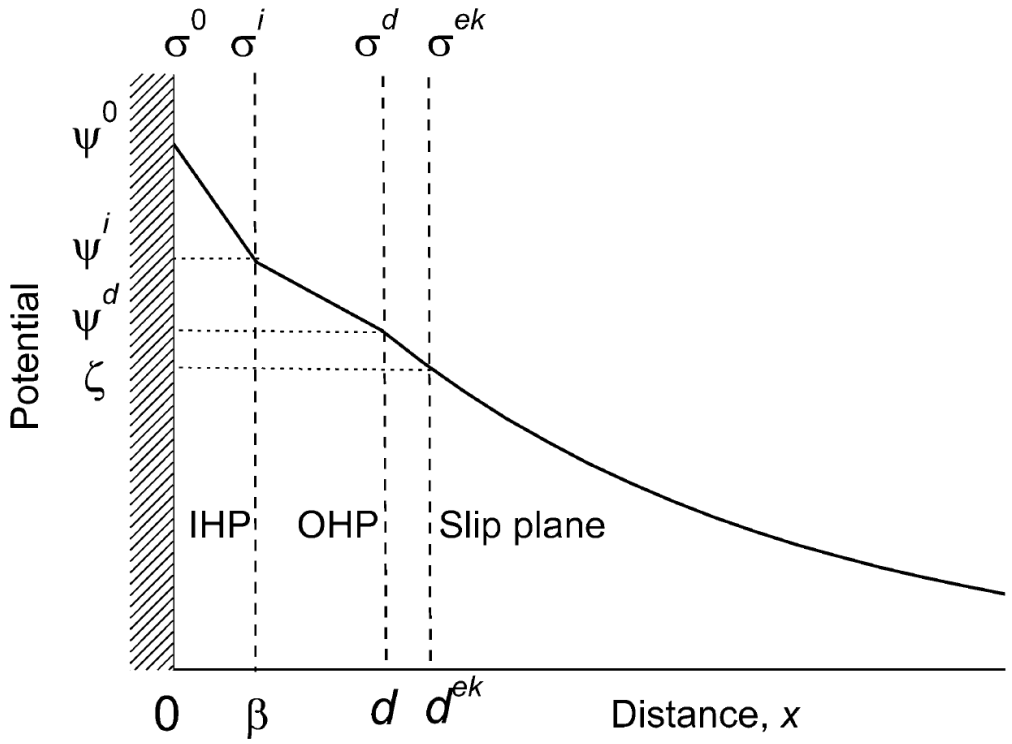

Fig. 2 Schematic representation of the charges and potentials at a positively charged solid – liquid interface [33]

By applying an external electric field (*electrophoresis, electro-osmosis*) or a mechanical force (*streaming potential, current*) to the suspension, a flow layer of tangential liquid along the charged solid surface was observed [34]. This layer (called hydrodynamically stagnant layer) extends from the surface to a specified distance (d^{ek}). In this distance, the hydrodynamic slip plane is assumed to exist, and its potential is identified as the *electrokinetic* or *zeta-potential*, ζ. In other words, within the diffuse layer there is an estimated boundary known as the slip plane, in which the particle acts as a single entity. The potential at this boundary is known as the zeta potential. Therefore, the charge of the slip plane equals the *electrokinetic* (*particle*) *charge,* σ^{ek} [31, 35 - 37].

The stability of a colloidal system is evident from its zeta potential value. Low ζ potential values refer to a very weak or almost no repulsion force existing between the colloidal particles which then can agglomerate. While in case of a very high potential, flocculation is prevented due to the large repulsion between the particles which introduces stability into the dispersion system. It was noticed that when the zeta potential value is higher than + 30 mV or lower than - 30 mV, the colloidal system should be stable [38].

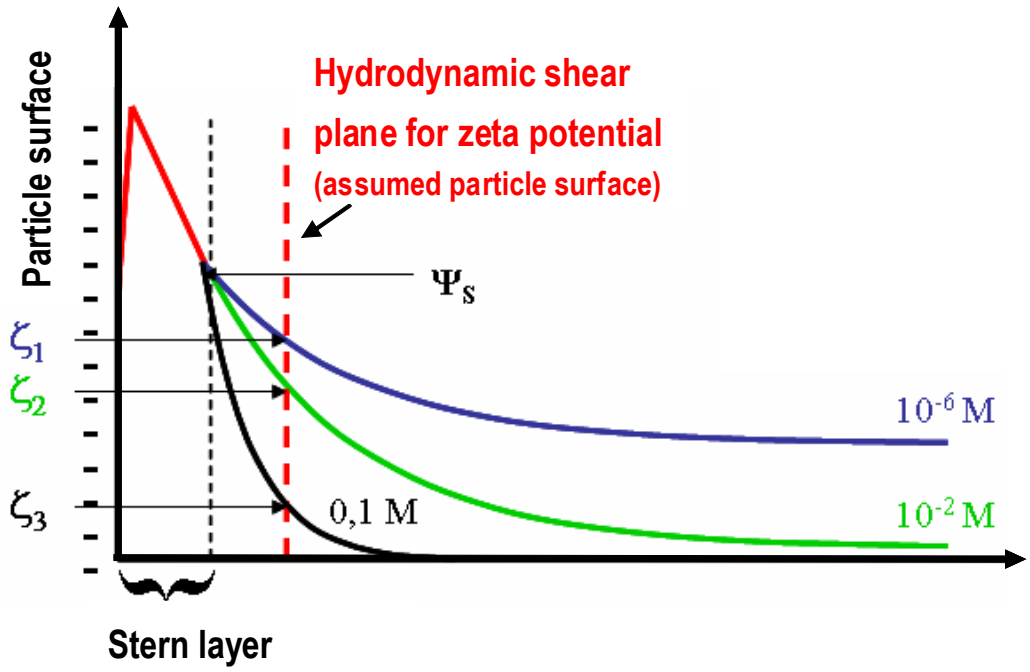

Fig. 3 Relation between ionic strength and zeta potential of a solid particle **[**39**]**

There are three factors which can significantly affect the zeta potential measurement; pH value, ionic strength and the concentration of the colloid. The higher the pH value, the more negative the zeta potential is, and vice versa at low pH value. As has been described before, by increasing the ionic strength the conductivity of the pore solution will increase too, thus compressing the EDL. The zeta potential will decrease as well (**Fig. 3**). Finally, the concentration of colloidal particles is important to understand the interplaying factors for the dispersion stability.

2.2 ADSORPTION

The term "adsorption" is normally used to refer to the adhesion of *adsorbate* (atoms, ions or molecules) onto a solid surface (*adsorbent*). The adhesion can be established through chemical or physical interactions. The physical adsorption (typically resulting from Van der Waals forces) is somehow weaker compared to chemical adsorption. The chemical adsorption is related to particle size, form and other physical properties of the adsorbate and only occurs when strong chemical bonds between the adsorbate and adsorbent are established. The chemical bonds can be formed by ionic attraction or covalent bonding. Adsorption is usually described through isotherms which express the amount of adsorbate present on the surface of adsorbent as a function of its pressure (gas) or concentration (liquid) at constant temperature. In general, adsorption can occur according to two different models expressed by *Langmuir* or *BET* isotherms. They can be determined by calculating the adsorption degree (θ_A). Both adsorption models are discussed here briefly.

2.2.1 LANGMUIR ADSORPTION ISOTHERM

This model was developed by Irving Langmuir in 1916 [40]. There are four assumptions in the Langmuir adsorption model:

1. Only a monolayer of the adsorbate is deposited on the available adsorbent surface at the maximum adsorption degree;
2. The ratio of adsorbate molecule to adsorptive site is constant;

3. All adsorption sites are energetically homogeneous (the adsorption enthalpy is similar for all adsorption sites and independent of the level of saturation);
4. The interaction between adsorbate molecules is negligible.

The Langmuir adsorption isotherm is applicable if these conditions exist in a system. **Fig. 4** shows a Langmuir adsorption isotherm. At the beginning, the adsorption degree is increased by increasing the partial pressure (in gaseous phase) or concentration (in aqueous phase) of the adsorbate. This way, the adsorptive sites are proportionally occupied by the adsorbate. When the adsorbate content reaches a certain value, a saturation plateau will be achieved. It signifies that the adsorptive sites are totally occupied with adsorbate.

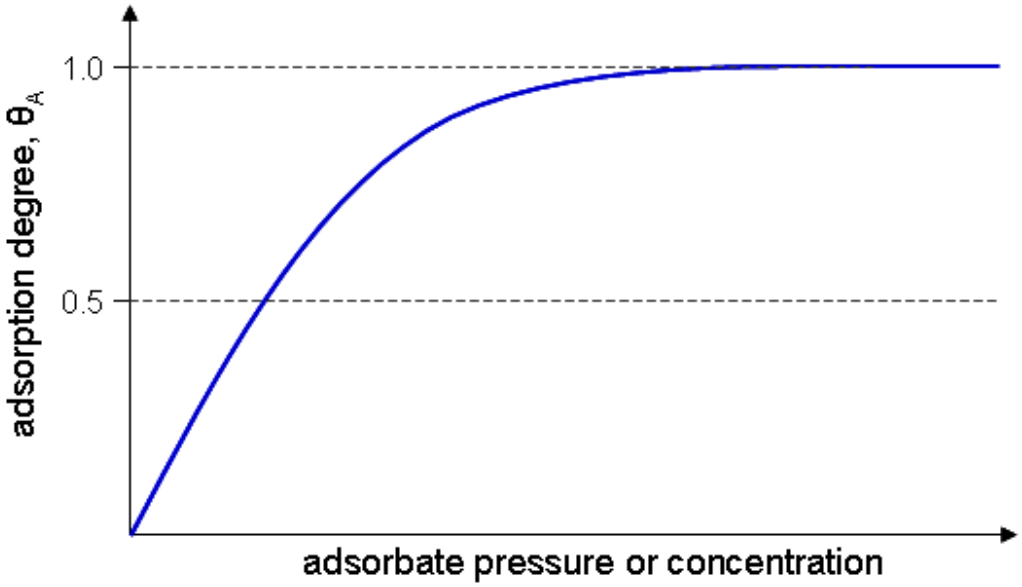

Fig. 4 Langmuir adsorption isotherm

It was found that the adsorption of polycondensates on cement follows the Langmuir adsorption model. One layer of anionic polymer particles coats the cement grains, thus producing repulsion between the negatively charged surfaces of cement. Electrostatic repulsion between the anionic polycondensate molecules also prevents the formation of double or multiple layers of polycondensate.

2.2.2 BET ADSORPTION ISOTHERM

This model was developed and published by Stephen Brunauer, Paul Hugh Emmett and Edward Teller in 1938 [41]. It describes the adsorption process in a double or multiple-layer model. There are several assumptions made in this adsorption model:

1. Infinite number of layers formed by adsorption;
2. No interaction between each adsorption layer occurs;
3. The Langmuir theory can be applied to each layer.

To achieve the infinite layering, the adsorption should reach the saturation point (θ_A= 1). **Fig. 5** shows as an example a BET adsorption isotherm. It can be observed here that the curve reaches the saturation plateau twice. The first is similar to a Langmuir isotherm (reaching a mono-layer saturation). Afterwards, the adsorption degree continues to rise until reaches a second saturation plateau (the formation of double-layer).

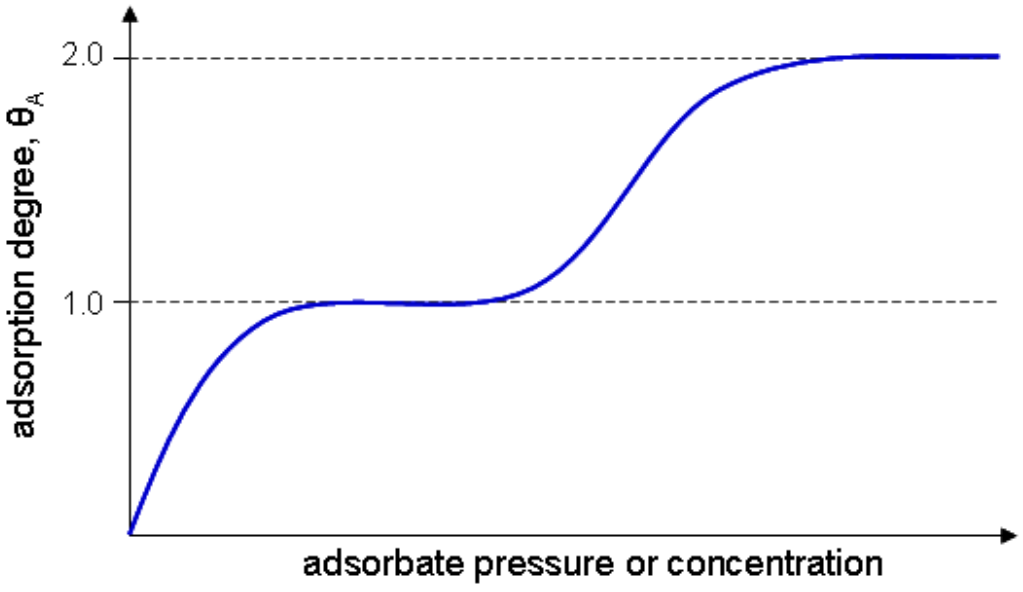

Fig. 5 BET adsorption isotherm showing further adsorption after monolayer saturation

2.3 POLYMER ADSORPTION EFFECT ON THE SURFACE CHEMISTRY OF COLLOIDAL PARTICLES

Polymers can provide an additional stabilizing effect for dispersed particles by adsorption either directly on the positively charged surface of the colloidal particles, or on the first positive ion-layer which covers the negatively charged surface. Depending on the structure of the adsorbed polymers, their repulsion effect is often comparable or greater than the range of Van der Waals attraction between colloidal particles.

Different repulsion mechanisms were found when SPs adsorb onto the surface of cement particles, which relate to the chemical structure of the polymer. When strongly anionic polycondensates adsorb onto cement particles, electrostatic repulsion occurs, as is illustrated in **Fig. 6**. On the contrary, the comb-shaped, weakly ionic PCEs attach to the particles producing a steric hindrance between them (**Fig. 6** and **7**) [42].

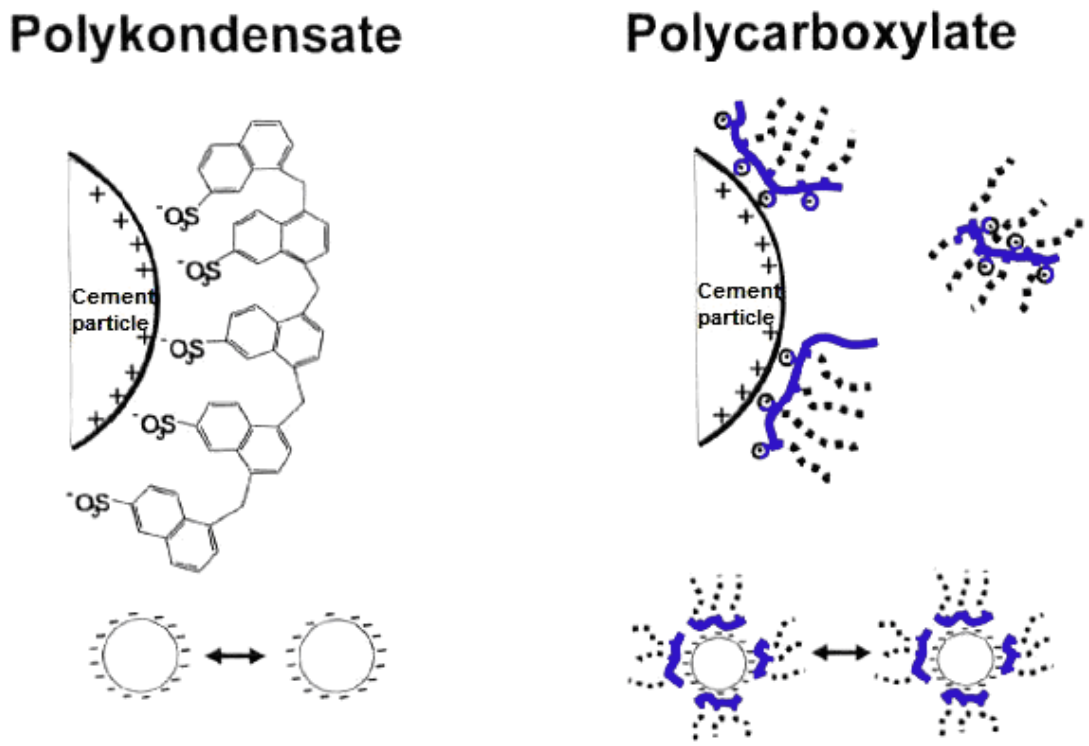

Fig. 6 Working mechanism of concrete superplasticizers [42]

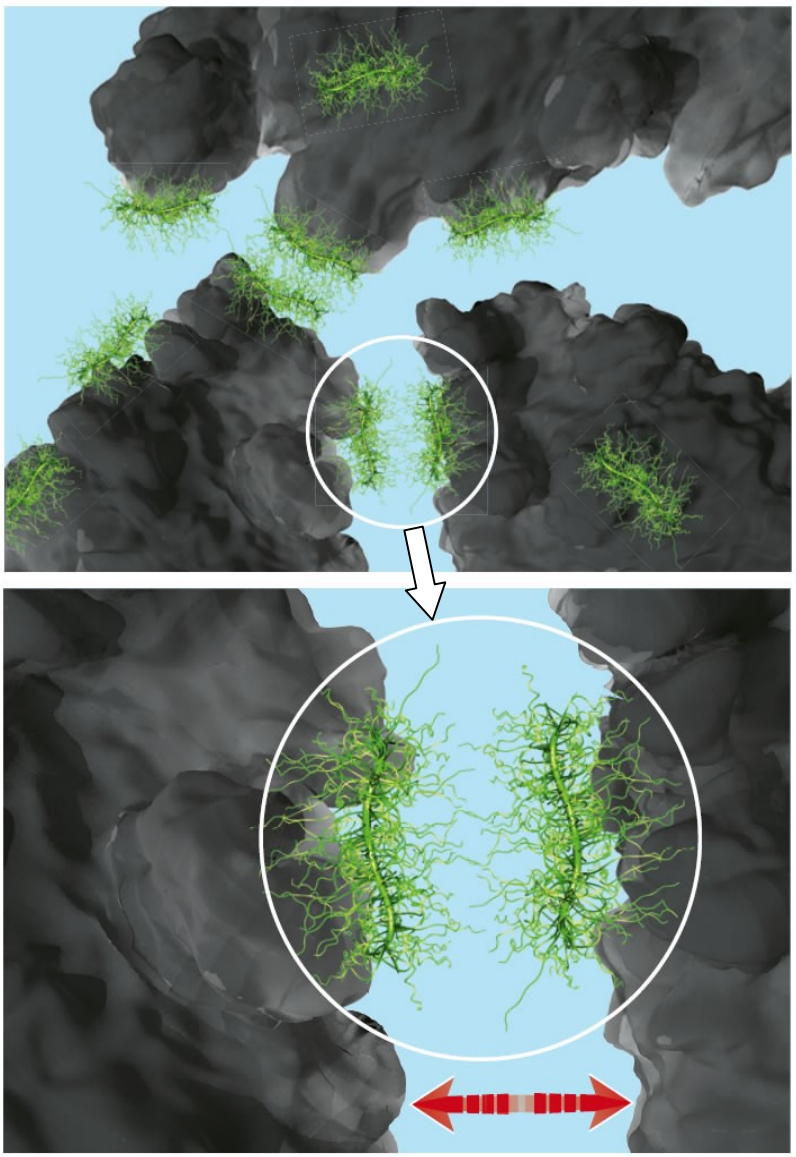

Fig. 7 Adsorption and the steric effect of PCE superplasticizers [43]

The impact of polymer adsorption on the surface chemistry of cement can be explained by the displacement of the hydrodynamic shear plane, which is dependent on the adsorbed polymer. For the comb-type PCEs it was observed that the long PEO side chains shift the shear (or slip) plane of the zeta potential to greater distances away from the cement surface (as is shown in **Fig. 8**) [44, 45]. At those distances from the particle surface, the potential curve in the diffuse layer can approach the isoelectric point (IEP).

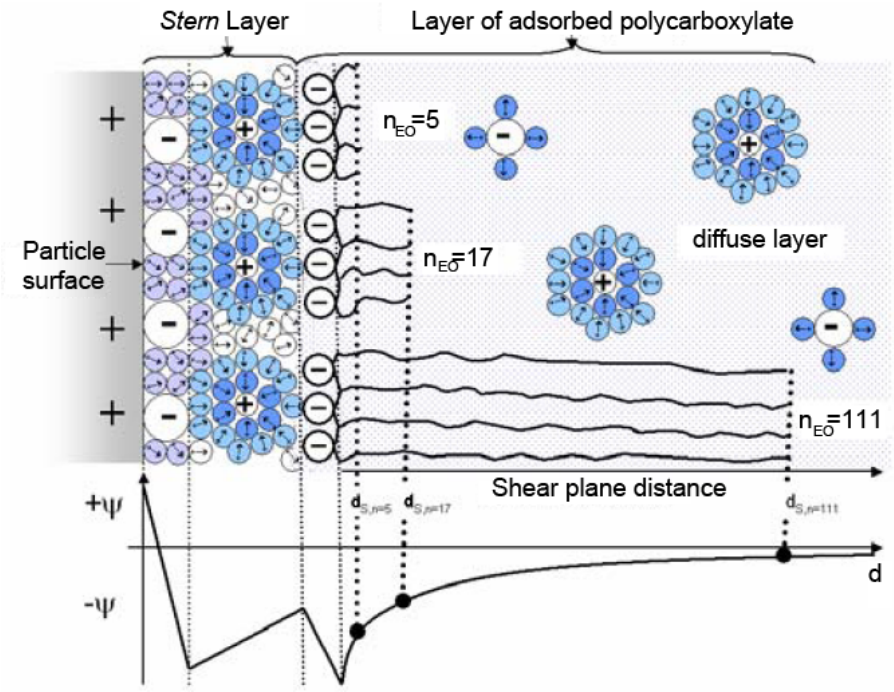

Fig. 8 Electrical double layer on the surface of a colloid particle with adsorbed comb-shaped polymers [45]

Generally, the adsorption mechanism of PCEs depends on several variables, such as strength and distribution of particle surface charge, chemical structure of the polymer, the specific charge amount of PCE, and ionic strength of the solution.

2.4 FORMATION OF ORGANO-MINERAL PHASES

During the hydration process of cement and in the presence of SPs, the interaction of SPs with hydrating cement not only involves surface adsorption, but a part of these polymers may intercalate (chemisorb) into lamellar calcium aluminate hydrates, thus leading to the formation of organo-mineral phases (OMP) [46, 47]. The formation of OMPs during the preparation of calcium aluminate hydrates with polynaphthalene sulfonate was confirmed *via* FTIR spectroscopy (chemical bond of the sulfonate groups condensate in BNS to the principal layers) [13]. It was also found that the initial molar ratios of sulfonate in BNS to the sulfate in solution impact the formation of both ettringite and OMPs [13].

Intercalation of PCE *via* formation of calcium aluminum layered double hydroxides incorporating PCE superplasticizers (Ca-Al-PCE-LDHs) was confirmed later [47, 48]. These studies observed that the formation of either OMP or ettringite is strongly related to the molar ratio of SO_3/C_3A (see **Fig. 9**). At high SO_3/C_3A ratios, sulfate occupies the interlamellar space thus preventing the intercalation of the PCE. Consequently, the intercalation of PCE occurs only at SO_3/C_3A ratios ≤ 1 [14]. Another research group mentions that the intercalation of PCEs depends greatly on the chemical structure of the PCE, as well as the amounts of calcium and sulfate present in the system. The lower the concentration of sulfate in the pore solution, the faster the formation of OMP occurs. On the other hand, no intercalation of PCE can be observed at high sulfate contents [49].

In general, if SPs are intercalated, they are no longer available for the superplasticizing effect which requires surface adsorption on the cement grains. Therefore, a higher dosage of SP will be required to compensate the polymer lost by chemical absorption.

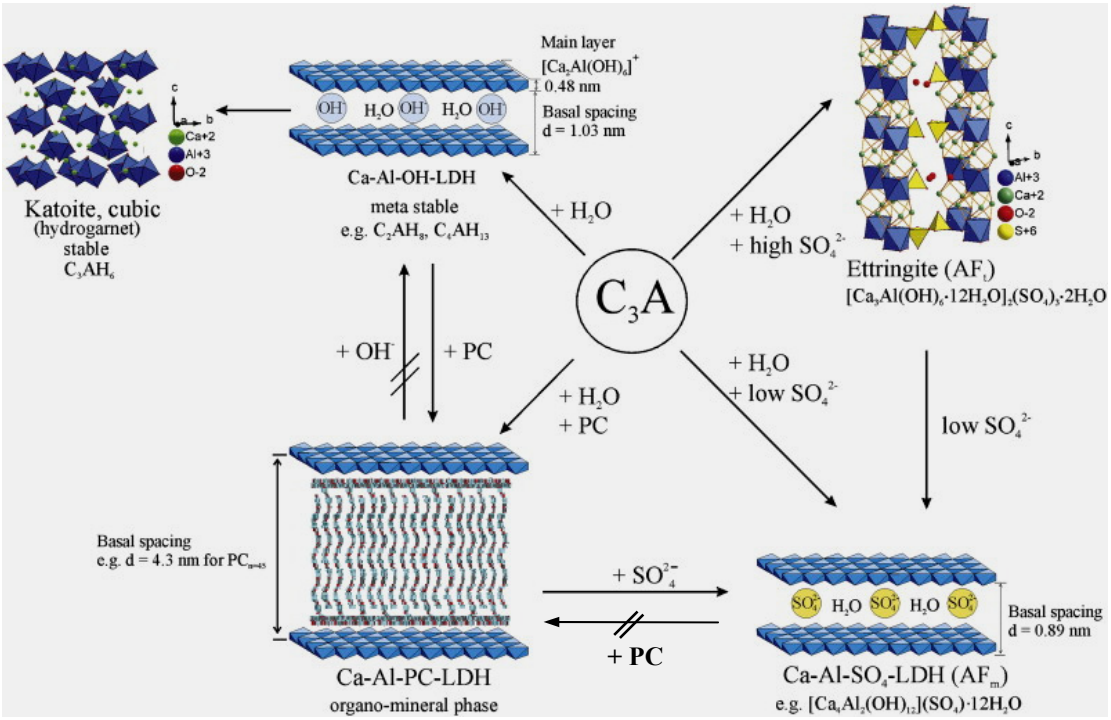

Fig. 9 Representation of C_3A hydrating at different SO_4^{2-} concentrations and in presence and absence of PCE (or PC) superplasticizer [14]

3. AIMS AND SCOPE

This work aims to study the synergistic and the antagonistic impacts of sulfate ions present in cement pore solution on the dispersing performance of different PCE based SPs. The dispersing power of PCE polymers is the main parameter which determines the workability achieved from them. Therefore, it was necessary to detect the tolerance of PCE for sulfate ions, and find solutions to overcome their negative effect on specific PCE molecules by modification of the PCE structure, or optimizing the electrolyte content in the PCE solution to achieve the best workability.

Previous studies on the interaction between PCEs and sulfate ions focused only on the negative impact of sulfate on the dispersing performance of PCE, while positive effects were neglected. Hence, also the synergistic impact of SO_4^{2-} on the dispersing effectiveness of PCEs was studied in this thesis.

This study was performed utilizing an inert system (namely limestone), a semi-inert system (GGBFS) and an active system (cement). The reason for this variation is on one hand to conduct the experiments in the absence or presence of the hydration process (during cement hydration, sulfate ions are released into the pore solution in different amounts, depending on the specific composition of the cement sample). On the other hand, different systems were used to investigate the individual effects of PCEs on each component (cement, slag or limestone) which could add up in blended cements.

The following research steps were taken to develop a model explaining the effects of PCEs at the solid-liquid interface in the absence and the presence of sulfate:

- The electrical surface charge developed by GGBFS when suspended in water, $CaCl_2$ solution and SCPS, respectively was determined using a zeta potential instrument.

- The interaction between PCE and either GGBFS, limestone or cement was studied *via* adsorption and zeta potential measurement in order to assess whether PCE and sulfate actually undergo competitive or concomitant adsorption.
- The influence of electrolytes in solution, of cementitious material used, of the PCE architectures and the addition time of PCE on the fluidity of the slurries utilizing the '*mini slump*' test was determined.
- The effect of sulfate ions on PCE properties such as its anionic charge amount and hydrodynamic radius were measured.
- Adsorption of PCE and sulfate on the inert $CaCO_3$ particles employing TOC measurements for PCE and ion chromatography for SO_4^{2-} analysis was studied.

These experiments allowed an understanding of the synergistic and antagonistic effects of sulfate ions by determination of the competitive and concomitant adsorption of both PCE polymers and sulfate ions on the mineral surfaces. Additionally, they allowed to determine which sulfate compound present in cement has the most impact on the formation of OMPs during the early addition of SPs to the cement paste. In consequence, this work explains the fundamental mechanisms underlying the positive or negative effects of sulfate ions, and clearly identifies PCE structures which either can benefit or suffer from sulfate.

4. MATERIALS

This chapter presents a general overview of all applied materials used during this research. Additional details about the materials have been presented in the publications which are part of this thesis.

4.1 POLYCARBOXYLATE SUPERPLASTICIZERS

Eight different PCE superplasticizers were synthesized and used in this study. Six of them were first generation PCEs (*x*PC*y*) based on methacrylic acid – *co* – ω-methoxy poly(ethylene glycol) (MPEG) methacrylate ester. Their general chemical structure is shown in **Fig. 10**. The number "*x*" refers to the ethylene oxide units (n_{EO}) present in the side chains of the PCE comb polymers and were 8.5, 17, 25, 45 or 111, whereas "*y*" refers to the molar ratios of methacrylic acid to MPEG methacrylate ester which were 6:1, 3:1 and 1.5:1 respectively. Aqueous radical copolymerization was utilized to synthesize these copolymers; initiator was sodium peroxodisulfate, and methallyl sulfonic acid was employed as a chain transfer agent.

The synthesis was curried out as follows: In a 1L-five-neck reaction flask was equipped with a reflux condenser, a nitrogen inlet pipe, a stirrer, a contact thermometer and a dispenser for the initiator. A certain amount of methacrylic acid was added to 87.5 mL water in the flask, and the pH value of the solution was adjusted to 9 by using 30 wt.% NaOH solution. Poly (ethylene glycol) methacrylate ester and 3.26 g of the chain transfer agent (methallyl sulfonic acid, sodium salt) were added to the flask at once. After that, 175 mL water were added too and the pH value of the mixture was adjusted once again to 9.2 using 30 wt.% NaOH solution. The mixture was heated up to a temperature of 60 °C. Over a period of 90 min, the initiator solution (2.5 g of $Na_2S_2O_8$ solved in 15 mL water) was added dropwise employing an ISMATEC MPC dosage pump. This reaction was curried out under nitrogen atmosphere, because of the instability of the initiator in oxygen atmosphere. The stirring was continued for additional 30 min at the same temperature (60 °C), and then the whole mixture was heated up to 80 °C for one hour. At the end of the reaction, heating was stopped allowing the solution to cool down to room temperature.

The solids content was between 15 and 25 wt.% which was determined by employing an infrared drying balance at 120 °C for 10 min. The color of the final product varied from transparent, yellow and orange to reddish brown, which depended on the amount of ethylene oxide units in the side chain of the poly(ethylene glycol) methacrylate ester used. After copolymerization, the polymer solutions were neutralized with sodium hydroxide and dialyzed using a 6,000 – 8,000 Da cellulose cut-off membrane (Spectra/Pro, Spectrum Laboratories Inc., Rancho Dominguez, CA, USA). **Table 1** shows the feed amounts of each component used in the synthesis of each copolymer.

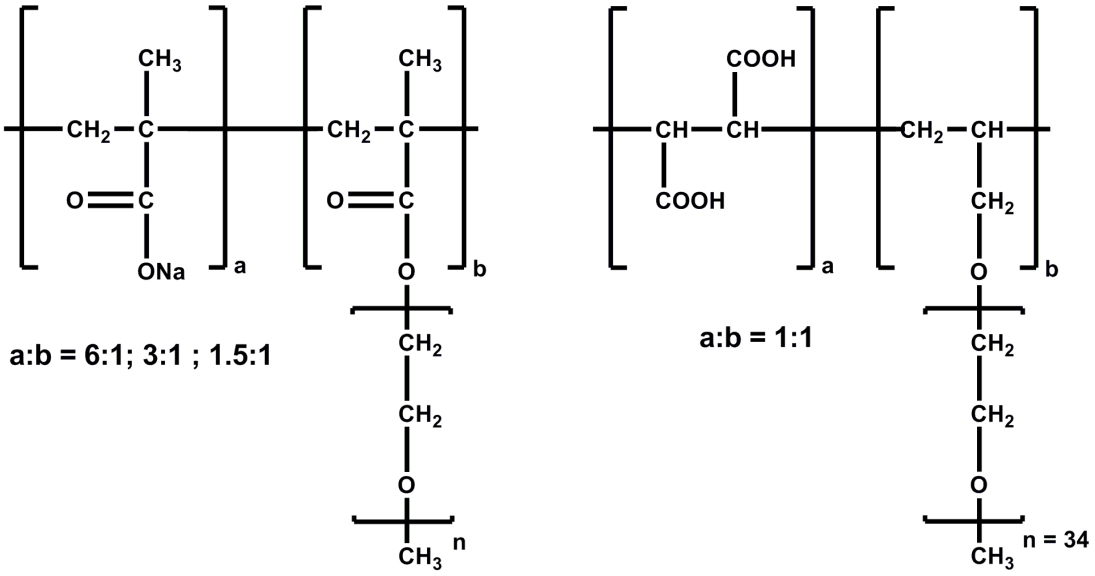

Fig. 10 Chemical structure of the MPEG-type (left) and the APEG-type (right) polycarboxylate copolymers

Table 1: Raw materials for the polycarboxylate syntheses

Sample	H_2O [g]	MA [g] pur	MPEG/ME [g]	n_{EO}	Chain transfer agent [g]	Initiator solution	
						$Na_2S_2O_8$ [g]	H_2O [g]
8.5PC6	262.5	51.6	47.4	8.5	3.26	2.5	15
17PC6	262.5	51.6	84.8	17	3.26	2.5	15
25 PC 3	262.5	25.8	120	25	3.26	2.5	15
45 PC 1.5	262.5	12.9	208	45	3.26	2.5	15
45 PC 6	262.5	51.6	208	45	3.26	2.5	15
111PC6	262.5	51.6	498.4	111	3.26	2.5	15

The other two dispersants, 34APEG and *m*34APEG polymers were from the second generation which are based on α-allyl-ω-methoxy polyethylene glycol - maleic anhydride. The 34APEG polymer was synthesized by free radical copolymerization in bulk from allyl ether macromonomer and maleic anhydride at a molar of ratio 1:1. The novel *m*34APEG was synthesized following the same procedure but using allyl maleate monomer as an additional new building block (molar of ratio 1:1:1). These polymers were synthesized at the Chair for Construction Chemicals, and the synthesis procedure is presented in detail in **paper 3**.

All polymers were characterized using Waters 2695 gel permeation chromatography (GPC) separation module, and the data obtained from GPC are presented in the published papers which are part of this thesis.

4.2 GROUND GRANULATED BLASTFURNACE SLAG

In this study, three GGBFS samples from different sources in Germany were employed: Slag # I from Schwenk cement company, Karlstadt; Slag # II from Holcim's Salzgitter plant, Salzgitter; and Slag # III from Holcim's Hansa Bremen plant, Bremen. To determine the oxide composition of the slag samples, X-ray fluorescence analysis was employed. It was found that all slag samples contained large contents of CaO ranging from 42.8 wt. % in slag # I to 36.4 wt. % in slag # II and 38.6 wt. % in slag # III. The slags also incorporated large amounts of SiO_2: 35.9 wt. %, 36.3 wt. % and 38.6 wt. % for slag # I, II and III respectively, while the Al_2O_3 contents were comparable in all slag samples (~ 11.5 wt. %). Slag # II exhibited a particularly high content of MgO (11.5 wt. %), compared to slags # I and III (~ 6.4 wt. %). Other oxides such as TiO_2, Fe_2O_3, Mn_3O_4, and SrO were present in low amounts (up to 0.8 wt. %). The physical properties of all slag samples such as density, specific surface area (*Blaine*) and d_{50} value (average particle size) are presented in **papers 1 and 2**.

Mineralogical characterization of the slag samples was attempted *via* powder XRD analysis and by scanning electron microscopy. Because of the amorphous character of the slags, no sharp reflections indicative of crystalline constituents were found in the XRD

spectra (exhibited in **paper 2**). Additionally, utilizing SEM glass-like appearances were observed for all samples (shown in **paper 1**).

4.3 PORTLAND CEMENT SAMPLE

Six different cement samples, all ordinary Portland cements, were used in this thesis. The chemical composition and the phase composition as determined by X-ray fluorescence analysis (XRF) and by X-ray diffraction analysis using *Rietveld* refinement respectively were listed in **papers 3** and **5**.

4.4 CALCIUM CARBONATE (LIMESTONE)

Compared to cement, the $CaCO_3$ system allows controlling and analyzing precisely the sulfate concentrations in the dissolved and adsorbed state. Moreover, no hydration process takes place, which can alter the ion concentrations in the pore solution or the surface chemistry of the solids particles. For this reason we chose to conduct the study in a model inert system (limestone suspension) as presented in **paper 4**.

The limestone powder used was "SCHAEFER Precal 18" from Schäfer Kalk GmbH & Co KG, Diez, Germany. It has a density of 2.69 g/cm^3, an average particle size (d_{50} value) of 12.58 μm, and a specific surface area of 0.283 m^2/g (BET, N_2) or 0.269 m^2/g (Blaine method). Its purity was 98.4 % calcite (Q-XRD using *Rietveld* refinement).

4.5 SYNTHETIC CEMENT PORE SOLUTION (SCPS)

Pore solution is a term commonly used throughout the cement industry for filtrates collected from aqueous suspensions of cement, slag or other constituents dispersed in water or any aqueous solution at specified water-to-solids ratios. The SCPS used in the study was composed based on characteristic ion concentrations found in the pore solutions of an OPC (CEM I). It contained (g/L) Ca^{2+} 0.4, K^+ 7.1, Na^+ 2.25 and SO_4^{2-} 8.29. The pH of the SCPS was 12.6. Preparation of the SCPS was described in **paper 2**.

5. METHODS

An overview of the essential methods utilized in this study is presented here. The working principles and scopes of the techniques used are described. Additional details about the sample preparation for the measurements can be found in the papers.

5.1 MINI SLUMP TEST

Flowability of the aqueous pastes studied here was determined utilizing a '*mini slump*' test according to DIN EN 1015 [50]. The test was carried out as follows: Over one minute, 300 g of powder were filled into a porcelain casserole which contained a certain amount of DI water (related to the w/s ratio), then left to soak for another minute and stirred again manually with a spoon for two minutes. Immediately after stirring, the paste was poured into a Vicat cone (height 40 mm, top diameter 70 mm, bottom diameter 80 mm) placed on a glass plate filled to the brim (**Fig. 11**), and then the cone was vertically removed. The resulting diameter of the paste represents the flow value of the slurry. This spread was measured twice; the second measurement being perpendicular to the first and averaged. Each test was performed three times, and the average of the paste flow diameters was reported as the slump flow value. The margin of error was ± 3%. This method was utilized to detect the water-to-solid ratios for each material studied by obtaining the spread target of 18 ± 0.5 cm. According to these w/s ratios, the dosage of SPs required to reach a spread of 26 ± 0.5 cm were determined by employing this method. When aqueous SP solutions were employed, then the amount of the water contained in the SP solution was subtracted from the volume of mixing water, to maintain a constant w/s ratio.

5.2 ADSORPTION

The amount of PCE retained in the suspension after contact with the different cementitious materials (cement, slag or limestone) was designated as "adsorbed amount". This infers that PCE interacts with the solids studied here only by surface adsorption, while chemisorption (intercalation) of PCE is considered to be negligent. The adsorbed

amounts of the copolymers on the different cementitious materials were determined using the depletion method. Different dosages of copolymer were added to the suspensions, shaken and then centrifuged. The adsorbed amount of PCE was obtained by subtracting the concentration of PCE found in the centrifugate from the initial PCE concentration existing prior to its addition to the suspension.

Fig. 11 Pouring a studied cement slurry into a Vicat cone on glass plate when performing the '*mini slump*' test

For quantification of organic carbon in the supernatants of each sample, a High TOC II apparatus from Elementar (Hanau, Germany) was used. There, the sample is oxidized in a glass tube at 1000°C on a platinum catalyst using synthetic air. The exhaust gas is dried with phosphorous pentoxide and the carbon dioxide is determined in a NDIR-Cell. The amount of organic carbon present in the sample is calculated based on the values obtained for mono potassium phthalate which is used as calibration standard.

5.3 ZETA POTENTIAL

The zeta potential is the potential difference between the layer of the sheared diffuse cloud and the pure dispersion medium (**Fig. 12**) [51]. The instrument measures a vibration current which is induced by sending an acoustic wave through the suspension that causes a frequent motion of the liquid relative to the particles. Therefore, and relative to the diffuse double layer, charge separation from the particles occurs which generates a short time dipoles. This measureable, alternating current is known as the colloid vibration current effect (CVI). Thus, the potential difference can be measured and assigned as zeta potential. In comparison to other zeta potential measuring techniques such as the electrophoresic or osmosic methods, the electroacoustic device is capable of measuring the zeta potential in highly concentrated solid suspensions.

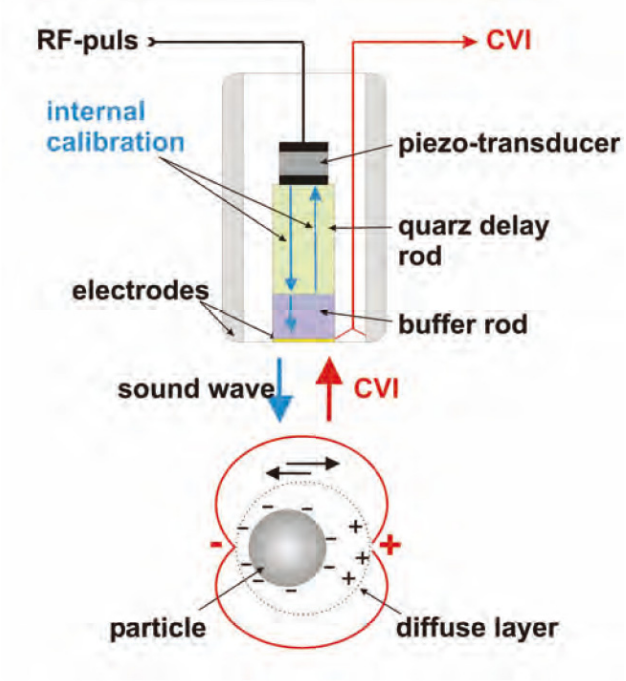

Fig. 12 Electroacoustic measurement principle for zeta potential determination [51]

The electrokinetic properties of the slurries studied were measured using a Model DT-1200 Electroacoustic Spectrometer (Dispersion Technology, Inc., Bedford Hills, NY, USA). The highly solids loaded suspension requires such an electroacoustic instrument

which can measure in undiluted condition. This instrument allows to measure the zeta potential of the highly solids loaded pastes used in this work [52, 53].

In the study of suspensions, 300 g of the solid were added to a certain volume of DI water or SCPS (depending on the w/s ratio) within one minute. The mixture was allowed to soak for one minute before it was stirred manually for another two minutes. After that, the paste was poured into a glass container and stirred continuously at 200 rpm and room temperature. For measuring the zeta potential of SP-free suspensions over time, zeta potential electrode, temperature probe and pH meter were inserted into the mixture. The surface properties of the solids were monitored *via* zeta potential measurement for 180 min. In order to investigate the impact of SPs, Ca^{2+} and/or SO_4^{2-} ions on the surface chemistry, the titrator probe was inserted too and zeta potential titrations with known concentrations of PCE, $CaCl_2$ or Na_2SO_4 solutions were carried out.

5.4 ANIONIC CHARGE AMOUNT

The anionic charge amounts of the copolymers used were determined by polyelectrolyte titration using a particle charge detector PCD 03 pH (BTG Mütek GmbH, Herrsching, Germany), which is shown in **Fig. 13**. The streaming current produced by the charged polymer molecules which adsorb on a moving surface can be measured employing this instrument. The neutralization of charge is achieved by addition of an oppositely charged polyelectrolyte, whereby a polyelectrolyte complex is formed.

The charge detector consists of a PTFE cylinder with an oscillating PTFE piston in the centre. The polyanionic polymer adsorbs onto the Teflon surface, while the counter ions are being separated from the polymer due to the piston movement. Thus, the streaming current induced is measured by two Platinum electrodes inside the Teflon cylinder. During the polyelectrolyte titration, a cationic polyelectrolyte (0.001 N poly(diallyl-dimethy lammonium chloride), polyDADMAC) was added dropwise and treated with PCE until the isoelectric point (point of zero charge) was reached. The amount of negative charge per gram of polymer was then derived from the final titration value. Three titrations were carried out for each sample and the mean value was taken.

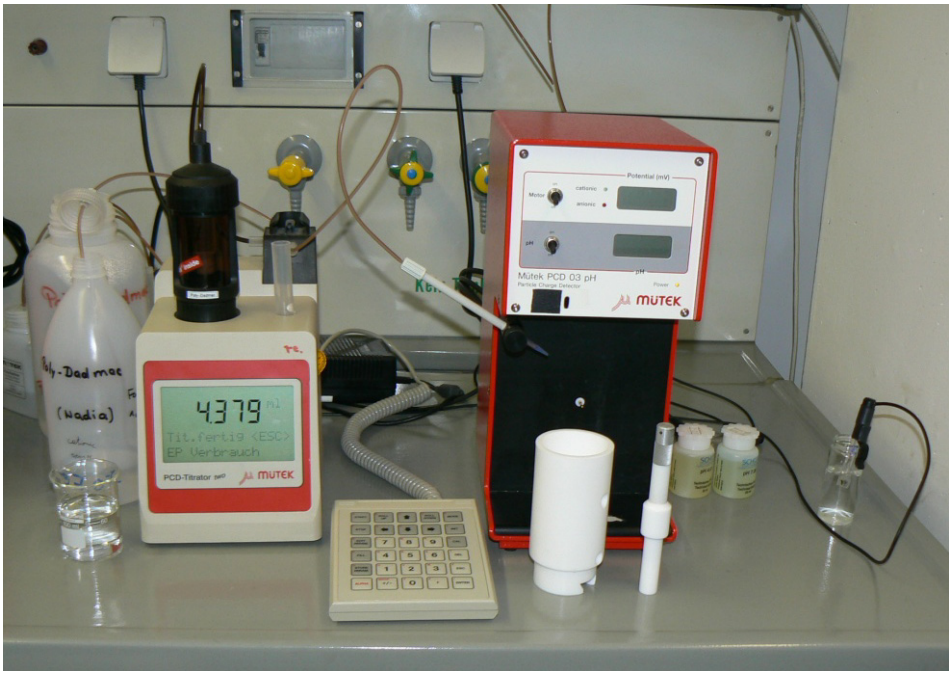

Fig. 13 Instrument used for the charge titration of polycarboxylate

5.5 IONIC CONCENTRATION OF PORE SOLUTIONS

In order to determine the changes in the ionic concentrations of the different suspensions, at a constant interval of 20 minutes small volumes of pore solution were collected and analyzed employing AAS (atomic absorption spectroscopy) Model 1100 B, Perkin Elmer, Überlingen, Germany and an IC (ion chromatography) instrument ICS-2000 from Dionex, Sunnyvale, CA, USA. Pore solutions were obtained by pulling 10 mL samples from the suspensions/slurries, centrifuging them for 10 minutes (Heraeus International, Osterode, Germany) followed by diluting the centrifugates at 1:20 (v/v %) with 0.1N HCl to avoid precipitation of calcium carbonate.

5.5.1 ATOMIC ABSORPTION SPECTROSCOPY (AAS)

This method was employed to identify cations and to determine their concentration in pore solutions. After absorbing a fixed amount of energy (radiation of a known wavelength), electrons in cations are first promoted to the excited state. Each element has a specific absorbed wavelength. The blank radiation flux (without a sample) and the one with a sample were measured using a detector in the instrument, and the ratio between

these two values gave the absorbance. Thus, each specific cation was identified based on this known absorbance. The absorbance was converted to a cation concentration utilizing the Beer-Lambert Law. The pore solutions prepared were directly used in the AAS analysis, and the concentrations of the cations Ca^{2+}, Na^{+} and K^{+} were determined.

5.5.2 ION CHROMATOGRAPHY (IC)

This method was utilized to determine and monitor the changes in the concentration of sulfate anion in the pore solutions over time. For quantification, a calibration curve employing different sulfate concentrations was developed by preparing and measuring a series of standard sulfate solutions as reference for calculation (20, 40, 60, 100 and 150 mg/L). The adsorbed amount of SO_4^{2-} was determined by subtracting the amount of sulfate found in the pore solution from the initial amount added. All measurements were repeated three times and averaged.

In the IC instrument the sample was charged onto the separator column where it was separated according to the ion exchange principle. Different ions in the sample migrate through the separator column at different speeds. The speed of migration of ions mainly depends on their interactions with the ion exchange sites. Later, the eluent carried the ions to the suppressor which selectively enhanced the ions detection by suppressing the conductivity of the eluent. After the suppressor, the conductivity of the sample ions was measured. By comparing with the results obtained from the standard solutions, the signal was then quantified and the concentration of sulfate ions was automatically determined from the chromatographic results displayed.

5.6 HYDRO DYNAMIC RADIUS OF POLYMER MOLECULES

Different polymer solutions were prepared by dissolving 10 g of PCE in 1L of different pore solutions, and the average particle size (hydro dynamic radius) of individual PCE molecules were determined by dynamic light scattering measurement using a Horiba LB-550 instrument (HORIBA, Ltd., Kyoto, Japan). Each sample was measured four times, and the average was reported as the hydrodynamic radius of PCE.

5.7 OTHER TECHNIQUES

The chemical compositions of solid samples, the specific surface area and the particle size distribution were determined utilizing an X-ray fluorescence apparatus (Axios from PANalytical, Philips, Eindhoven, the Netherlands), a Blaine instrument (Toni Technik, Berlin, Germany) and a Laser granulometer (Cilas 1064, Marseille, France), respectively. Additionally, a scanning electron microscope (XL30 ESEM FEG instrument from Philips, FEI Company, Eindhoven, the Netherlands) and an X-ray diffractometer (Bruker D8 advance, Bruker-AXS, Karlsruhe, Germany) were employed to analyse the mineralogical composition of the neat samples and to monitor the formation of new crystalline phases during hydration of the samples which were washed in acetone and dried at 50° C for one day.

Moreover, FT-IR and ^{1}H NMR were employed in this work to prove the formation of a 5-membered ring in the novel polymer *m*34APEG. For ^{1}H NMR analysis, a 250 MHz spectrometer from Bruker BioSpin, Karlsruhe/Germany was utilized, while FT-IR was conducted using a Vertex 70 instrument from Bruker Optics, Karlsruhe/Germany.

6. RESULTS AND DISCUSSION

This chapter contains the main results which are presented in the publications.

6.1 DISPERSING EFFECT OF POLYCARBOXYLATE ON DIFFERENT SLAG SLURRIES (PAPER 1)

Depending on the results obtained from the zeta potential measurements and the changes in the ion concentrations in the pore solution of different slag slurries (slag dispersed in DI water), it was found that the surface charge of slag is related to its chemical composition and the mineral properties of each slag. These two parameters determine the releasing rate of alkali and earth alkali cations into the pore solution. With progressing release, these cations start to adsorb onto the negatively charged surface of slag (see **Fig. 14**). Depending on the amount of cations present, particularly of divalent Ca^{2+} ions, the surface of slag will either become less negative or overall positively charged. This way, the final surface charge of slag suspended in water is the result of dissolution processes and subsequent ion adsorption. Ca^{2+} is the charge determining ion in this system.

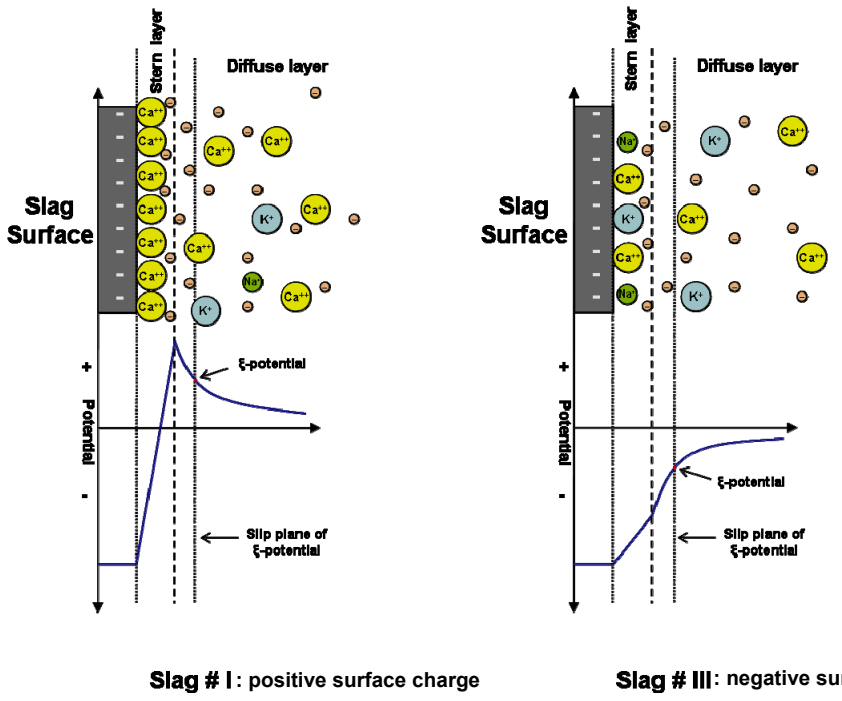

Fig. 14 Schematic illustration of the electrochemical double layer existing on the surfaces of slags dispersed in water and their surface charge as evident from zeta potential

Consequently, when added to cement or concrete, all slag samples will adsorb sufficient amounts of Ca^{2+} ions to reach the saturation which is characterized by a positive surface charge. Thus, they become suitable substrates for interaction with anionic dispersants.

The presence of a layer of adsorbed Ca^{2+} cations on the surface of slag is the precondition for its ability to adsorb anionic PCEs. The packing density of the adsorbed Ca^{2+} ions determines the quantity of adsorbed PCE. Nevertheless, the adsorbed amounts of PCE are comparable to those known for Portland cement [54]. Hence, in a cement paste containing slag, competition between the surfaces of cement and slag for PCE will occur.

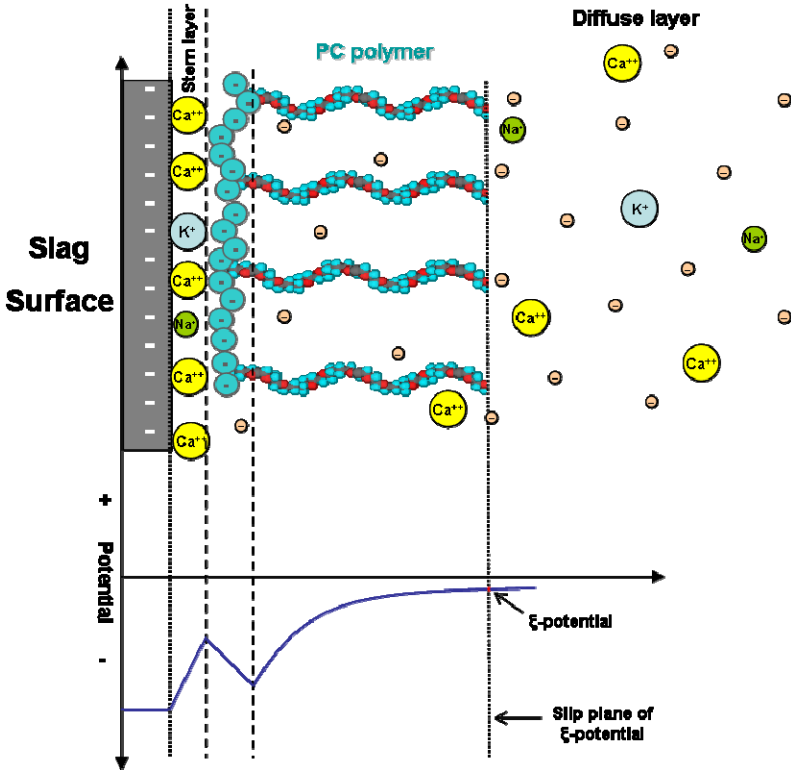

Fig. 15 Schematic representation of the electrochemical double layer existing on slag # III when dispersed in water, illustrating the steric effect of the side chain of adsorbed 45PC6 on the value of zeta potential (size of ions/atoms not to scale)

The dispersing effect of PCEs was probed employing a *mini slump* test such that increasing the fluidity of the slag slurry by adding PCEs. The dispersing effect is owed to the adsorption of PCE on the surface of slag, which was detected utilizing TOC and

ζ potential measurements. TOC analysis revealed a considerable consumption of PCE by slag, while the ζ potential proved an adsorption of PCE by changing the surface charge of slag from positive to almost 0 mV. The reason behind the zero charge on the slag surface is a steric effect of the side chains of PCEs which shifts the shear plane of the ζ potential to greater distances away from the surface (**Fig. 15**). At those distances from the particle surface, the potential curve in the diffuse layer approaches the isoelectric point.

6.2 INFLUENCE OF SULFATE ON WORKABILITY OF PCE IN DIFFERENT SLAG SLURRIES (PAPERS 2 AND 6)

Here, slag samples were dispersed in SCPS instead of DI water that to study the specific effects of the simultaneous presence of calcium and sulfate ions in the pore solution on the surface chemistry of slag, and to investigate its impact on PCE adsorption. This fluid media is more similar to an actual cement slurry.

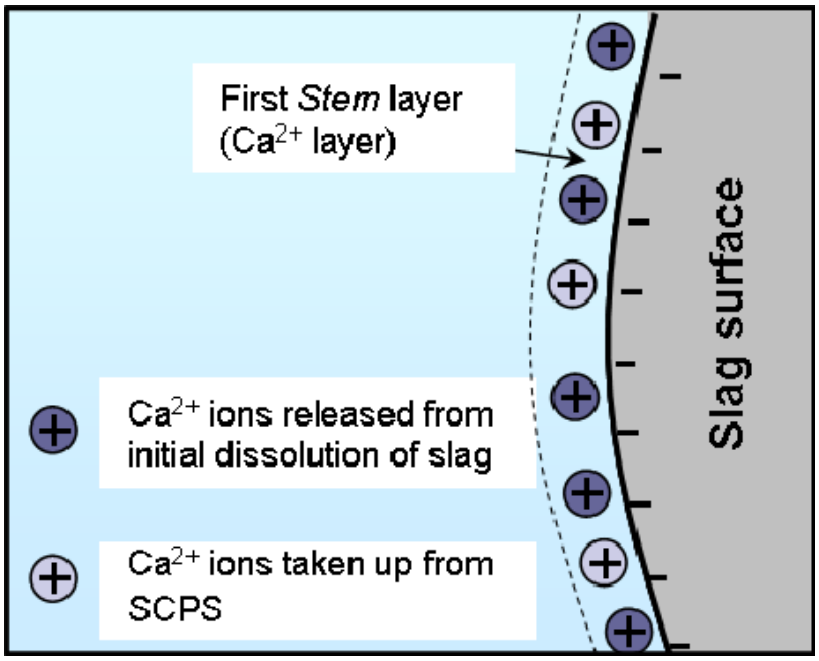

Fig. 16 Schematic illustration of the composition of the first *Stern* layer (Ca^{2+} layer) existing on the surface of slag dispersed in SCPS.

Based on the results obtained from AAS, IC and ζ potential measurements it can be summarized that the surface charge of slag dispersed in SCPS is the result of interaction

between the slag surface and the ions present in the pore solution. Because of the high pH value of SCPS, all slag samples initially possess a highly negative surface charge stemming from silanolate groups. Onto this surface, Ca^{2+} ions adsorb forming a first positive layer; the Ca^{2+} ions adsorbed originate from slag dissolution as well as from SCPS (**Fig. 16**). Subsequently, sulfate ions present in SCPS adsorb onto the positive calcium layer, thus forming a second ion layer. A model of the electrochemical double layer existing on the surface of slag particles suspended in SCPS is displayed in **Fig. 17**.

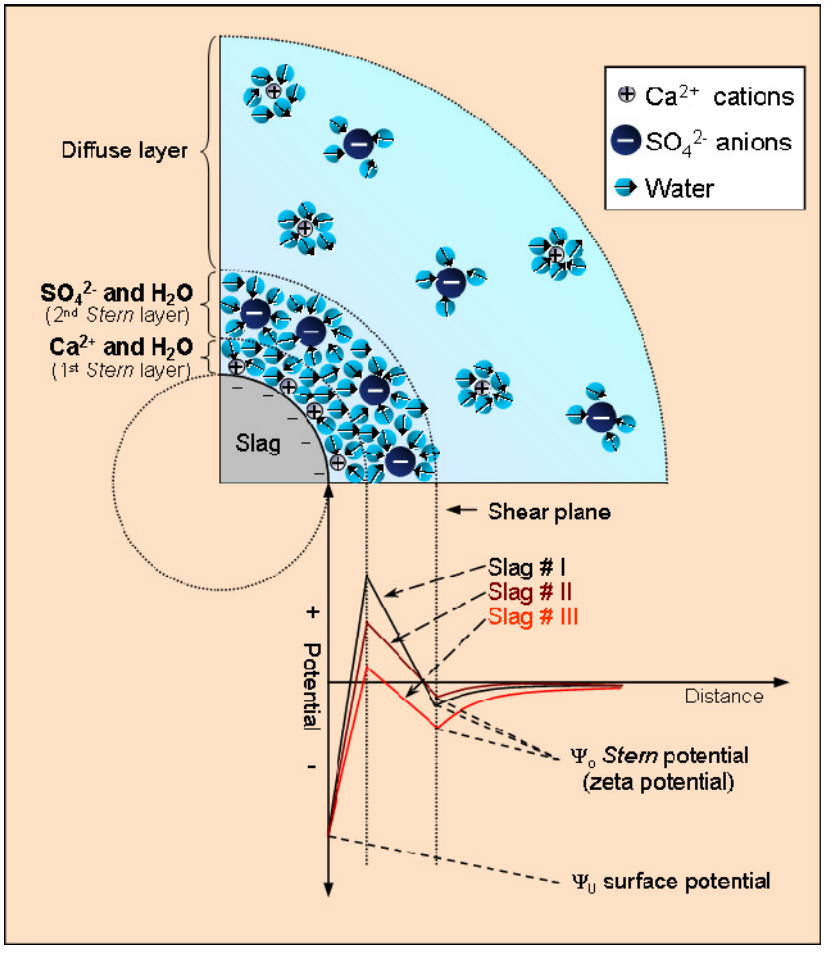

Fig. 17 Schematic illustration of the electrochemical double layer existing in the equilibrium state on the surface of the slag samples dispersed in SCPS, and the resulting surface charges as evidenced by zeta potential measurement

Another effect of the Ca^{2+} ions in SCPS was detected by decreasing the anionic charge amount of PCEs, which negatively affected their adsorption capability. The *mini slump*

test revealed that in case of slag dispersed in SCPS; dosages of 45PC6 comparable to those in DI water were required to achieve the target spread. Obviously, 45PC1.5 is a less effective dispersant for slag cements.

Furthermore, competitive adsorption between the PCEs and sulfate ions present in SCPS for the positive sites existing on slag surface occurs. Based on TOC and ζ potential measurements, no significant difference in the adsorption behavior of 45PC6 on slag surface when dispersed in DI water or SCPS was observed, while adsorption was significantly lower in case of using 45PC1.5 (**Fig. 18**). Obviously, polymer 45PC6 which is sufficiently high anionic can occupy the positive surface without any significant competition from sulfate ions. Contrary, 45PC1.5 is not sufficiently anionic to compete with SO_4^{2-} and hence cannot adsorb in large amount on the surface of slag.

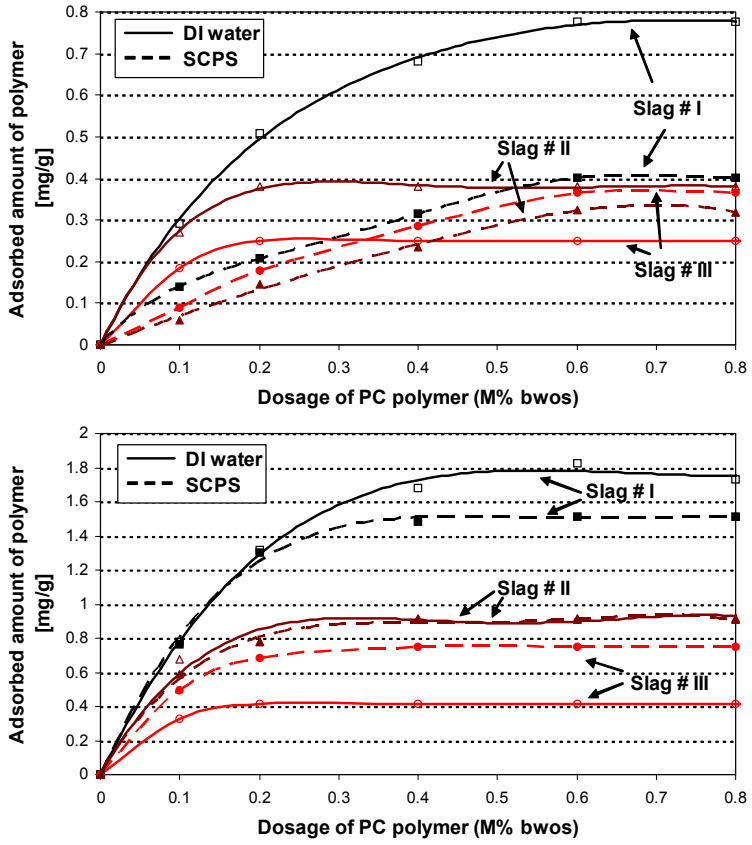

Fig. 18 Adsorption isotherms for PCE polymers 45PC1.5 (top) and 45PC6 (bottom) on slag samples dispersed in DI water and in SCPS

6.3 MODIFIED PCE POSSESSING ENHANCED CEMENT COMPATIBILITY (PAPER 3)

In this paper we evaluated the performance of our novel synthesized APEG-type polymer *m*34APEG with respect to robustness in different cements and sulfate tolerance. Two mechanisms are responsible for the negative effect of sulfate anions on PCE samples: First, competitive adsorption between sulfate and PCE, whereby highly anionic sulfate ions preferably adsorb onto cement and occupy most of the surface area of hydrates available for adsorption. This way, PCE is prevented from adsorption in sufficient amount on cement. The second mechanism is the shrinkage of PCE molecules, which will lead to more coiled molecules that cannot adsorb so easily on cement [21].

The novel PCE was synthesized by free radical copolymerization in bulk from allyl ether macromonomer, maleic anhydride and allyl maleate at a molar of ratio 1:1:1. The sequence of reactions occurring in the synthesis is described in **Scheme 1** (also see **paper 3**). Moreover, cyclization of the allyl maleate building block to a five – membered heterocyclus was proven by utilizing ^{1}H NMR analysis and FT-IR spectroscopy.

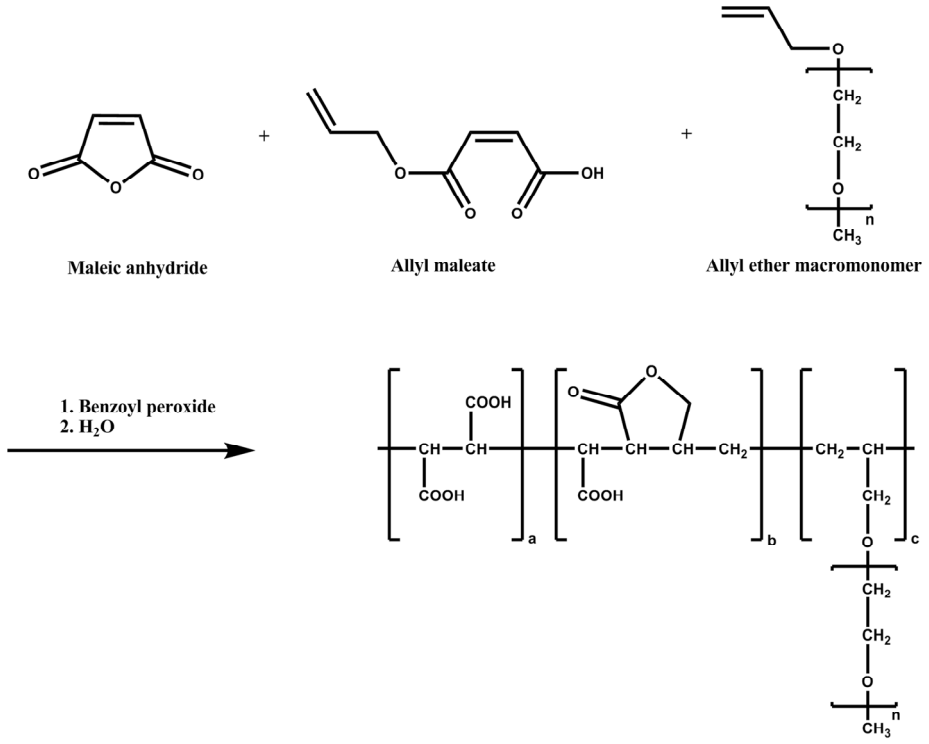

SCHEME 1 Reaction sequence leading to the formation of modified PCE polymer *m*34APEG

First, the dispersion ability of this new PCE molecule was compared with those from PCEs possessing conventional structures. To probe the robustness against variations in cement compositions, distinctly different cement samples were selected and tested. All non-modified PCE samples 34APEG and 25MPEG3 require substantially higher dosages than the modified PCE (**Fig. 19**). Consequently, incorporation of the new building block allyl maleate in *m*34APEG enhances its cement compatibility.

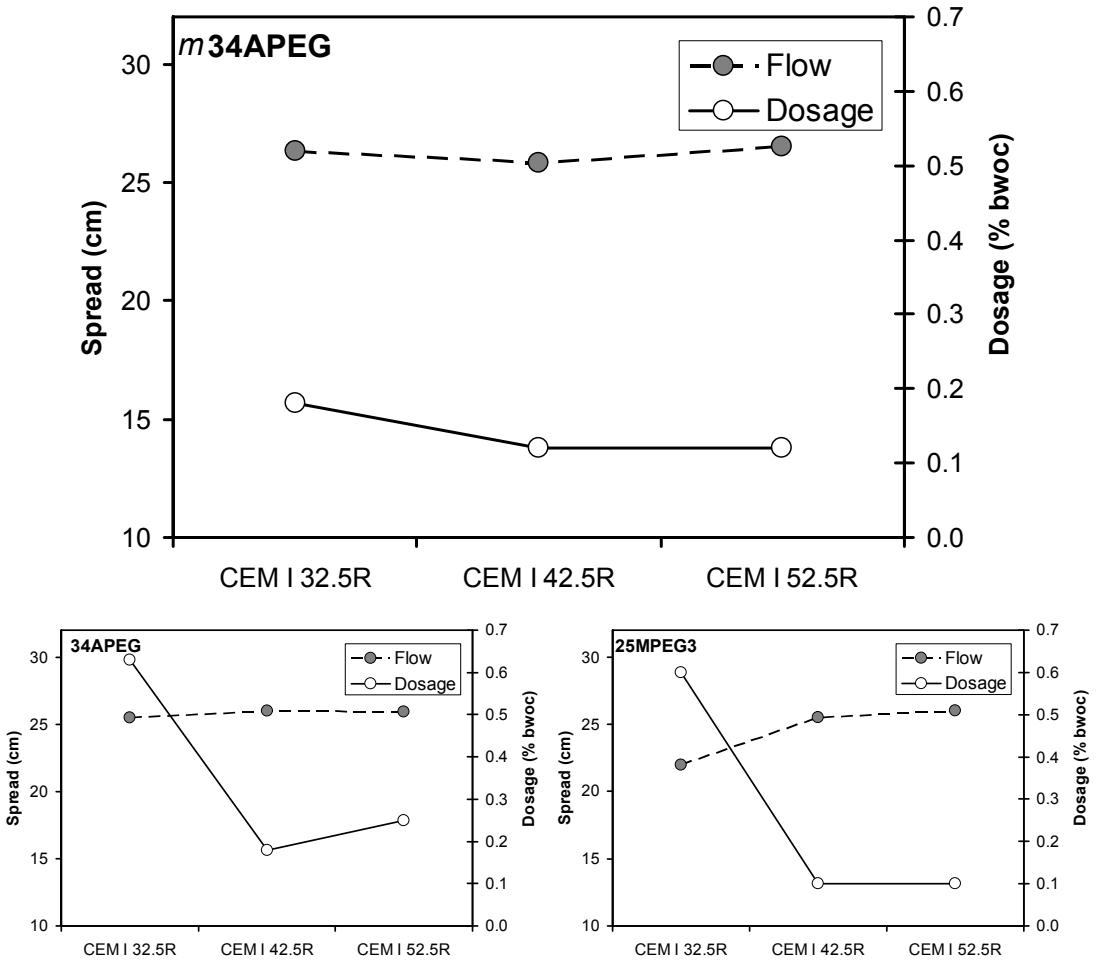

Fig. 19 Dispersing ability of PCE polymers *m*34APEG, 34APEG and 25MPEG3 in pastes (w/c = 0.3) prepared from different cement samples

Second, the impact of sulfate on the workability obtained from PCEs in cement slurries was determined based on *mini slump* and adsorption measurements. According to the results, it was found that the adsorption of the modified PCE is not perturbed by sulfate

ions, thus the adsorption of the novel PCE (*m*34APEG) is independent of the sulfate components present in blended cements.

Finally, to explain the superior behavior of the novel polymer, its steric size in pore solutions of the cement / K_2SO_4 blends was determined in order to see whether the PCE molecule is indeed compressed and shrinking. Surprisingly, the hydrodynamic radius of *m*34APEG is independent of sulfate concentration. Thus, for the polymer studied here the shrinkage mechanism presented earlier by Yamada et al. does not apply [21].

6.4 SYNERGISTIC EFFECT OF SULFATE ON THE DISPERSING POWER OF PCE (PAPER 4)

In this study, we first investigated the impact of sulfate ions on the workability of aqueous $CaCO_3$ slurries containing two differently composed polycarboxylate-based SPs. This experiment demonstrated that the positively charged surface of $CaCO_3$ does not only attract anionic polymers, but also can be occupied by small inorganic anions such as sulfate.

The next step was an adsorption study for PCE and sulfate on $CaCO_3$ particles employing TOC and IC measurements. This experiment demonstrated that the adsorption of PCE and sulfate presents a dynamic process whereby a final equilibrium is attained which may involve partial desorption of already adsorbed species by anions possessing a higher charge density.

From this data, a model was derived which can explain the structure-related differences in the behavior of PCEs in the presence of various sulfate concentrations (**Fig. 20**). It was observed that 45PC1.5 can only adsorb on surface sites which are not occupied by sulfate, causing only weak steric repulsion between the limestone particles. Contrary to this, sulfate does not much impact adsorption of 45PC6 polymer. Instead, a concomitant adsorption of both PCE and sulfate occurs whereby the small sulfate anions fill the interstitial space existing between the cylindrical volume spaces occupied by the PCE comb polymer. As a consequence of this synergistic effect between PCE and SO_4^{2-}, fluidity of the $CaCO_3$ slurry increased when both 45PC6 and sulfate were present.

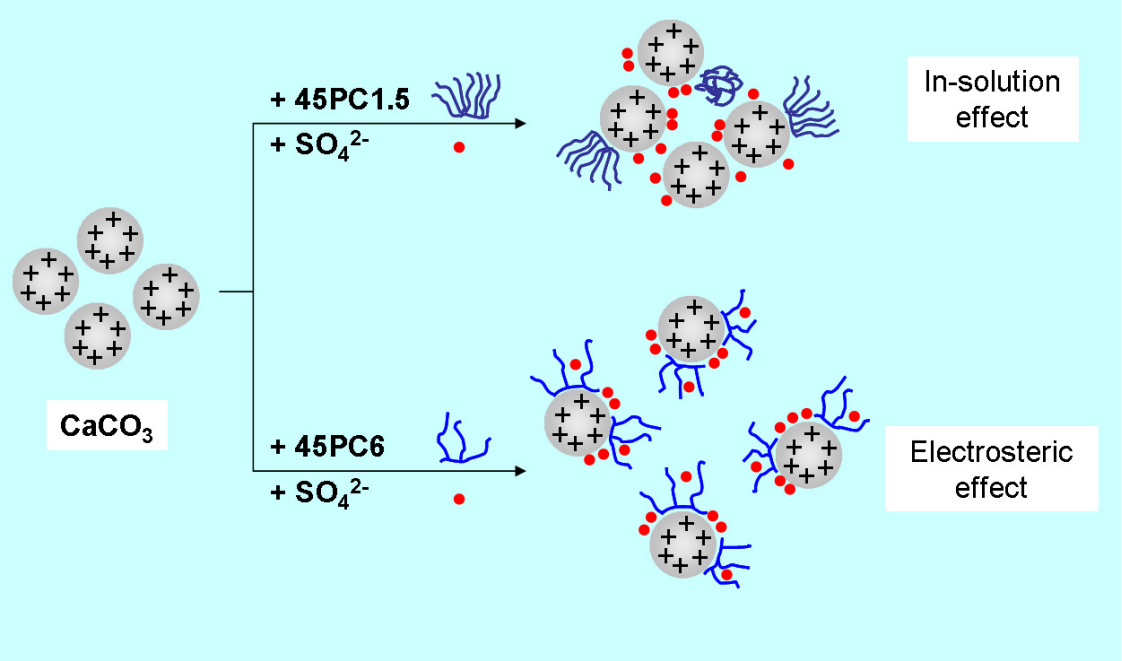

Fig. 20 Schematic representation of the adsorption behavior of the two PCE samples on $CaCO_3$ in the presence of sulfate, illustrating the electrosteric and in-solution effect (size of ions/atoms not to scale)

6.5 INTERCALATION OF SUPERPLASTICIZERS INTO AF_m PHASES (PAPER 5)

Here, we tried to explain the correlation between the paste flow at early and delayed PCE addition, the content of both alkali sulfate and C_3A in cement, and the intercalation tendency of the PCEs. For this purpose, we compared the spread flow values of pastes prepared from six different cements holding four different PCEs and a BNS for early and delayed addition of SPs.

Interestingly, a clear correlation was found to exist between the molar ratio of alkali sulfate and C_3A. By using cements containing low molar ratios of alkali SO_3/C_3A ($\leq$ 1.29), considerable differences between early and delayed addition were observed (**Fig. 21**). Apparently, in these systems the amount of dissolved sulfate which should chemisorb immediately to form enough monosulfo aluminate is insufficient. There, instead of sulfate, the SP will occupy the interlayer space of C–A–H phases forming OMPs. This way SP will be consumed in a chemical reaction. Whereas, when an excess

amount of alkali sulfates relative to C_3A is available (alkali SO_3/C_3A ratio is ≥ 2), then sulfate immediately converts C_3A into monosulfo aluminate (AF_m) or even ettringite (AF_t). In such a case, no chemical reaction between the SP and C–A–H phases takes place, and thus SP remains available for adsorption onto the surface of cement hydrates and can achieve dispersion. In this situation, only adsorption of the SP occurs, which is independent of the time of addition. This model can explain why here no significant difference in the dispersing effectiveness is observed between early and delayed addition of SP (**Fig. 21**).

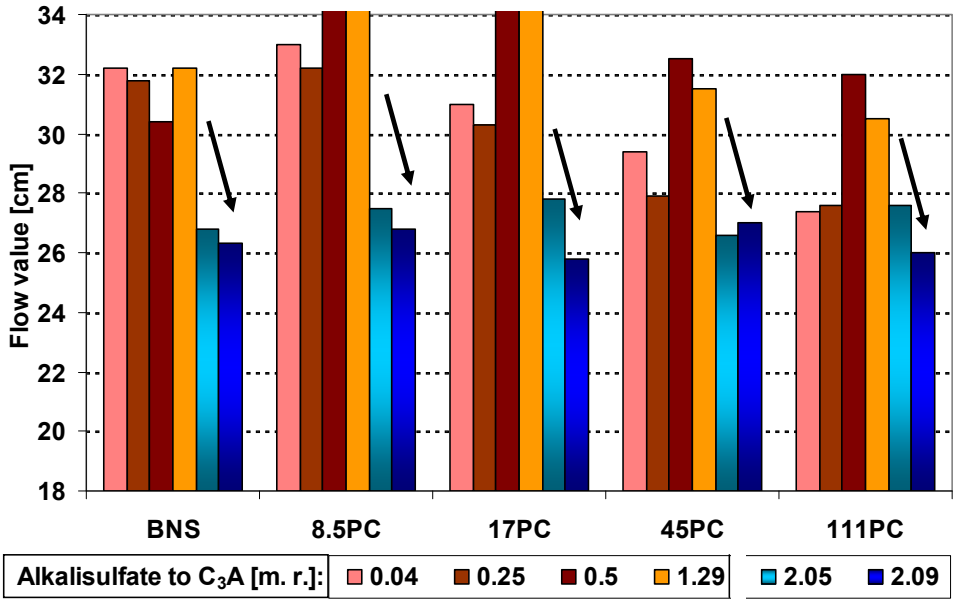

Fig. 21 Flow values of pastes prepared from different cement samples (alkalisulfate/C_3A molar ratios ranged from 0.04 to 2.09) at delayed addition of SP samples, while the spread values at the early addition of SP are 26 ± 0.5 cm

We also conclude from this work that the alkali sulfates apparently dissolve much faster than the calcium sulfates. Therefore, they and much less the calcium sulfates determine whether an SP can intercalate or not.

In addition, it was observed for those cement samples which reveal a huge difference in paste flow values after early and delayed addition, that the difference decreases with increasing side chain length of PCE. This behavior perfectly correlates with the intercalation tendency of the PCEs as was established before [14].

7. CONCLUSIONS AND OUTLOOK

This thesis focused on the dispersing effect of different PCE based SPs on different cementitious materials, and on the impact of sulfate ions on the workability of these polymers.

In a neat slag system, PCEs can effectively disperse its suspension. It was demonstrated that strong interaction between PCE and the surface of slag exists, and that in blended cements, PCE will interact with both Portland cement and slag. Moreover, when PCEs are added to blended cements containing slag, competitive adsorption between the polymers and sulfate ions for positively charged adsorption sites on the surfaces of slag can occur. The adsorbed amount of PCE, and hence its dispersing effectiveness, mainly depends on the difference in anionic charge of the copolymer and sulfate. It was found that a highly anionic PCE polymer (such 45PC6) is sufficiently strong to occupy enough adsorption sites on slag. Contrary to this, a low anionic PCE polymer (*e.g.* 45PC1.5) is not sufficiently strong to compete with SO_4^{2-} and thus cannot adsorb in large amounts on the surface of slag. Consequently, very high dosages of this polymer are required to obtain high workability of a concrete containing slag cement.

The slag study demonstrates that in general, the anionic charge amount of the SP and the packing density of Ca^{2+} ions adsorbed on the slag surface are the two main parameters which impact PCE adsorption on slag. This way, different saturated adsorbed amounts of PCE can result. Consequently, the dosages of SP required to instigate high flowability in concrete mixtures containing slag can vary significantly.

In calcium carbonate systems, sulfate can play a positive or negative role for the dispersing effectiveness of PCE. A negative impact can occur for PCE polymers possessing low anionic charge. Their adsorbed amount decreases in the presence of sulfate, which decreases the fluidity of the slurry. In case of a sufficiently anionic charged PCE, sulfate anions cannot prevent its adsorption. To the contrary, an additional amount of sulfate will adsorb in the interstitial spaces between the large macro molecules, thus

enhancing dispersion by a supplementary electrostatic effect. According to this finding, the dispersing performance of highly anionic PCEs can be improved by the addition of controlled amounts of sulfate salts to the liquid admixture. Utilizing this effect, a more economical SP could be attained.

Actually, the cement content of C_3A phase and alkali sulfate in cement has a significant influence on the dispersing performance of SPs. It was found that the molar ratio between alkali sulfate and C_3A determined whether a cement sample exhibits much or no significant difference between early and delayed addition of SP. In general, the effectiveness of SP is independent of its addition time when using a cement possessing a high molar ratio of alkali sulfate/C_3A content (~ 2). This effect seems to be independent of the chemical type of SP (polycondensate or polycarboxylate).

During the hydration of cement, the sulfate ions dissolved in the pore solution can significantly affect the adsorption of PCEs and thus their dispersing performance. A modified PCE polymer which contains a lactone ring in the main chain is more robust against sulfate than conventional PCE polymers. This property possibly is due to its high anionic charge and its small steric size which allows forming a more densely packed layer of polymer on the surface of cement particles.

The study demonstrates that in general, the impact of sulfate on the adsorption behavior of PCEs is dependent on:

- The contents of C_3A and alkali sulfate present in a cement sample.
- The concentration of sulfate ions in the pore solution.
- The dosage of PCE added to the slurry.
- The chemical structure of the PCE used (type and modification).
- The anionic charge amount of the PCE.
- The packing density of the Ca^{2+} ion layer adsorbed onto negatively charged sites on the mineral surface of the particle.
- Early and delayed addition of SP.

The work documented in this thesis includes a wide range of investigations on the impact of sulfate ions on the sorption behavior (adsorption and/or absorption/intercalation) of different PCEs on GGBFS, limestone and OPC. However, further studies are suggested to extend the results gained from this work and to explain other behaviors of specific PCEs. The researches suggested could be as follows:

- Study of the surface chemistry of other SCMs, such as burnt oil shale, pozzolan, fly ash …etc.

- Finding a suitable way to eliminate the chemisorption of PCEs at early addition to specific cement slurries by controlling the alkali sulfate content in the cement used e.g. by mixing a certain amount of alkali sulfate salt into the cement to achieve the value ~ 2 of the molar ratio alkalisulfate/C_3A.

- Optimization of the sulfate salt amount to be added to a specific PCE solution to achieve maximum concomitant adsorption between sulfate and PCE, thus giving optimal dispersing effect from this admixture.

- Clarification of the reason for the high tolerance of the novel PCE toward cements containing large amounts of C_3A and free lime.

- Analytical proof of the occurrence of intercalation of PCE into aluminate hydrates during the hydration of OPC under actual application conditions.

REFERENCES

[1] E. Sakai, K. Yamada, A. Ohta, "Molecular Structure and Dispersion-Adsorption Mechanisms of Comb-Type Superplasticizers Used in Japan", *J. Adv. Concr. Techn.*, 1 (2003) 16-25.

[2] J. Plank, C. Hirsch, "Superplasticizer Adsorption on Synthetic Ettringite", in: V. M. Malhotra (Ed.), Seventh CANMET/ACI Conference on Superplasticizers and Other Chemical Admixtures in Concrete, ACI, SP-217, (2003) 283-298.

[3] Lucia Ferrari, Josef Kaufmann, Frank Winnefeld, Johann Plank, "Interaction of cement model systems with superplasticizers investigated by atomic force microscopy, zeta potential and adsorption measurements", *Coll. Interf. Sci.*, 347 (2010) 15-24.

[4] K. Yamada, T. Takahashi, S. Hanehara, M. Matsuhisa, "Effects of the chemical structure on the properties of polycarboxylate-type superplasticizer", *Cem. Concr. Res*., 30 (2000) 197-207.

[5] S. Hanehara, K. Yamada, "Interaction between cement and chemical admixture from the point of cement hydration, adsorption behaviour of admixture, and paste rheology", *Cem. Concr. Res.*, 29 (1999) 1159-1165.

[6] N. Mikanovic, C. Jolicoeur, "Influence of superplasticizers on the rheology and stability of limestone and cement pastes", *Cem. Concr. Res.*, 38 (2008) 907-919.

[7] J. Plank, Ch. Hirsch, "Impact of zeta potential of early cement hydration phases on superplasticizer adsorption", *Cem. Concr. Res.*, 37 (2007) 537-542.

[8] E. Sakai, J. K. Kang, M. Daimon, "Action mechanisms of comb-type superplasticizers containing grafted polyethylene oxide chains", in: V. M. Malhotra (Ed.), 6th International

Conference on Superplasticizers and Other Chemical Admixtures in Concrete, Farmington Hills, MI, USA, CANMET/ACI, SP-195, (2000) 75-90.

[9] J. Dransfield, "Admixtures for concrete, mortar and grout" (Chapter 4): In Advanced Concrete Technology Set, J. Newman and B. S. Choo (Eds.), BUTTERWORTH HEINEMANN, London, (2003) 3-36.

[10] Ch. Z. Li, N. Q. Feng, Y. D. Li, R. J. Chen, "Effects of polyethlene oxide chains on the performance of polycarboxylate-type water-reducers", *Cem. Concr. Res.*, 35 (2005) 867- 873.

[11] J. Rieger, J. Thieme, C. Schmidt, "Study of precipitation reactions by X-ray microscopy: $CaCO_3$ precipitation and the effect of polycarboxylates", *Langmuir*, 16 (2000) 8300-8305.

[12] F. Ridi, L. Dei, E. Fratini, S. H. Chen, P. Baglioni, "Hydration kinetics of tri-calcium silicate in the presence of superplasticizers", *J. Phys. Chem*., B 107 (2003) 1056-1061.

[13] V. Fernon, A. Vichot, N. Le Goanvic, P. Colombet, F. Corazza, U. Costa, "Interaction between Portland cement hydrates and polynaphthalene sulfonates", 5th CANMET/ACI conference on superplasticizers in concrete, ACI, SP-173, (1997) 225-248.

[14] J. Plank, Z. Dai, H. Keller, F. von Hoessle, W. Seidl, "Fundamental mechanisms for polycarboxylate intercalation into C_3A hydrate phases and the role of sulfate present in cement", *Cem. Concr. Res.*, 40 (2010) 45-57.

[15] H. Uchikawa, D. Sawaki, S. Hanehara, "Influence of kind and added timing of the organic admixture on the composition, structure and property of fresh cement paste", *Cem. Concr. Res.*, 25 (1995) 353-364.

[16] P. W. Brown, "Kinetics of tricalcium aluminate and tetracalcium aluminoferrite hydration in the presence of calcium sulfate" *J Am Ceram Soc*, 76 [12], (1993) 2971-2976.

[17] M. Halaweh, "Effect of alkalis and sulfates on Portland cement systems", Dissertation, University of South Florida, Civil and Environmental Engineering, (2006). http://scholarcommons.usf.edu/etd/2542.

[18] Y. Nakajima, K. Yamada, "The effect of the kind of calcium sulfate in cements on the dispersing ability of poly β-naphthalene sulfonate condensate superplasticizer", *Cem. Concr. Res*., 34 (2004) 839-844.

[19] R. J. Flatt, J. Zimmermann, C. Hampel, C. Kurz, I. Schober, L. Frunz, C. Plassard, E. Lesniewska, "The role of adsorption energy in the sulfate-polycarboxylate competition", T. C. Holland, P. R. Gupta, V. M. Malhotra (Eds.), Proc. of the 9th ACI Int. Conf. on Superplasticizers and Other Chemical Admixtures in Concrete, *American Concrete Institute*, Detroit, SP-262-12, (2009) 153-164 .

[20] S. Hanehara, K. Yamada, "Rheology and early age properties of cement systems", *Cem. Concr. Res.*, 38 (2008) 175-195.

[21] K. Yamada, S. Ogawa, S. Hanehara, "Controlling of the adsorption and dispersing force of polycarboxylate-type superplasticizer by sulfate ion concentration in aqueous phase", *Cem. Concr. Res.*, 31 (2001) 375-383.

[22] A. Zingg, F. Winnefeld, L. Holzer, J. Pakusch, S. Becker, L. Gauckler, "Adsorption of polyelectrolytes and its influence on the rheology, zeta potential, and microstructure of various cement and hydrate phases", *Journal of Colloid and Interface Science*, 323 (2008) 301-312.

[23] ACI 233R-95, "Ground Granulated Blast Furnace Slag as a Cementitious Constituent in Concrete", *American Concrete Institute*, Farmington Hills, Michigan, (1995).

[24] V. Malagavelli and P. N. Rao, "High performance concrete with GGBS and robo sand", *International Journal of Engineering Science and Technology*, Vol. 2 [10], (2010) 5107-5113.

[25] P. J. Sandberg, L. R. Roberts, "Studies of cement-admixture interactions related to aluminate hydration control by isothermal calorimetry", in: V. M. Malhotra (Ed.), Seventh CANMET/ACI Conference on Superplasticizers and Other Chemical Admixtures in Concrete, ACI, SP-217, (2003) 529-542.

[26] L.R. Roberts, P.C. Taylor, "Understanding cement–SCM–admixture interaction issues", *Concr. Int.*, 29 (2007) 33-41.

[27] S. K. Agarwal, I. Masood, S. K. Malhotra "Compatibility of superplasticizers with different cements" *Construction and Building Materials*, 14 (2000) 253-259.

[28] R. Magarotto, I. Torresan, N. Zeminian, "Effect of alkaline sulfates on performance of superplasticizers", in: G. Grieve, G. Owens (Eds.), Proceeding of the 11th International Congress on the Chemistry of Cement: Cement's Contribution to Development in the 21st Century, Vol. 2, Durban, South Africa, May 11 – 16, (2003) 569-580.

[29] P. Somasundaran, S. C. Mehta, X. Yu, and S. Krishnakumar, "Colloid Systems and Interfaces Stability of Dispersions through Polymer and Surfactant Adsorption", In: Handbook of Surface and Colloid Chemistry, 3rd Ed. K. S. Birdi (ed.), *CRC Press,* Taylor & Francis Group, USA, (2009) 155-196.

[30] Richard Holdich, "Fundamentals of Particle Technology; Chapter 13: Colloids and agglomeration", Midland Information Technology and Publishing, UK, (2002) 131-140.

[31] J. J. Lyklema, A. de Keizer, B. H. Bijsterbosch, G. J. Fleer and M. A. Cohen Stuart. "Fundamentals of Interfaces and Colloid Science", Vol. II: solid-liquid interface, Academic Press, New York (1995).

[32] J. Lyklema, "Nomenclature, symbols, definitions and measurement for electrified interfaces in aqueous dispersions of solids", *Pure Appl. Chem*., 63 (1991) 895-906.

[33] A. V. Delgado, F. Gonzalez-Caballero, R. J. Hunter, L. K. Koopal, And J. Lyklema "Measurement and Interpretation of Electrokinetic Phenomena", International Union of Pure and Applied Chemistry, Technical Report, published in *Pure Appl.Chem.*, vol 77 [10], (2005) 1753-1805.

[34] J. Lyklema, S. Rovillard, J. de Coninck, "Electrokinetics: The Properties of the Stagnant Layer Unraveled" *Langmuir*, 14 [20], (1998) 5659-5663.

[35] A. S. Dukhin. "Electrochemical characterization of the surface of a small particle and nonequilibrium electric surface phenomena" *Adv. Collo. Interf. Sci.*, 61 (1995) 17-49.

[36] A. S. Dukhin, P. J. Goetz, "Characterization of Liquids, Nano- and Microparticulates, and Porous Bodies Using Ultrasound; Chapter 5: Electroacoustic Theory", *Studies in Interface Science*, 24 (2010) 187-237.

[37] H. Ohshima, "Interfacial Electrokinetic Phenomena"; *In*: 'Electrical Phenomena at Interfaces, Fundamentals, Measurements and Applications' 2nd edition, Hiroyuki Ohshima and Kunio Furusawa (Eds.), *Marcel Dekker, Inc.*, 76 (1998) 19-55.

[38] R. Wongsagonsup, S. Shobsngob, B. Oonkhanond, S. Varavinit, "Zeta potential (ζ) and pasting properties of phosphorylated or crosslinked rice starches". *Starch*, 57 (2005) 32-37.

[39] R. H. Müller, "Zetapotential und Partikelladung in der Laborpraxis", Band 37, *Wissenschaftliche Verlagsgesellschaft mbH*, Stuttgart, (1996) pp. 254.

[40] I. Langmuir "The Adsorption of Gases on Plane Surfaces of Glass, Mica and Platinum", *J. Am. Chem. Soc.*, 40 [9], (1918)1361-1403.

[41] S. Brunauer, P. H. Emmett, E. Teller, "Adsorption of Gases in Multi-molecular Layers", *J. Am. Chem. Soc.*, 60 [2], (1938) 309-319.

[42] C. Hirsch, "Investigation of the interaction between polymeric superplasticizers, cement and mineral phases of the early cement hydration", Dissertation, Technische Universität München, Chair for Construction Chemicals, (2005).

[43] http://www.sika.com, "Characteristics and Advantages of Polycarboxylate Ether Technology (PCE) ". (accessed on 06.08.2012).

[44] J. Plank and B. Sachsenhauser, "Impact of molecular structure on zeta potential and adsorption conformation of α-allyl-ω-methoxypolyethylene glycol - maleic anhydride superplasticizers", *J. Adv. Concr. Techn*., 4 [2], (2006) 233-239.

[45] J. Plank, R. Schwerd, D. Vlad, A. Brandl, P. Chatziagorastou, "Kolloidchemische Aspekte zur Verflüssigung von Zementleimen mit Polycarboxylaten", GDCh-Monographie, Band 31 (2004) 58-69.

[46] R. J. Flatt, Y. F. Houst, "A simplified view on chemical effects perturbing the action of superplasticizers", *Cem. Concr. Res.*, 31(2001)1169-1176.

[47] J. Plank, Z. Dai, P. R. Andres, "Preparation and characterisation of new Ca-Al-polycarboxylate layered double hydroxides", *Mater. Lett.*, 60 (2006) 3614-3617.

[48] J. Plank, H. Keller, P. R. Andres, Z. Dai, "Novel organo-mineral phases obtained by intercalation of maleic anhydride – allyl ether copolymers into layered calcium aluminium hydrates", *Inorg. Chim. Acta.*, 359 (2006) 4901-4908.

[49] C. Giraudeau, J.-B. d'Espinose de Lacaillerie, Z. Souguir, A. Nonat, R. Flatt, "Surface and intercalation chemistry of polycarboxylate copolymers in cementitious systems", *J. Am. Ceram. Soc*., 92 (2009) 2471-2488.

[50] DIN (the German Institute for Standardization), DIN EN 1015-3:2007-05: "Methods of test for mortar for masonry", (2007), DIN, Berlin, Germany.

[51] Near-process measurement of colloidal properties (zeta potential) by means of the electroacoustic devices DT-300 and DT-1200, Quantachrome Particle World, 3rd Ed. (May 2009) 21-26.

[52] A. S. Dukhin, V. N. Shilov, H. Ohshima, P. J. Goetz, "Electroacoustics Phenomena in Concentrated Dispersions. New Theory and CVI Experiment", *Langmuir*, 15 [20], (1999) 6692-6706.

[53] A. S. Dukhin, P. J. Goetz and S. Truesdail, "Titration of Concentrated Dispersions Using Electroacoustic ζ-Potential Probe", *Langmuir***,** 17 (2001) 964-968.

[54] J. Plank, C. Schröfl, M. Gruber, M. Lesti and R. Sieber "Effectiveness of Polycarboxylate Superplasticizers in Ultra-High Strength Concrete: the Importance of PCE Compatibility with Silica Fume", *J. Adv. Concr. Techn.*, **7** [1], (2009) 5-12.

Paper 1

Interaction between Polycarboxylate Superplasticizers and Amorphous Ground Granulated Blast Furnace Slag

Ahmad Habbaba and Johann Plank

Journal of the American Ceramic Society
93 [9] 2857-2853 (2010)

DOI: 10.1111/j.1551-2916.2010.03755.x

journal

J. Am. Ceram. Soc., 93 [9] 2857–2863 (2010)
DOI: 10.1111/j.1551-2916.2010.03755.x

Interaction Between Polycarboxylate Superplasticizers and Amorphous Ground Granulated Blast Furnace Slag

Ahmad Habbaba and Johann Plank†

Construction Chemicals, Technische Universität München, 85747 Garching, Germany

Ground granulated blast furnace slag produced in iron-making is an amorphous, glassy material, which is widely used in blended cements. Here, the surface chemistry of slag dispersed in water and its behavior in cement paste were studied in the absence and presence of anionic dispersants. Three different slag samples possessing different oxide compositions and two polycarboxylate (PC) dispersants based on methacrylic acid—*co*—ω-methoxy poly(ethylene glycol) methacrylate ester were investigated. When suspended in deionized water, all slag samples released different amounts of Ca^{2+}, K^+, Na^+, and OH^- ions, thus producing pore solutions possessing high pH. Electrokinetic properties of slag suspensions were determined by zeta potential measurement, revealing that initially negatively charged slag adsorbs considerable amounts of Ca^{2+} ions on its surface until saturation is reached. Through this mechanism, slag attains a strongly positive zeta potential in pore solutions containing Ca^{2+} ions. Onto this positively charged layer of adsorbed Ca^{2+} ions, anionic PC dispersants adsorb, producing a Langmuir-type adsorption isotherm. PC consumption generally correlates with the absolute value of the positive zeta potential of slag. The study demonstrates that when blended into cement, slag is not inert relative to anionic superplasticizers. Instead, competition occurs between cement and slag for the dispersant.

I. Introduction

Slag is an amorphous mineral by-product of various metal-refining processes. The slag produced in iron making derives from impurities contained in the metal oxides, coke, limestone, and other compounds. Slags occurring in the production of iron are generated at three different stages of processing and are classified as: blast furnace slag (the most common one), electric arc furnace slag, and ladle slag.[1–5] Blast furnace slag is obtained by quenching molten iron slag, which floats on top of the molten iron in a blast furnace (temperature 1400°–1600°C) with water or steam. This produces a glassy granular product, which is then dried and ground into a fine powder. It is known as "ground granulated blast furnace slag" (GGBS or GGBFS). This powder is essentially an amorphous calcium potassium glass, which contains huge amounts of silicon dioxide (SiO_2), earth alkali oxides (particularly CaO and some MgO), aluminum oxide (Al_2O_3), and alkali oxides (especially K_2O and few Na_2O). Besides, other oxides such as TiO_2, Fe_2O_3, Mn_3O_4, SrO, etc. are present in various amounts. GGBFS is a pozzolanic material, which in the presence of $Ca(OH)_2$ released from hydration of the calcium silicates contained in Portland cement reacts to form calcium silicate hydrates similar to those produced by ordinary Portland cement.[6,7] Currently, the iron-making industry produces hundreds of millions of tons of slag as a by-product.

GGBFS belongs to the group of secondary cementitious materials (SCMs), which are commonly blended with Portland cement clinker to produce Portland composite cements (e.g., CEM II and CEM III cements). Such blended cements show a lower carbon footprint than common Portland cement (CEM I). Recently, they have become very popular because they allow the cement industry to lower their CO_2 emission considerably. In 2008, approximately 2.7 billion tons of cement were produced worldwide, resulting in about 5% of global CO_2 emission.[8] The use of SCMs enables to reduce the CO_2 emission from ~850 kg CO_2 per ton of ordinary Portland cement clinker to ~650 kg CO_2 per ton for a blended cement. Consequently, the cement industry has significantly accelerated its efforts to increase the consumption of slag.[9]

Slag cements allow to build high strength and durable concrete structures similar to those achieved with ordinary Portland cement.[10,11] Yet, the interaction occurring between the slag and common concrete admixtures such as superplasticizers has been poorly investigated so far.

The aim of using superplasticizers in concrete is to improve its flow properties, and/or to reduce the water-to-cement ratio (w/c) in order to reach high strength and durability. Polycarboxylate (PC) superplasticizers are high performance admixtures used in advanced concrete formulations such as self-compacting or ultra-high-strength concrete.[12] The interaction between superplasticizers and cement is generally well understood,[13–15] however, the effects of superplasticizers on SCMs are less known. Here, we report on the interaction between PC-based superplasticizers and GGBFS. First, the electrical surface charge developed by GGBFS when suspended in water was determined using a zeta potential instrument. Next, the interaction between PC and GGBFS was studied by adsorption and zeta potential measurements were performed in slag pore solutions. Pore solution is a term commonly used throughout the cement industry for filtrates collected from aqueous suspensions of cement, slag or other constituents dispersed in water at specified water-to-solids ratios. Based on these results, a model for the electrochemical double layer existing on GGBFS surface in water and cement pore solution was developed. Finally, the relationship between the surface properties of slag and the dispersing performance obtained from the PCs will be presented.

II. Experimental Procedure

(1) Blast Furnace Slag

Three GGBFS samples from different sources in Germany (Slag # I from Schwenk Cement Company, Karlstadt, Germany, Slag # II from Holcim, Salzgitter Plant, Salzgitter, Germany, and Slag # III from Holcim, Hansa Bremen Plant, Bremen, Germany) were used in this study. Table I lists their chemical compositions as determined by X-ray fluorescence analysis (XFA). The instrument used was Axios from PANalytical, Philips, Eindhoven, the Netherlands. Their specific surface area and particle size distribution (d_{50} value) were determined using a

G. Scherer—contributing editor

Manuscript No. 27147. Received November 23, 2009; approved February 26, 2010.
This work has been supported by a grant from the German Research Foundation (Deutsche Forschungsgemeinschaft).
†Author to whom correspondence should be addressed. e-mail: johann.plank@bauchemie.ch.tum.de

Table I. Oxide Composition and Properties of GGBFS Samples Studied

Oxide content (wt%)	Slag # I	Slag # II	Slag # III
SiO_2	35.9	36.3	38.6
CaO	42.8	36.4	38.6
Al_2O_3	11.4	11.5	12.4
MgO	6.44	11.50	6.40
TiO_2	0.82	0.78	0.82
K_2O	0.33	0.66	0.53
Na_2O	0.27	0.34	0.45
Fe_2O_3	0.45	0.26	0.46
Mn_3O_4	0.28	0.22	0.26
SO_3	2.40	2.57	1.55
SrO	0.09	0.09	0.09
ZrO_2	0.03	0.03	0.03
BaO	0.13	0.19	0.00
P_2O_5	0.00	0.00	0.00
Specific surface area (Blaine) (cm^2/g)	4000	3480	4080
d_{50} value (μm)	9.53	10.19	9.25
Density (g/cm^3)	2.86	2.91	2.91
Water/slag ratio	0.55	0.52	0.46

GGBFS, ground granulated blast furnace slag.

Blaine instrument (Toni Technik, Berlin, Germany) and a laser granulometer, respectively (Cilas 1064, Cilas, Marseille, France).

The amorphous character of the slag samples was evidenced by X-ray diffraction (Bruker D8 advance, Bruker-AXS, Karlsruhe, Germany). There, all three samples showed no reflections indicative of crystalline constituents. Additionally, glass-like appearances were observed for all samples by scanning electron microscopy performed using an XL30 ESEM FEG instrument from Philips, FEI Company, Eindhoven/the Netherlands. A representative sample from slag # II is shown in Fig. 1.

(2) PC

Two methacrylic acid—*co*—ω-methoxy poly(ethylene glycol) (MPEG) methacrylate ester-based superplasticizers denominated 45PC1.5 and 45PC6, respectively, were synthesized and used in this work. Their general chemical structure is shown in Fig. 2. The number in front of PC refers to the number of ethylene oxide units (n_{EO}) present in the side chains of the PC comb polymers, whereas the number behind PC refers to the molar ratio between methacrylic acid and MPEG methacrylate ester, which either was 1.5:1 or 6:1. The copolymers were synthesized via radical copolymerization in aqueous solution using sodium

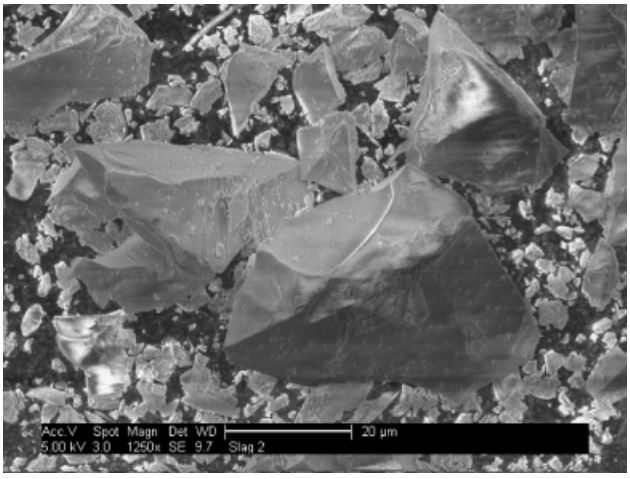

Fig. 1. Scanning electron microscopic micrograph of slag # II, demonstrating its glassy character.

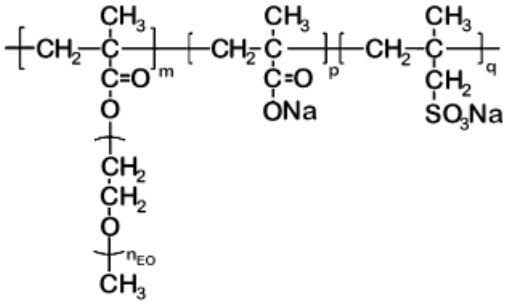

Fig. 2. Chemical structure of the synthesized polycarboxylate copolymers.

peroxodisulfate as an initiator and methallyl sulfonic acid as a chain transfer agent. Details of the synthesis process have been disclosed before.[16] After copolymerization, the polymer solutions were neutralized with sodium hydroxide and dialyzed using a 6000–8000 Da cellulose cut-off membrane (Spectra/Pro, Spectrum Laboratories Inc., Rancho Dominguez, CA).

The copolymers were characterized using Waters 2695 gel permeation chromatography (GPC) separation module equipped with a refractory index detector (2414 module, Waters, Eschborn, Germany) and a Dawn EOS 3 angle static light scattering detector (Wyatt Technology, Clinton, IA). A d*n*/d*c* of 0.135 mL/g (value for poly(ethylene oxide)) was utilized to determine molar masses.[17] Ultrahydrogel columns 500, 250, and 120 (Waters, Eschborn, Germany) with an operating range (PEO/PEG) of M_W between 100 and 1 000 000 Da were used. The eluent was 0.1 N $NaNO_3$ at pH = 12 adjusted using NaOH. The data obtained from GPC are presented in Table II.

(3) Slump Flow Test

Flowability of pastes obtained by dispersion of the slag samples in water was determined utilizing a "mini slump test" according to DIN EN 1015. The test was carried out as follows: In a porcelain casserole, 300 g of slag were added to the specific amount of water as shown in Table I (water/slag ratio) to produce a target slump flow of 18 ± 0.5 cm. The mixture was manually stirred with a spoon for 1 min, then allowed to soak for another minute, and then stirred manually again for 2 min. Immediately after the stirring, the paste was poured into a Vicat cone (height 40 mm, top diameter 70 mm, bottom diameter 80 mm) placed on a glass plate and the cone was vertically removed. The resulting diameter (spread) of the paste correlates with the flow value of the slurry. This spread was measured twice; the second measurement being perpendicular to the first and averaged to give the slump value. Each test was performed three times, and the average of the paste flow diameters was reported as the slump flow value. The margin of error was $\pm 3\%$. The water-to-slag ratios required to obtain the target slump flow of 18 ± 0.5 cm using this method are shown in Table I.

(4) Zeta Potential

Zeta potential was measured using Model DT-1200 Electroacoustic Spectrometer (Dispersion Technology Inc., Bedford Hills, NY). This instrument allows to measure the zeta potential of highly solids loaded suspensions such as the slag/water pastes used in this work.[18] For the determination of the zeta potential, aqueous solutions of the copolymers (concentration 10 wt%, pH = 7) were stepwise titrated to the slag suspended in water. The water-to-slag ratios were those reported in Table I. The zeta potential of the slurry was recorded as a function of copolymer concentration.

(5) Anionic Charge Amount of PC

Anionic charge amount of the copolymers used were determined by polyelectrolyte titration using a particle charge detector PCD 03 pH (BTG Mütek GmbH, Herrsching, Germany). The charge

Table II. Molar composition and characteristic properties of the synthesized polycarboxylates (PC) comb polymers

Copolymer	Molar ratio methacrylic acid:ester	Side chain n_{EO}	M_W (g/mol)	M_n (g/mol)	Polydispersity index (M_W/M_n)	Hydrodynamic radius $R_{h(avg.)}$ (nm)
45PC1.5	1.5	45	196 300	51 900	3.8	8.7
45PC6	6.0	45	222 300	52 340	4.2	10.4

n_{EO}, number of ethylene oxide units; avg., average.

detector consists of a PTFE cylinder with an oscillating PTFE piston in the center. The polyanionic polymer adsorbs onto the Teflon surface, while the counter ions are being separated from the polymer when the piston is moving. This creates a streaming current, measured by two Pt electrodes inside the Teflon cylinder. During the polyelectrolyte titration, a cationic polyelectrolyte (0.001 N poly(diallyl-dimethylammoniumchloride), PolyDADMAC) was added dropwise to the pore solution obtained by centrifugation of the slag suspension and treated with PC until the point of zero charge (isoelectric point) was reached.

(6) Adsorption of PC

Adsorbed amount of copolymers on slag was determined using the depletion method. The amount of PC retained in the suspension after contact with slag was designated as the "adsorbed amount". This infers that PC interacts with slag only by surface adsorption, while no chemical absorption (intercalation) of PC into slag hydrates will occur. This assumption is only valid for slag, but not for cement.[19,20] Different dosages of copolymer were added to the slag suspension (water-to-slag ratio as listed in Table I), which was stirred for 2 min, and then centrifuged for 10 min at 8500 rpm. For the quantification of organic carbon in filtrate samples, a high TOC II apparatus from Elementar (Hanau, Germany) was used. Centrifugates were diluted 20:1 (v/v) with 0.1 N HCl to remove inorganic carbonates and to prevent the solving of carbon dioxide in the alkaline solution. The sample is oxidized in a glass tube at 1000°C on a platinum catalyst using synthetic air. The exhaust gas is dried with phosphorous pentoxide and carbon dioxide is determined in a NDIR-Cell. The amount of organic carbon present in the sample is calculated based on the values obtained for mono potassium phthalate, which is used as the calibration standard. The adsorbed amount of PC is obtained by subtracting the concentration of PC found in the centrifugate (which was determined by TOC measurement) from the initial PC concentration added to the slag paste.

III. Results and Discussion

To understand the interaction between PCs and slag, it is necessary to study the surface chemistry of slag in water. First, the electrical surface charge of the slag samples dispersed in DI water was obtained by using a zeta potential instrument. Additionally, the ion concentrations present in pore solutions of slag–water slurries were determined.

(1) Zeta Potential of Slag Dispersed in Water

Zeta potential is the potential at the shear plane between the suspended solid particles and the liquid phase.[21] As a first step, the zeta potential of superplasticizer-free slag suspensions in distilled water was measured over time.

The initial zeta potentials of the three different slag suspensions range from a negative value for slag # III (−20 mV) followed by an almost neutral value for slag # II (+1 mV) to a strongly positive value for slag # I (+17 mV). It becomes obvious that depending on the chemical composition of an individual slag sample, its surface charge can be anything between highly positive and highly negative. Measurement of time-dependent zeta potential over a period of ~2 h revealed that the zeta potential values of all slag samples increase to either less negative or more positive values (see Fig. 3). This behavior indicates that partial dissolution of components present in slag is occurring over time, as was confirmed by the time-dependent pH measurement (see Fig. 4). There, all slag pastes show different pH values ranging from 12.0 to 12.6. Over time, these pH values increase to 12.2–12.8.

To explain the increase in zeta potential and pH value of the slag suspensions, we determined the concentrations of ions present in the pore solutions of the slag slurries.

(2) Ion Concentrations in Slag Pore Solution

Pore solutions of the three slag slurries were obtained by pulling 10 mL samples from the slag suspensions in 20 min intervals over a period of 160 min, centrifuging them for 10 min followed by dilution at 1:20 (v/v%) with 0.1 N HCl to avoid the precipitation of calcium carbonate. Time-dependent ion concentrations present in the slag pore solutions were measured by atomic absorption spectroscopy Model 1100 B (Perkin Elmer, Überlingen, Germany).

From the results shown in Fig. 5, the differences in pH values for each slag sample can be explained. Pore solution of slag # I shows the highest initial concentrations of alkali and earth alkali cations (Ca^{2+} 361 mg/L, K^+ 205 mg/L, and Na^+ 72 mg/L). These electrolyte contents result from a partial dissolution of the respective oxides contained in the slag. Therefore, slag # I develops the highest pH value (pH 12.6) of all slag samples. Next is the pore solution of slag # II which exhibits lower ion concentrations (Ca^{2+} 214 mg/L, K^+ 56 mg/L, and Na^+ 39 mg/L), thus producing a lower pH value (pH 12.5). The pore solution of slag # III contains by far the lowest contents of cations (Ca^{2+} 91 mg/L, K^+ 16 mg/L, and Na^+ 32 mg/L). This results in a much lower pH value (pH 12.0) than for the other slag samples. Additional measurements of the Si content present in the aqueous phase revealed that this element practically is not leached from the slag (Si concentrations found were ~2 mg/L).

Surprisingly, for all slag samples, the concentrations of Ca^{2+}, K^+, and Na^+ ions found immediately after the preparation of the suspensions do not correlate with their CaO, K_2O, and Na_2O contents as determined by XFA (see Table I). Apparently, the slag samples tested here incorporate the alkalis and earth

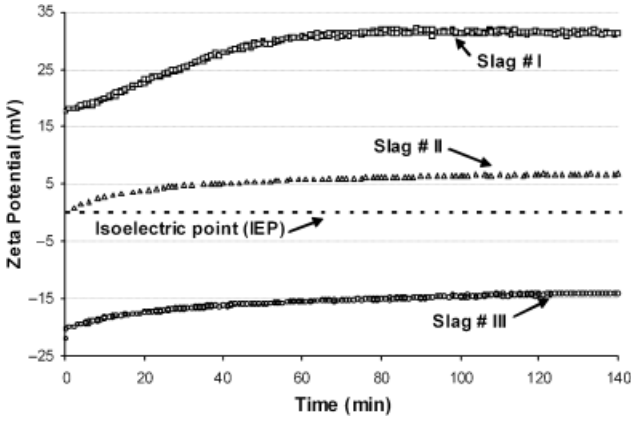

Fig. 3. Time-dependent zeta potentials of slag samples dispersed in DI water (w/s ratios: 0.55 for slag # I, 0.52 for slag # II, and 0.46 for slag # III).

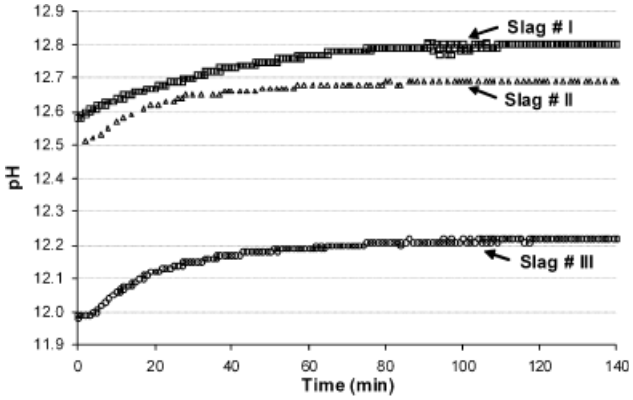

Fig. 4. Time-dependent pH values of slag samples dispersed in DI water (w/s ratios: 0.55 for slag # I, 0.52 for slag # II, and 0.46 for slag # III).

alkalis in different modes. Consequently, their dissolution behavior varies.

Additionally, the time-dependent evolution of ion concentrations during stirring of the slag samples in water was determined (Fig. 5). Here, it becomes obvious that slag # I continuously releases significant amounts of Ca^{2+}, K^+, and Na^+ into the pore solution. This process is not yet completed even after ~3 h. In comparison, slag # II releases a significantly lower amount of ions, whereas slag # III is the least reactive. It exhibits only a relatively minor change of ion concentrations over time.

The experiments clearly demonstrate that when dispersed in water, slag is not an inert material, but reacts with water to release ions at concentrations that are close to those observed for aqueous suspensions of cement.[22] The main difference being that in the case of slag, a much greater variability can be observed, depending on its chemical composition.

Based on the results obtained for the ion concentrations, the zeta potential and pH values of the slag samples can now be explained. In general, slag samples exhibiting high pH values in aqueous suspension (>12.5) produce high concentrations of Ca^{2+} and alkali cations and show a positive zeta potential. Whereas, slag samples showing a lower pH value (~12.0) in water dissolve significantly lesser ions and possess a negative surface charge.

The differences in the surface charges of slag samples are owing to fundamental processes occurring at the interface between the slag and the pore solution. As it is apparent from the initial zeta potential of slag # III (Fig. 3), all slags appear to possess initially a highly negative surface charge, which might be, for example, caused by deprotonated silanol groups present at the surface of SiO_2 when dispersed in alkaline solution.[23]

With the progressing release of alkali and earth alkali cations into the pore solution, these cations start to adsorb onto the negatively charged slag surface (see Fig. 6). Depending on the amount of cations present, particularly of divalent Ca^{2+} ions, in the equilibrium state the surface of slag will either become less negative (slag # III) or overall positively charged (slag # I and II). This way, the final surface charge of slag suspended in water is the result of dissolution processes and subsequent ion adsorption, with Ca^{2+} being the charge-determining ion.

To prove that the Ca^{2+} ion concentration instigates the main effect on the surface charge of slag, extra amounts of calcium ions contained in a 10 g/L aqueous $CaCl_2$ solution were titrated dropwise to the slag-water suspensions. The development of zeta potential with the increasing Ca^{2+} ion concentration is shown in Fig. 7.

All slag samples exhibit increasing zeta potential values after the addition of the calcium chloride solution until they reach a stable state, which is characterized by the saturated adsorption of Ca^{2+} ions onto the slag surface. In this equilibrium state, no more changes in the zeta potential are observed. Apparently, the amount of Ca^{2+} ions adsorbed depends on the initial surface charge of the slag sample. A negatively charged slag particle (slag

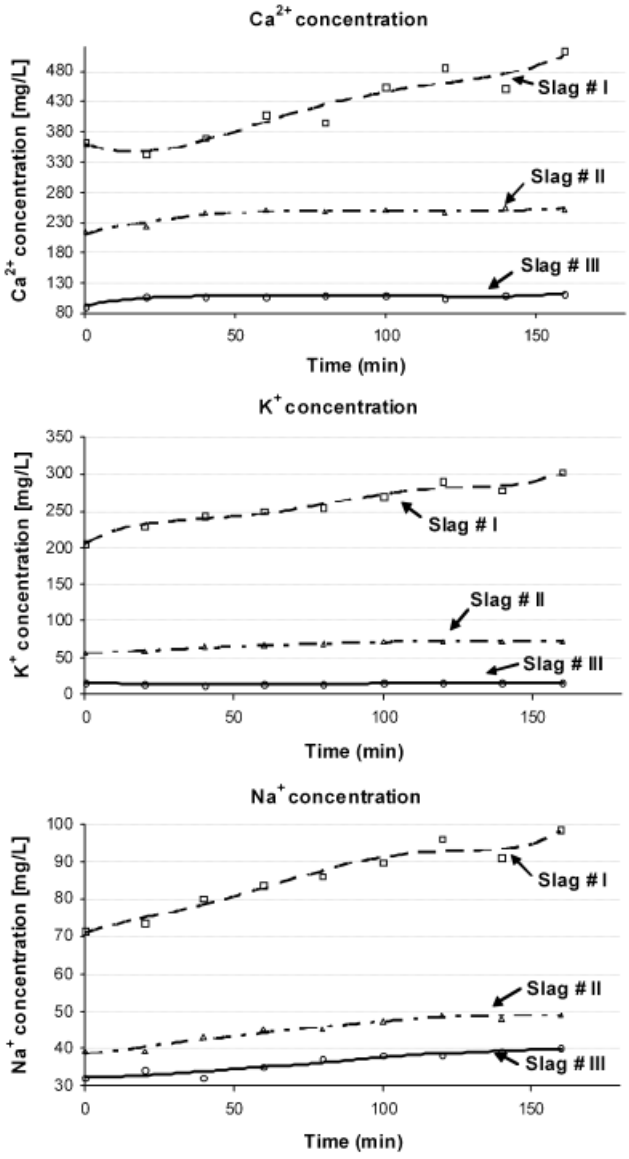

Fig. 5. Time-dependent evolution of Ca^{2+}, K^+, and Na^+ concentrations in pore solutions from slag samples suspended in DI water (w/s ratios: 0.55 for slag # I, 0.52 for slag # II, and 0.46 for slag # III).

III) exhibits a higher uptake of Ca^{2+} ions than a slag possessing neutral (slag # II) or positive charge (slag # I). Because of this mechanism, the final zeta potentials of all three slag samples are quite similar (~20–30 mV), in spite of their huge differences in surface charge immediately after dispersion in water.

In aqueous cement slurries, a huge excess of Ca^{2+} ions always exists in the pore solution, as a result of dissolution and hydrolysis of the calcium silicates.[3,4] Consequently, when added to cement or concrete, all slag samples will adsorb sufficient amounts of Ca^{2+} ions to reach their saturation and equilibrium state, which is characterized by a positive surface charge. In this way they become suitable substrates for interaction with anionic dispersants.

(3) Anionic Charge Amount of PC

After clarification of the surface chemistry of slag in aqueous suspension, we can now study the interaction between the PC dispersant and slag. At first, we want to understand the behavior of PC dissolved in the slag pore solution, which is characterized by high pH and the presence of significant amounts of electrolytes.

The concentration of calcium ions and the pH value have a significant effect not only on the surface charge of slag, but also

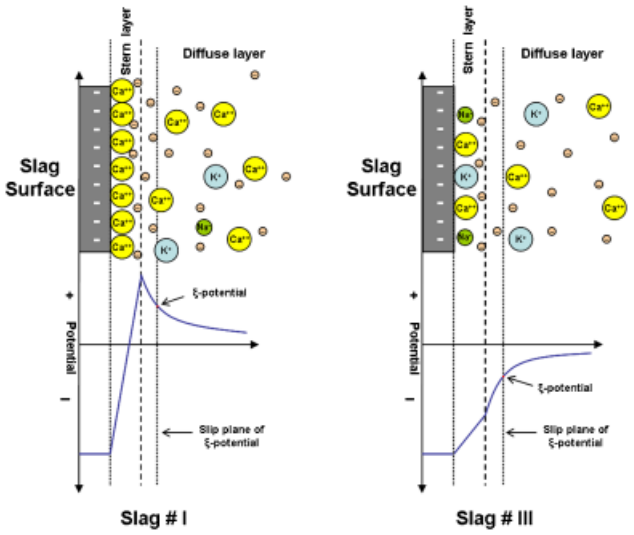

Fig. 6. Schematic illustration of the electrochemical double layer existing at a near equilibrium state on the surfaces of slags # I (left) and slag # III (right) dispersed in water, and their surface charge as evident from the zeta potential.

on the anionic charge amount of the PC polymers. To investigate, the anionic charge amount of the PC polymers (concentration: 0.2 g/L) was determined in pore solutions of the three slag samples. The results obtained are shown in Table III.

It is generally known that the anionic charge amount of PCs will increase with the increasing methacrylic acid content in the polymer.[24] Thus, the anionic charge amount of our PC samples follows the order: 45PC6 > 45PC1.5. Additionally, it becomes obvious that in suspensions containing higher concentrations of dissolved Ca^{2+} ions as is the case for slag # I, the anionic charge of PC is particularly low. This signifies that not only slag but also PC can take up calcium ions here through the complexation of the carboxylate functionalities present in the polymer.[24]

(4) Effect of PC on Rheological Properties of Slag Suspension

It is commonly known that anionic dispersants work by adsorption onto the positively charged surface of a substrate.[13,14] This way, electrostatic repulsion and steric hindrance between the solid particles is created which leads to improved the flowability of the suspension. Because of the differences in the anionic charge amounts of the PC polymers found here, one can expect that their dispersing ability for slag may differ. To investigate, mini slump tests were performed to determine the rheological properties of slag suspensions in the presence of PCs. The dosages of superplasticizer required to obtain a target slump

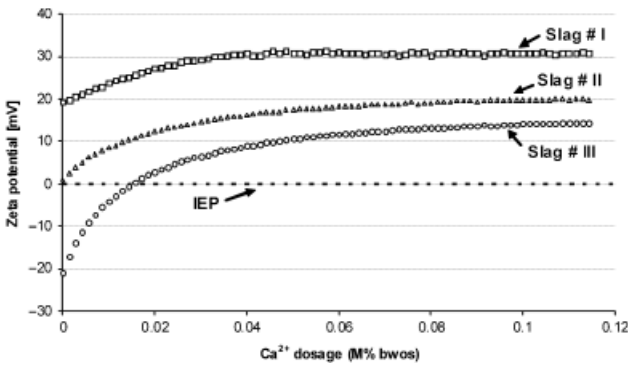

Fig. 7. Zeta potential of slag samples dispersed in DI water as a function of the increasing Ca^{2+} ion concentration (w/s ratios: 0.55 for slag # I, 0.52 for slag # II, and 0.46 for slag # III).

Table III. Anionic charge amount of polycarboxylates (PC) measured in filtrates of slag suspensions

	Anionic charge amount of PC polymer (μ eq/g)	
Sample	45PC1.5	45PC6
Slag # I	298	1235
Slag # II	306	1261
Slag # III	460	1437

flow of 26±0.5 cm were determined. The results are shown in Fig. 8.

The experiments show that for all slag samples, highly anionic 45PC6 dispersant requires significantly lower dosages to achieve the target spread of 26±0.5 cm, compared with its lesser anionic counterpart 45PC1.5. It also becomes obvious that the adsorbed amount of PC is determined by the final surface charge (zeta potential) of a slag sample. For example, slag # I, which exhibits the most positive zeta potential (Fig. 7), consistently requires a higher PC dosage than slag # II, which exhibits a less positive surface charge or slag # III, which possesses the lowest positive surface charge.

(5) Adsorption of PCs on Slag

Normally, the dispersing effectiveness of cement dispersants shows a correlation with the adsorbed amount of dispersant. Thus, the adsorbed amounts of PCs on all slag samples dispersed in DI water were determined for each copolymer by adding different dosages of PCs to the slag slurries, which were then centrifuged and the residual PC content was determined. The adsorption isotherms for the PCs are shown in Fig. 9.

The adsorbed amounts of all PCs increase with increasing superplasticizer dosage until the point of saturation is reached. Adsorption isotherms of the Langmuir type are observed. Once the saturation point of adsorption was attained, any extra amount of added copolymer will remain dissolved in the aqueous phase. Table IV shows the maximum adsorbed amounts of the copolymers.

Apparently, the PC sample possessing a higher anionic charge amount (45PC6) generally adsorbs in a significantly higher amount on all slag samples, compared with the lesser anionic 45PC1.5 polymer. Additionally, it becomes evident that slags possessing a more pronounced positive surface charge such as slag # I, attract more PC than slag # III which shows the lowest positive surface charge. It can be concluded that the presence of a layer of adsorbed Ca^{2+} cations is the precondition for the ability of slag to adsorb anionic polyelectrolytes. The packing density of the adsorbed Ca^{2+} ions determines the quantity of PC that is bound at the point of saturation.

It should be noted that the adsorbed amounts of PC found here (0.25–1.8 mg/g slag) are comparable with those known for Portland cement.[25] This signifies that in a blended cement such

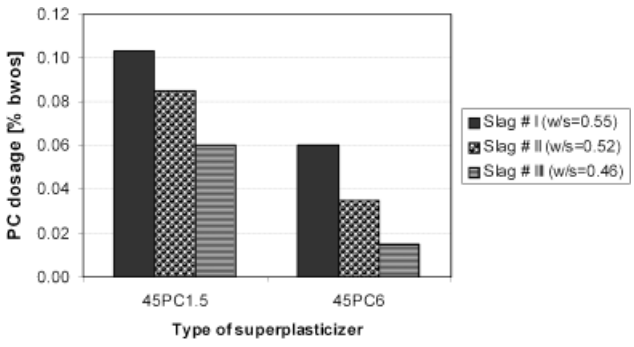

Fig. 8. Dosages of polycarboxylate superplasticizers required to obtain a target slump flow of 26±0.5 cm for aqueous slag suspensions.

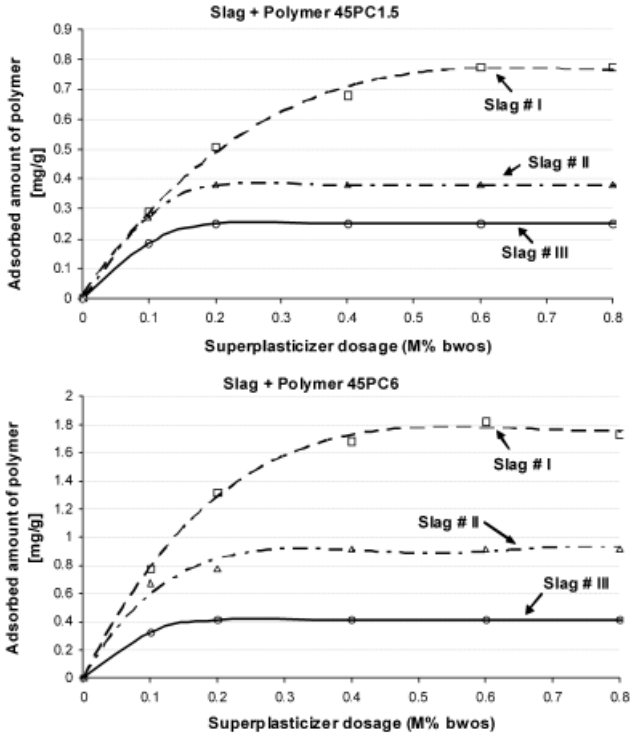

Fig. 9. Adsorption isotherms for the polycarboxylate dispersants 45PC1.5 and 45PC6, respectively, on the slag samples.

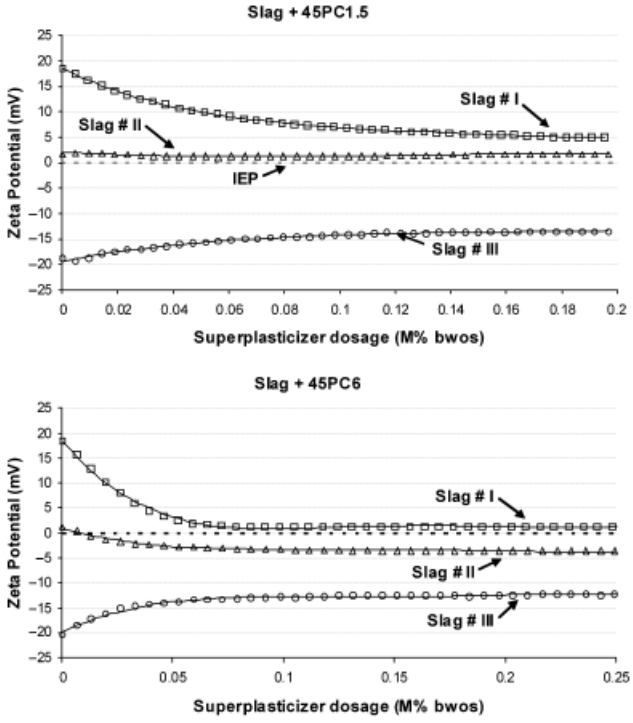

Fig. 10. Effect of polycarboxylate comb polymers on the zeta potential of slag suspensions.

as CEM III, some slags may consume amounts of PC that are comparable with those characteristic for Portland cement, and other slags may take up less PC than cement. Hence, in a cement paste or in concrete-containing slag, competition between the surfaces of cement and slag for PC will occur, and the respective surface areas and values of positive charge for the two components will determine the relative adsorbed amounts of PC on each surface in the equilibrium state.

(6) Effect of PCs on Zeta Potential of Slag Suspensions

To further investigate the interaction between PC and the surface of slag, zeta potentials of aqueous slag suspensions were measured while the PCs were gradually dosed in. The results are shown in Fig. 10.

For all copolymers, a similar effect on zeta potential was observed; that is, they modify the zeta potential of slag suspensions toward the isoelectric point. This observation confirms again that interaction between the PCs and the slag surface is occurring. In the case of slags possessing an initially positive surface charge such as slag # I and II, PC adsorption results in a decrease of the zeta potential that halts at the isoelectric point, because of the steric effect exercised by the PC side chains. While for slag # I and II, the direction of the shift of the zeta potential can be easily explained by the addition of anionic polyelectrolytes onto the slag surface, the change in the zeta potential value for slag # III toward less negative values appears to contradict the model derived from the electric charges present on this surface.

The reason behind this different behavior is a steric effect of the PEO side chains present in the PCs. As reported previously, long PEO side chains shift the shear (or slip) plane of the zeta potential to greater distances away from the slag surface.[26] This situation is schematically illustrated in Fig. 11. At these distances from the particle surface, the potential curve in the diffuse layer approaches the isoelectric point. This way, it is explained that an even adsorption of anionic polyelectrolytes onto the slag surface produces less negative particle charge.

Table IV. Polycarboxylates (PC) dosages required for surface saturation and saturated adsorbed amounts of PC on slag samples

	PC dosages for surface saturation (% bwos)		Saturated adsorbed amounts of PC on slag (mg/g)	
Sample	45PC1.5	45PC6	45PC1.5	45PC6
Slag # I	0.6	0.6	0.78	1.80
Slag # II	0.2	0.4	0.38	0.92
Slag # III	0.2	0.2	0.25	0.41

IV. Conclusion

When dispersed in water, GGBFS produces a highly alkaline pH value (12–12.6) and releases significant amounts of Ca^{2+}, K^+, and Na^+ ions. This dissolution process lasts for approximately 2 h until equilibrium is achieved. The final ion concentrations, pH values, and zeta potentials of slag suspensions vary, depending on the chemical composition of the slag. Consequently, the surface charges of slags dispersed in water can be positive or negative. The final charge mainly depends on the concentration of calcium ions released into the pore solution. Different amounts of calcium ions were shown to adsorb onto the surfaces of the slag samples tested here, depending on the initial surface charge of each slag in water. In cement pore solution where always an excess of Ca^{2+} ions is present, slag adsorbs additional amounts of calcium ions until the point of saturation is reached, which is characterized by a positive zeta potential. Through this mechanism, slag becomes a suitable substrate for the adsorption of anionic dispersants such as PCs.

PC superplasticizers can effectively disperse slag suspensions. Effectiveness is particularly strong from PCs possessing a high anionic charge amount. Their dispersion mechanism is based on adsorption onto the positively charged layer of Ca^{2+} ions present on the surface of slag. The electrostatic and steric working mechanism was proven by zeta potential measurements.

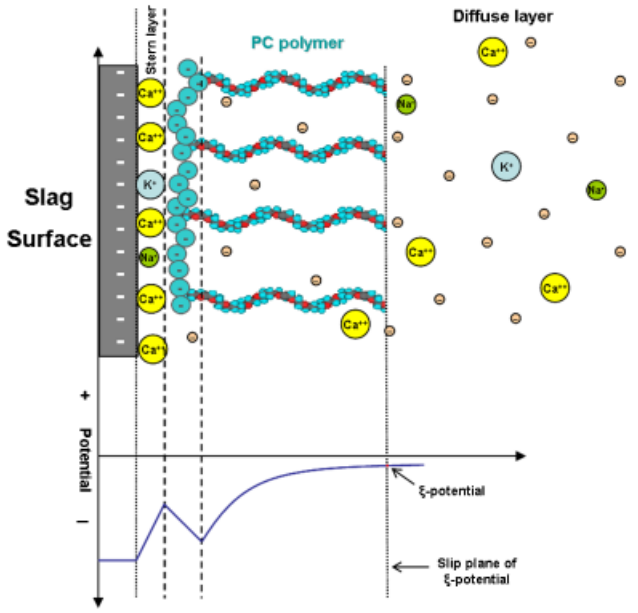

Fig. 11. Schematic representation of the electrochemical double layer existing on slag # III when dispersed in water, illustrating the steric effect of the side chain of adsorbed 45PC6 on the value of zeta potential (size of ions/atoms not to scale).

The results demonstrate that a strong interaction between PC and the surface of slags exists, and that in blended cements, PC will interact with both Portland cement and slag. Consequently, slag is not inert toward PC, and higher or lower PC dosages compared with pure Portland cement-based systems have to be considered when formulating concretes containing slag. The ratios of surface area and positive surface charge between cement and slag will determine the distribution of the adsorbed polymer between the two components.

Acknowledgment

A. H. would like to thank Al-Baath University in Homs, Syria for a stipend to finance his study.

References

[1]W. Kramer, "Blast Furnace Slags and Slag Cements"; pp. 957–81 in *Proceedings of the 4th International Symposium on the Chemistry of Cement*, Vol. II, Washington, 1960.

[2]F. Schröder, "Blast Furnace Slags and Slag Cements"; pp. 149–99 in *Proceedings of the 5th International Symposium on the Chemistry of Cement*, Vol. IV, Tokyo, 1968.

[3]R. W. Nurse, "Slag Cements"; pp. 37–68 in *The Chemistry of Cements*, Vol. 2, Edited by H. F. W. Taylor. Academic Press, London, 1964.

[4]M. Moranville, "Cement made from Blast Furnace Slag"; pp. 637–78 in *Lea's Chemistry of Cement and Concrete*, 4th edition, Edited by Peter Hewlett. Elsevier Science & Technology Books, Oxford, 2004.

[5]E. Lang, "Blast Furnace Cements"; pp. 310–25 in *Structure and performance of cements*, Edited by J. Bensted, and P. Barnes. Spon Press, London, 2002.

[6]R. Kumar, S. Kumar, S. K. Jena, and S. P. Mehrotra, "Hydration of Mechanically Activated Granulated Blast Furnace Slag," *Metall. Mater. Trans.*, **B 6**, 473–84 (2005).

[7]M. Luckman and S. V. Venkateswaran, "Cementitious and Pozzolanic Behavior of Electric Arc Furnace Steel Slags," *Cem. Concr. Res.*, **39** [2] 102–9 (2009).

[8]M. Malhotra, "Reducing CO_2 Emissions," *ACI Concr. Int.*, **28** [9] 42–5 (2006).

[9]A. Ehrenberg, "CO_2 Emissions and Energy Consumption of Granulated Blast Furnace Slag"; pp. 151–66 in *Proceedings of the 3rd European Slag Conference*, EUROSLAG Publication, 2, Keyworth, U.K., 2002.

[10]L. Jianyong and T. Pei, "Effect of Slag and Silica Fume on Mechanical Properties of High Strength Concrete," *Cem. Concr. Res.*, **27** [6] 833–7 (1997).

[11]G. J. Osborne, "Durability of Portland Blast-Furnace Slag Cement Concrete," *Cem. Con. Comp.*, **21** [1] 11–21 (1999).

[12]V. S. Ramachandran and V. M. Malhotra, "Superplasticizers"; pp. 410–517 in *Concrete Admixtures Handbook*, 2 edition, Edited by V. S. Ramachandran. Noyes publications, New Jersey, 1996.

[13]K. Yoshioka, E. Sakai, M. Daimon, and A. Kitahara, "Role of Steric Hindrance in the Performance of Superplasticizers for Concrete," *J. Am. Ceram. Soc.*, **80** [10] 2667–71 (1997).

[14]A. Ohta, T. Sugiyama, and Y. Tanaka, "Fluidizing Mechanism and Application of Polycarboxylate-Based Superplasticizers"; pp. 359–78 in *SP-173: 5th CANMET/ACI International Conference on Superplasticizers and Other Chemical Admixtures in Concrete*, Edited by V. M. Malhotra. ACI Publication, Rome, Italy, 1997.

[15]K. Yamada, T. Takahashi, S. Hanehara, and M. Matsuhisa, "Effects of the Chemical Structure on the Properties of Polycarboxylate-Type Superplasticizer," *Cem. Concr. Res.*, **30** [2] 197–207 (2000).

[16]J. Plank, K. Pöllman, N. Zouaoui, P. R. Andres, and C. Schaefer, "Synthesis and Performance of Methacrylic Ester Based Polycarboxylate Superplasticizers Possessing Hydroxy Terminated Poly(Ethylene Glycol) Side Chain," *Cem. Concr. Res.*, **38** [10] 1210–6 (2008).

[17]M. Teresa, R. Laguna, R. Medrano, M. P. Plana, and M. P. Tarazona, "Polymer Characterization by Size-Exclusion Chromatography with Multiple Detection," *J. Chromatogr. A*, **919** [1] 13–9 (2001).

[18]A. S. Dukhin and P. J. Goetz, "Acoustic and Electroacoustic Spectroscopy," *Langmuir*, **12**, 4336–44 (1996).

[19]R. J. Flatt and Y. F. Houst, "A Simplified View on Chemical Effects Perturbing the Action of Superplasticizers," *Cem. Concr. Res.*, **31**, 1169–76 (2001).

[20]J. Plank, H. Keller, and B. Yu, "Conditions Determining the Formation of Organo-Mineral Phases in Concrete"; pp. 235–56 in *9th CANMET/ACI Conference on Superplasticizers and Other Chemical Admixtures in Concrete (Supplementary Papers)*, Edited by V. M. Malhotra. ACI, Seville, 2009.

[21]E. Nägele, "The Zeta Potential of Cement," *Cem. Concr. Res.*, **15** [3] 453–62 (1985).

[22]A. L. Kelzenberg, S. L. Tracy, B. J. Christiansen, J. J. Thomas, M. E. Clarage, S. Hodson, and H. M. Jennings, "Chemistry of the Aqueous Phase of Ordinary Portland Cement Pastes at Early Reaction Times," *J. Am. Ceram. Soc.*, **81** [9] 2349–59 (1998).

[23]J. Plank, C. Schröfl, M. Gruber, M. Lesti, and R. Sieber, "Effectiveness of Polycarboxylate Superplasticizers in Ultra-High Strength Concrete: The Importance of PCE Compatibility with Silica Fume," *J. Adv. Concr. Technol.*, **7** [1] 5–12 (2009).

[24]J. Plank and B. Sachsenhauser, "Experimental Determination of the Effective Anionic Charge Density of Polycarboxylate Superplasticizers in Cement Pore Solution," *Cem. Concr. Res.*, **39** [1] 1–5 (2009).

[25]J. Plank and Ch. Hirsch, "Superplasticizer Adsorption on Synthetic Ettringite"; pp. 283–98 in *SP 217–19, Seventh CANMET/ACI Conference on Superplasticizers in Concrete*, Edited by V. M. Malhotra. ACI, Berlin, 2003.

[26]J. Plank and B. Sachsenhauser, "Impact of Molecular Structure on Zeta Potential and Adsorption Conformation of α-Allyl-ω-Methoxypolyethylene Glycol—Maleic Anhydride Superplasticizers," *J. Adv. Concr. Techn.*, **4** [2] 233–9 (2006). □

Paper 2

Surface Chemistry of Ground Granulated Blast Furnace Slag in Cement Pore Solution and Its Impact on the Effectiveness of Polycarboxylate Superplasticizers

Ahmad Habbaba and Johann Plank

Journal of the American Ceramic Society
95 [2] 768-775 (2012)

DOI: 10.1111/j.1551-2916.2011.04968.x

journal

J. Am. Ceram. Soc., 95 [2] 768–775 (2012)
DOI: 10.1111/j.1551-2916.2011.04968.x

Surface Chemistry of Ground Granulated Blast Furnace Slag in Cement Pore Solution and Its Impact on the Effectiveness of Polycarboxylate Superplasticizers

Ahmad Habbaba and Johann Plank†

Chair for Construction Chemicals, Technische Universität München, 85747 Garching, Germany

The surface chemistry of slag dispersed in synthetic cement pore solution (SCPS) was studied in absence and presence of polycarboxylate (PC) superplasticizers. Three different slag samples and two PCs based on methacrylic acid–*co*–ω–methoxy poly(ethylene glycol) methacrylate ester were employed. Zeta potential measurement of slag suspensions in SCPS revealed that all slags initially possess a negative surface charge owed to the highly alkaline pH (formation of silanolate groups). Onto this surface, at first, calcium and subsequently sulfate ions present in SCPS adsorb, thus forming a double ion layer; the first positively charged layer consisting of Ca^{2+} ions and the second negatively charged layer containing SO_4^{2-} anions. Consequently, the final surface charge of slag dispersed in SCPS is always negative. Upon addition of PC superplasticizer, competitive adsorption between the sulfate ions and PC occurs. Highly anionic PCs can desorb SO_4^{2-} and adsorb in high amount onto the Ca^{2+} ion layer, thus producing a strong dispersing effect. However, less anionic PCs cannot adsorb and do not fluidify the slag suspension. The total adsorbed amount of PC is determined by the packing density (positive charge) of the Ca^{2+} ion layer present on the surface of slag.

I. Introduction

One of the main challenges facing the concrete industry in the 21st century is to reduce the high energy demand and greenhouse gas (GHG) emission associated with the manufacturing of Portland cement. At the same time, there is a growing public interest in ecologic and economic disposal of millions of tons of industrial by-products, such as slag, fly ashes, and dusts, that can be safely incorporated into cement and concrete as secondary cementitious materials.

Slag is a by-product obtained in iron making from iron ore, coke (carbon-rich residue resulting from the distillation of coal) and flux (limestone or dolomite).[1] At the end of the smelting process, lime has combined with other components present in the iron ore and coke, forming molten blast furnace slag which floats atop of the liquid iron. The slag is then separated from the liquid metal and cooled rapidly. There are several different ways by which slag can be quenched, the most common being air-cooling and water-cooling. Both methods produce a glassy, amorphous, granular product which is then dried and ground into a fine powder which is known as "ground granulated blast furnace slag" (GGBFS). Blast furnace slag essentially consists of calcium, magnesium and alkali silicates, and alumosilicates.[2,3] Due to its latent hydraulic properties, GGBFS belongs to the group of supplementary cementitious materials (SCMs) which not only act as a mere filler or aggregate, but enhance the properties of hardened concrete through chemical reactions with cement. The GGBFS is applied either already in the cement production process by premixing the slag with Portland cement clinker to produce a blended cement, or by adding the slag as a mineral component to concrete containing Portland cement.[4–6] Concrete containing GGBFS exhibits reduced permeability and better durability, but takes longer to develop its final strength.[7–10]

Carbon dioxide is considered as the main GHG contributing to climate change, and the cement industry is a major CO_2 emittant, owed to the huge global production of cement, which in 2010 amounted to almost 3 billion tons. Currently, cement is directly responsible for roughly 7% of the world's total CO_2 emission.[11] This value corresponds to about 2 billion tons of CO_2. Due to a reduced clinker content, blended cements (CEM II/III) show a lower carbon footprint than common Portland cement (CEM I). Recently, they have become more popular because they allow the cement industry to lower their CO_2 emission considerably.

Polycarboxylate (PC) superplasticizers are applied in the construction industry to produce highly flowable concrete (such as self-compacting) and/or high strength concrete possessing a low water-to-cement ratio (w/c). Some PC superplasticizers also show fluidity retention over time. The mechanism behind the dispersing effect of PCs is based on steric hindrance as well as electrostatic repulsion forces between the cement particles.[12]

The interaction between PC dispersants and cement is generally well understood.[13–15] However, the effects of superplasticizers on SCMs, such as GGBFS, are less known. Most research studies on this topic focus on the interaction between superplasticizers and the entire cement system, including SCM, but do not differentiate between the individual components which are present therein.[16–18] For that reason, the focus of this study was on the behavior of slag as a single component in cement pore solution and the specific interactions occurring between PC superplasticizers and slag.

In previous work by the authors, the surface chemistry of slag dispersed in DI water has been studied extensively. There, a major observation was that calcium ions released from partial dissolution of slag adsorb onto the surface of slag. Depending on the quantity of Ca^{2+} dissolved, either a negative or a positive surface charge of slag can result. Moreover, interaction of PC superplasticizers with the surface of GGBFS in that system (which is free of sulfate) and the resulting dispersing performance of PC were discussed.[19] In this work here, interaction between PC and GGBFS in synthetic cement pore solution (SCPS) and thus in presence of both calcium and sulfate ions was studied. The concentrations of Ca^{2+} and SO_4^{2-} ions contained in the SCPS were comparable to those occurring in actual cement pore solution. At first, the electrical surface charge of GGBFS suspended in $CaCl_2$ solution and SCPS, respectively, was

C. Jantzen—contributing editor

Manuscript No. 29868. Received June 14, 2011; approved October 20, 2011.
†Author to whom correspondence should be addressed. e-mail: johann.plank@bauchemie.ch.tum.de.

determined using a zeta potential instrument. Next, interaction between PC and GGBFS was studied via adsorption and zeta potential measurements. The effect of the simultaneous presence of calcium and sulfate ions on the surface charge of slag was given particular attention, and the behavior was compared with that of slag dispersed in DI water only. Based on the results, a model for the electrochemical double layer existing on GGBFS surface in cement pore solution is proposed and the consequences for interaction of PC with that surface are presented.

II. Experimental Procedure

(1) Slag Samples

Three GGBFS samples from different sources in Germany (Slag # I from Schwenk Cement Company, Karlstadt, Germany; Slag # II from Holcim's Salzgitter Plant, Salzgitter, Germany; and Slag # III from Holcim's Hansa Bremen Plant, Bremen, Germany) were employed in this study. According to X-ray fluorescence analysis (XRF instrument Axios from PANalytical, Philips, Eindhoven, the Netherlands), all slag samples contained large contents of CaO ranging from 42.8 wt% in slag # I to 36.4 wt% in slag # II and to 38.6 wt% in slag # III. The slags also incorporated large amounts of SiO_2: 35.9 wt%, 36.3 wt%, and 38.6 wt% for slag # I, II, and III, respectively, while Al_2O_3 contents were comparable in all slag samples (~11.5 wt %). Slag # II exhibited a particularly high content of MgO (11.5 wt%) compared to slags # I and III (~6.4 wt%). Other oxides, such as TiO_2, Fe_2O_3, Mn_3O_4, and SrO, were present in less amounts (up to 0.8 wt%). The slag compositions are tabulated in a previous article.[19] The physical properties of all slag samples, such as density, specific surface area (*Blaine*), and d_{50} value (average particle size) are presented in Table I. Particle size distribution was measured by utilizing a laser granulometer (Cilas 1064; Cilas, Marseille, France), while the Blaine instrument was from ToniTechnik, Berlin, Germany.

Mineralogical characterization of the slag samples was attempted via powder XRD analysis (Bruker D8 advance instrument; Bruker-AXS, Karlsruhe, Germany). The instrument was equipped with a scintillation detector using Cu-Kα (λ = 1.5406 Å) radiation with a scanning range between 10° and 60° 2θ. The scan rate was set at 0.5°/min. As expected, all three samples did not show any sharp reflections indicative of crystalline constituents because of the amorphous character of the slags. The XRD spectra are exhibited in Fig. 1.

(2) Polycarboxylates

Two PC superplasticizers designated as 45PC*x* (*x* = 1.5 or 6) were synthesized and used in this work. These copolymers are based on methacrylic acid–*co*–ω–methoxy poly(ethylene glycol) (MA-MPEG) methacrylate ester. Their general chemical structure is displayed in Fig. 2. In the designation, the number "45" refers to the number of ethylene oxide units

Table I. Physical Properties and Water-To-Solids Ratios of the GGBFS Samples Used in the Study

Property	Slag # I	Slag # II	Slag # III
Water/slag ratio	0.55	0.52	0.46
SCPS/slag or $CaCl_2$ sol./slag ratio	0.59	0.53	0.505
d_{50} value (μm)	9.53	10.19	9.25
Density (g/cm^3)	2.86	2.91	2.91
Specific surface area (*Blaine*) (cm^2/g)	4000	3480	4080

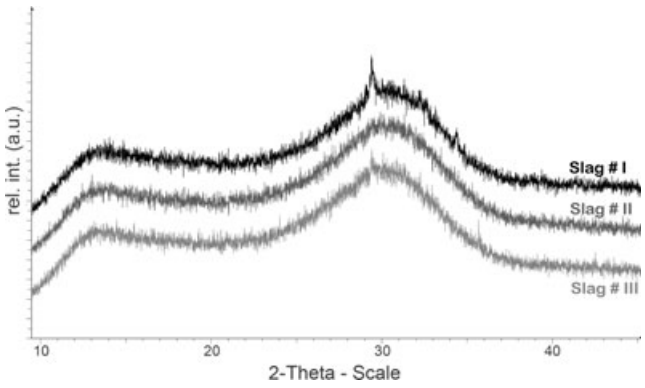

Fig. 1. Powder XRD spectra of the slag samples used in the study.

(n_{EO}) present in the side chain of the PC comb polymers, whereas "*x*" refers to the molar ratio of methacrylic acid to MPEG methacrylate ester, which was either 1.5:1 or 6:1. Free aqueous radical copolymerization was employed to synthesize the copolymers using sodium peroxodisulfate as initiator, and methallyl sulfonic acid acted as chain transfer agent. A detailed description of the synthesis process is provided in previous work.[20] The characteristic properties of the copolymers are presented in Table II.

(3) Synthetic Cement Pore Solution

The term "pore solution" (PS) generally describes the aqueous phase loaded with electrolytes which occurs between cement, slag, or other particles when dispersed in water at specific water-to-solids ratios. The SCPS used in this work was composed based on characteristic ion concentrations found in the pore solutions of a common Portland cement (CEM I).[21,22] It contained (g/L) Ca^{2+} 0.4, K^+ 7.1, Na^+ 2.25, and SO_4^{2-} 8.29. The pH of the SCPS was 12.6.

To prepare the SCPS, 1.72 g of $CaSO_4 \cdot 2H_2O$ was dissolved in 850-mL deionized water by stirring at 900 rpm until complete dissolution was achieved (~1 h). As a next step, two individual beakers were filled with 150 mL each of the prepared calcium sulfate solution. In one beaker, 6.959 g of anhydrous Na_2SO_4 was dissolved completely under stirring. In the other beaker, 4.757 g of K_2SO_4 was dissolved. Then, these two solutions and the rest of the $CaSO_4 \cdot 2H_2O$ solution were combined in a 1-L flask, and 100 mL of potassium hydroxide solution (71.2 g/L) was added dropwise to the flask under stirring at 900 rpm to achieve a pH of 12.6. To finalize, the solution was filled to 1 L by adding ~50 mL of DI water.

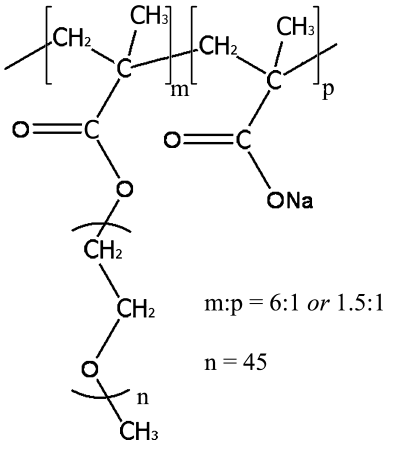

Fig. 2. Chemical structure of the synthesized polycarboxylate copolymers.

Table II. Characteristic Properties of the Synthesized PC Comb Polymers

Copolymer	Molar ratio methacrylic acid:ester	Side chain n_{EO}	Molar masses		Polydispersity index (M_W/M_n)	Hydrodynamic radius $R_{h(avg)}$ (nm)
			M_W (g/mol)	M_n (g/mol)		
45PC1.5	1.5	45	196 300	51 900	3.8	8.7
45PC6	6.0	45	222 300	52 340	4.2	10.4

(4) Methods

Rheologic properties of all slag samples dispersed in SCPS were determined using a "mini slump" test according to DIN EN 1015; there, over 1 min, 300 g of slag was filled into a porcelain cup which contained the specific amount of SCPS as described in Table I, then left to soak for another minute, and stirred again manually with a spoon for 2 min. Immediately after stirring, the slurry was poured into a Vicat cone (height 40 mm, top diameter 70 mm, bottom diameter 80 mm) placed on a glass plate, filled to the brim and the cone was removed vertically. The resulting diameter (spread) of the paste represents the flow value of the slurry. The spread was measured twice; the second measurement being perpendicular to the first and averaged to give the slump value. Each test was repeated three times, and the average of the past flow diameter was reported as the slump flow value. The margin of error was ±3%. The water-to-slag and SCPS-to-slag ratios required to obtain a target slump flow of 18 ± 0.5 cm are shown in Table I.

Electrokinetic properties were measured using Model DT-1200 Electroacoustic Spectrometer (Dispersion Technology Inc., Bedford Hills, NY, USA). The highly solids loaded suspensions used in this work require an electroacoustic instrument to obtain zeta potential values which are representative of the conditions occurring in actual concrete.[23] For determination of the zeta potential, aqueous solutions of the copolymers (concentration 10 wt%, pH = 7) were titrated stepwise to the slags suspended in SCPS. The SCPS-to-slag ratios were those reported in Table I. Zeta potential of the slurry was recorded as a function of copolymer concentration. To determine the effect of sulfate on the surface charge of the slag samples, zeta potentials were recorded during dropwise addition of 1 *M* Na_2SO_4 solution to slag suspension in $CaCl_2$ solution (0.4 g/L). The $CaCl_2$ solution-to-slag ratios were similar to those of the SCPS/slag system (see Table I).

Anionic charge amount of the copolymers used was determined by polyelectrolyte titration using a particle charge detector PCD 03 pH (BTG Mütek GmbH, Herrsching, Germany). The anionic charges were determined by titrating PC dissolved in slag pore solution (SPS) and in SCPS using poly (diallyldimethylammonium chloride) as cationic counter-polyelectrolyte.

Adsorbed amount of PC on slag surface was determined according to the depletion method. Different dosages of copolymer were added to the individual slag suspensions (SCPS-to-slag ratios as listed in Table I) which were stirred for 2 min and centrifuged for 10 min at 8500 rpm. For quantitation of the organic carbon content in the filtrates, a High TOC II apparatus from Elementar (Hanau, Germany) was used. Centrifugates were diluted 20:1 (v/v) with 0.1 N HCl to remove inorganic carbonates and to prevent the solving of carbon dioxide in the alkaline solution. The samples were oxidized in a glass tube at 1000°C on a platinum catalyst using synthetic air, the exhaust gas was dried with phosphorous pentoxide, and the carbon dioxide was determined in a NDIR-Cell. The amount of organic carbon present in the sample was calculated based on the values obtained for mono potassium phthalate which was used as calibration standard. The adsorbed amount of PC was obtained by subtracting the concentration of PC found in the centrifugate from the initial PC concentration existing prior to contact with slag.

The experiments for determination of ion concentrations in slag pore solution and SCPS were conducted as follows: in 20 min intervals, 10 mL of the slag suspensions in SCPS was pulled, centrifuged for 10 min, and diluted 1:20 (v/v%) with 0.1 N HCl to avoid precipitation of calcium carbonate. Total test period was 160 min. Time-dependent ion concentrations present in the filtrates were obtained from an atomic absorption spectroscope Model 1100 B (Perkin Elmer, Überlingen, Germany). The sulfate concentrations were determined by utilizing ionic chromatography (instrument ICS-2000 from Dionex, Sunnyvale, CA, USA).

Formation of new crystals (ettringite needles) on the surface of slag was monitored by scanning electron microscopy (SEM) performed on a XL30 ESEM FEG instrument from Philips FEI Company, Eindhoven/Netherlands. The sample was collected from the slag/SCPS slurry, filtrated, washed with acetone three times, and dried at 50°C for 1 day.

III. Results and Discussion

The surface chemistry of GGBFS dispersed in DI water and the role of Ca^{2+} ions therein, have been clarified before.[19] Here, the specific effects of the simultaneous presence of calcium and sulfate ions in the pore solution on the surface chemistry of slag and its impact on PC adsorption are presented.

(1) Zeta Potential of Slag Dispersed in SCPS

In the previous study, it was found that when dispersed in DI water, the initial surface charge of the GGBFS samples was either positive or negative, ranging from −20 mV for slag # III to an almost neutral value (+1 mV) for slag # II, and to a positive one (+17 mV) for slag # I. It became obvious that the surface charge mainly depends on the concentration of calcium ions released from the slag into the pore solution.[19] The different dissolution behavior of the slag samples is owed to variable contents of amorphous calcium compounds present in the slags.

Here, time-dependent zeta potential measurements of the slag samples dispersed in DI water, $CaCl_2$ solution containing 0.4 g/L Ca^{2+} (this value corresponds to the concentration of calcium ions present in SCPS) and SCPS were taken and compared. The data obtained from DI water and $CaCl_2$ solution, were distinctly different from that in SCPS. In DI water and $CaCl_2$ solution, a strong impact of Ca^{2+} on the surface charge of slag was observed (Fig. 3). There, in general, all zeta potential values increased over time until a stable value was attained after ~2 h. For slags # I and II, the initial zeta potential values in DI water which were already positive become even more positive in $CaCl_2$ solution, while for slag # III, the initial surface charge changed from a strongly negative (−20 mV) to an almost neutral value (−0.5 mV). In the $CaCl_2$ solution, the final zeta potential values for slags # I, II, and III were +32, +14, and +4 mV, respectively. These results indicate that Ca^{2+} is the charge determining ion for the slags. The higher the adsorbed amount of calcium ions, the higher becomes the positive charge of slag.

Opposite to before, when the slags are now dispersed in SCPS which holds sulfate anions, then the initial zeta potential values become negative for all three samples (−5, −5.5,

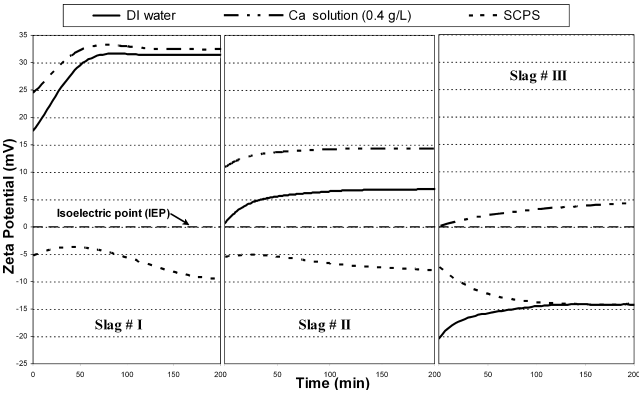

Fig. 3. Time-dependent zeta potentials of slag samples dispersed in DI water[19], $CaCl_2$ solution, and SCPS (w/s ratios as in Table I).

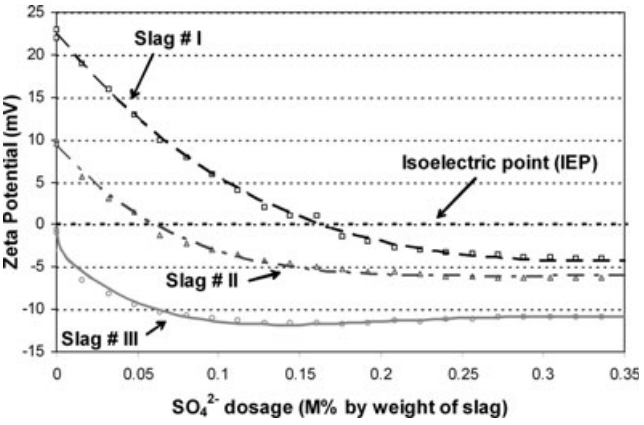

Fig. 4. Zeta potential of slag samples dispersed in $CaCl_2$ solution as a function of SO_4^{2-} ion concentration (w/s ratios: 0.59 for slag # I, 0.53 for slag # II, and 0.505 for slag # III).

and −7 mV for slags # I, II, and III, respectively). Note that in $CaCl_2$ solution, all zeta potentials were positive. This effect can be attributed to the adsorption of sulfate anions onto the layer of adsorbed Ca^{2+} ions. Over time, the surface charges decreased further and stabilized after ~3 h (Fig. 3).

To confirm that SO_4^{2-} ions are indeed responsible for alteration of the surface charge of slag to negative values, additional amounts of sulfate anions were titrated dropwise as 1 *M* Na_2SO_4 solution to the slag dispersed in $CaCl_2$ solution. There, for all slag samples, a strong decrease in zeta potential was found as a result of increasing SO_4^{2-} concentration (Fig. 4). After addition of 0.3% bwos (by weight of solids) of SO_4^{2-}, the surface charge of slag # I decreased from +23 to −4.5 mV; for slag # II, from +10 to −7 mV; and for slag # III, from −0.5 to −12 mV. Consequently, the crucial effect of sulfate anions on the final charge of slag dispersed in SCPS becomes apparent.

The total amount of SO_4^{2-} ions adsorbed on individual slag samples appears to depend on the initial zeta potential of the slag dispersed in $CaCl_2$ solution. Strongly positively charged slags (slags # I and II) exhibit a higher uptake of SO_4^{2-} ions than a slag possessing neutral charge (slag # III). Due to this mechanism, the final zeta potentials of all three slag samples are quite similar (~−4 to −12 mV), in spite of their large differences in surface charge immediately after dispersion in calcium chloride solution which varies from +23 to −0.5 mV.

(2) Ion Concentrations in Slag Pore Solution and SCPS

In the previous study, it was found that when the slag samples were dispersed in DI water, their filtrates (pore solutions) contained dissolved Ca^{2+} ions at initial concentrations of 0.35, 0.2, and 0.1 mg/L for slags # I, II, and III, respectively.[19] These Ca^{2+} concentrations correlated well with zeta potential values: the higher the Ca^{2+} concentration, the more positive is the zeta potential of the slag suspension. Thus, it was concluded that the positive surface charge is the result of adsorption of calcium ions dissolved from slag which then form a positive *Stern* layer (Ca^{2+} layer) on the slag surface.

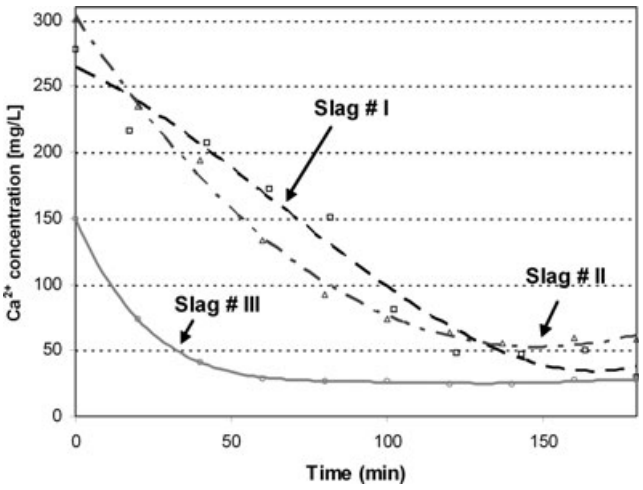

Fig. 5. Time-dependent evolution of Ca^{2+} concentration in pore solutions from slag samples suspended in SCPS (w/s ratios as shown in Table I).

However, when dispersed in SCPS, additional amounts of calcium ions are available to adsorb onto slag, thus further increasing the density of the calcium layer existing on the slag surface. This effect can be tracked by depletion of Ca^{2+} ions from SCPS and a concomitant increase of the positive charge on the slag surface.

Consumption of Ca^{2+} ions from SCPS was indeed observed for all slag samples when dispersed in SCPS. For slags # I and II, after contact with slag, the Ca^{2+} concentration present in SCPS decreased initially from 400 to 300 mg/L (Fig. 5). Slag # III consumed an even higher amount of Ca^{2+}, as was evidenced by a decrease in the Ca^{2+} concentration in SCPS from 400 to 150 mg/L. In SCPS, over time, no significant continuous release of calcium ions from slag into the solution occurred, which is different from the slag–water system.[19] This behavior becomes apparent by a decrease of time-dependent zeta potentials, as displayed for all slag/SCPS systems in Fig. 3. On the contrary, as evidenced by the continuous depletion of Ca^{2+} ions from SCPS over time, adsorption of Ca^{2+} originating from SCPS onto slag proceeds until a state of equilibrium is attained. This way, a layer of mixed Ca^{2+} ions stemming from slag dissolution as well as from SCPS is formed (Fig. 6).

Next, time-dependent evolution of SO_4^{2-} concentrations present in the pore solutions of all slag suspensions was studied. There, in accordance with the zeta potential results exhibited in Fig. 4, formation of a sulfate layer on the slag surface was confirmed by a corresponding depletion of sulfate from the pore solution of slag/SCPS suspensions (Fig. 7). At first, and because of the sulfur compounds present in the slags, all slag samples release different, yet minor quantities of SO_4^{2-} into the SCPS (356 mg/L sulfate from slag # I, 286 mg/L from slag # II, and 110 mg/L from slag #III, as evidenced by IC). This way, the initial SO_4^{2-} concentrations found for all slag suspensions are higher than that in SCPS which was 8.29 g/L. Next, continuous adsorption of sulfate onto the surfaces of the slag samples occurs, as is evidenced by a decrease over time of the SO_4^{2-} concentrations found in the pore solutions (Fig. 7). For slag # II, the sulfate concentration dropped initially from 8.59 to 8.05 g/L

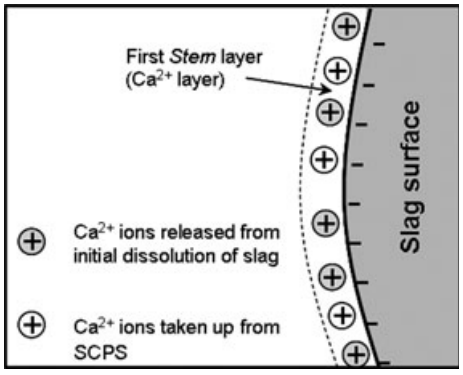

Fig. 6. Schematic illustration of the composition of the first *Stern* layer (Ca^{2+} layer) existing on the surface of slag dispersed in SCPS.

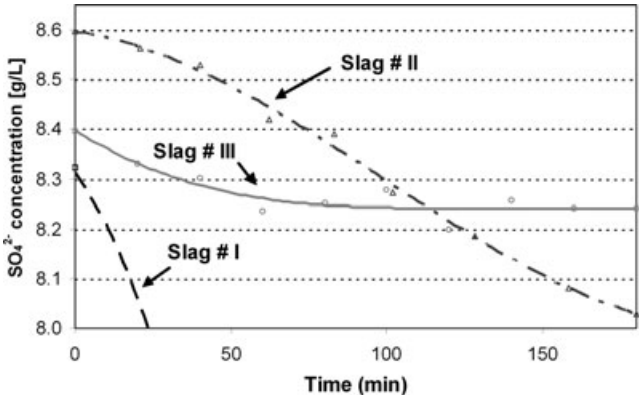

Fig. 7. Time-dependent evolution of SO_4^{2-} concentration in pore solutions of slag samples suspended in SCPS (w/s ratios as shown in Table I).

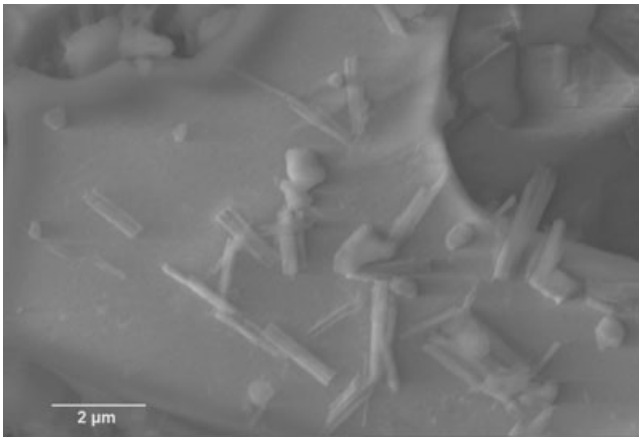

Fig. 8. SEM micrograph of slag # I dispersed in SCPS for 180 min, showing needle-shaped ettringite crystals.

and for slag # III, from 8.40 to 8.25 g/L, thus indicating a substantial uptake of SO_4^{2-} onto the Ca^{2+} layer existing on the surface of slag. Surprisingly, slag # I consumed a much larger amount of SO_4^{2-} from SCPS. There, the sulfate concentration dropped from 8.32 to 3.1 g/L within 180 min. A potential explanation for this effect is additional formation of ettringite in this suspension.[24]

To clarify, SEM images of the solids collected after filtration of slag # I dispersed for 180 min in SCPS were taken (Fig. 8). There, characteristic needle-shaped ettringite crystals were observed on the surface of slag # I, thus proving our concept. Obviously, aluminate leached from the slag reacts

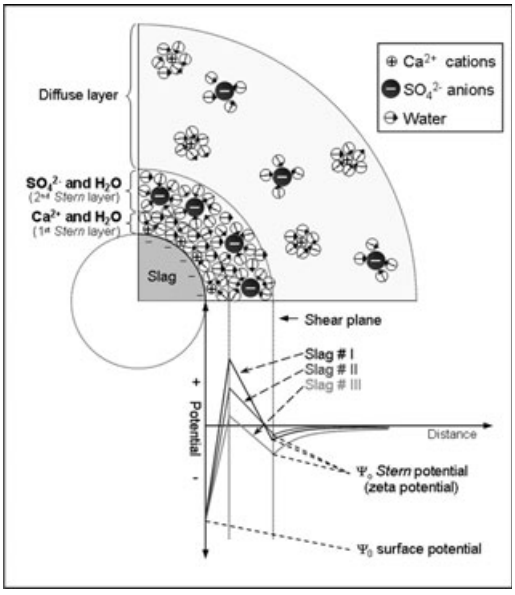

Fig. 9. Schematic illustration of the electrochemical double layer existing in the equilibrium state on the surface of the slag samples dispersed in SCPS, and the resulting surface charges as evidenced by zeta potential measurement.

Table III. Specific Anionic Charge Amount (µeq/g) of PC Samples Measured in SPS and SCPS

	Pore solution [µeq/g]			
PC polymer	SPS # I	SPS # II	SPS # III	SCPS
45PC1.5	298	306	460	175
45PC6	1235	1261	1437	1200

SPS, slag pore solution; SCPS, synthetic cement pore solution.

with calcium and sulfate present in SCPS to form calcium aluminate trisulfate (ettringite) crystals. Comparative SEM images (not shown here) revealed no ettringite crystals being present on the particulate surfaces of slags # II and # III, respectively.

To summarize, the surface charge of slag dispersed in SCPS is the result of interaction between the slag surface and the ions present in the pore solution. Due to the high pH value of SCPS, all slag samples initially possess a highly negative surface charge stemming from silanolate groups. Onto this surface, Ca^{2+} ions adsorb to form a first ion layer, which is neutral for slag # III or positive for slags # I and II. Subsequently, sulfate ions present in SCPS adsorb onto the positive calcium layer, thus forming a second ion layer. Over time, further deprotonation of silanol groups existing on the surface of slag continues, thus allowing for adsorption of more calcium and sulfate ions onto the slag surface. Accordingly, zeta potential values decrease until a final state of equilibrium is reached. A model of the electrochemical double layer existing on the surface of slag particles suspended in SCPS is displayed in Fig. 9.

(3) Anionic Charge of PC Samples

The dispersing power of PCs is generally correlated to their anionic charge amount, which is affected by the pH value and the presence of significant amounts of electrolytes (especially Ca^{2+}). Table III shows the anionic charge amounts of the PCs used in this study as measured in different pore solutions.

In general, the anionic charge amount of PC increases with increasing methacrylic acid content of the polymer.[25]

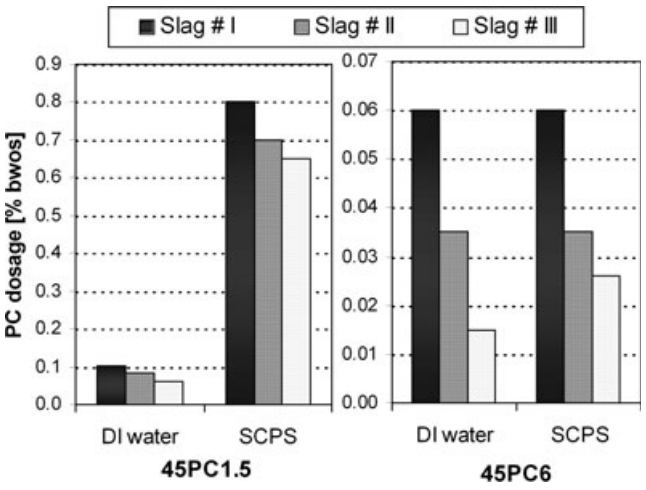

Fig. 10. Dosages of polycarboxylate superplasticizers required to obtain a target slump flow of 26 ± 0.5 cm for slag suspensions in DI water[19] or SCPS.

Accordingly, independent of the type of pore solution, the anionic charge amount of 45PC6 is considerably higher than that of 45PC1.5. It is also evident that in the pore solution from slag # III which contains the lowest concentration of Ca^{2+}, both PC polymers exhibit the highest anionic charge amount.

(4) Effect of PC on Rheology of Slag Suspension

'Mini slump' tests according to DIN EN 1015 were utilized to investigate the dispersion force of the PC samples on the slag suspensions. The dosages of PC polymers required to obtain a target slump flow of 26 ± 0.5 cm were determined (Fig. 10). For the slag pastes using DI water, lower dosages of 45PC6 (0.01–0.06% bwos) were required to attain the same spread as when 45PC1.5 was used (0.06–0.11% bwos).[19] This result is owed to the higher anionic charge amount of 45PC6. In case of slag samples dispersed in SCPS, dosages of 45PC6 comparable to those in DI water were required to achieve the target spread (Fig. 10). However, the dosages of 45PC1.5 became extremely high (0.65–0.8% bwos). Obviously, 45PC1.5, which is a polycarboxylate typically used in ready-mix concrete is a less effective dispersant for slag cements. To clarify the mechanism behind this effect, adsorption of 45PC1.5 and 45PC6, respectively on slag was compared.

(5) Adsorption of PC on Slag

First, adsorption isotherms for 45PC6 in both slag–water[19] and slag–SCPS systems were measured using the TOC method. In both systems, the adsorbed amount of 45PC6 increases with dosage until it reached a saturation point (*Langmuir* type isotherm; see Fig. 11). The saturated adsorbed amounts of this PC are lowest for slag # III and highest for slag # I.

Apparently, the main difference between the slags dispersed in water and SCPS is the saturated adsorbed amount of polymer. The anionic charge amount of PC and the positive surface charge (first *Stern* layer) arising from adsorption of Ca^{2+} ions onto slag are the two main parameters which determine the maximum amount of PC which can adsorb on slag. Take, for example, the system with slag # I and PC polymer 45PC6: when slag # I is dispersed in water or SCPS, the same final charge of the first *Stern* layer at ~+32 mV was observed (see Fig. 3). Whereas, the anionic charge amount of 45PC6 in SCPS is lower than those found in the SPSs (Table III). This, results in a slightly lower adsorbed amount of 45PC6 on slag # I dispersed in SCPS, compared to that in SPS (1.8 mg/g vs 1.51 mg/g). For slag # II, due to the different anionic charge amount of 45PC6 in each solution, PC adsorption should be lower in SCPS than in SPS. However, the opposite trend is observed. This effect is explained by the higher adsorbed amount of Ca^{2+} present on the surface of slag # II in SCPS which instigates a greater affinity of PC, thus resulting in similar amounts of PC adsorbed in both systems (~0.91 mg/g). Higher adsorption of calcium ions occurs for slag # III dispersed in SCPS than in DI water. This leads to an increased adsorbed amount of the copolymer (0.75 mg/g) in SCPS, compared to the water–slag system (0.41 mg/g).

In general, the amounts of 45PC6 adsorbed on the slag samples dispersed in SCPS follow the order: slag # I > II > III. This trend correlates well with the positive surface charges of the individual slag samples observed in $CaCl_2$ solution (see Fig. 3). In other words, the packing density of the layer of adsorbed Ca^{2+} ions determines the maximum quantity of adsorbed polymer.

The saturated adsorbed amounts of 45PC6 on slag found in this work (0.75–1.51 mg/g) are comparable to those measured previously for Portland cement.[26] Therefore, this PC exhibits a similar affinity for cement and slag, and competitive adsorption between the surfaces of cement and slag may occur in an actual concrete. The relative adsorbed amounts of PC on each surface in the equilibrium state are determined by the respective surface areas and the values of the positive surface charge for cement and slag.

Compared to 45PC6, adsorption of 45PC1.5 on slag # I was much lower (~0.4 mg/g at saturation point vs 1.5 mg for 45PC6) (Fig. 12). Surprisingly, in SCPS, similar adsorbed amounts were found for all three slag samples. This suggests that adsorption of this type of PC mainly is driven by a gain in entropy, and not by electrostatic attractive forces, as it is independent of the positive surface charges of the different slags.[27] This low adsorption explains why 45PC1.5 is not an effective dispersant for these slag suspensions, as is shown in Fig. 10.

(6) Effect of PC on Zeta Potential of Slag Suspensions

To support the adsorption data, zeta potentials were measured during dropwise addition of PC polymer 45PC6 to all slag samples suspended in DI water (the results were presented in previous work[19]) and SCPS, respectively. The results are exhibited in Fig. 13.

When PC is added, for all slag pastes, a shift in zeta potential values toward the isoelectric point (IEP) occurs, thus confirming that adsorption of PC on slag does indeed occur. In general, the shift in zeta potential toward the IEP instigated by adsorption of superplasticizer can be attributed to the steric effect of the polyethylene oxide (PEO) side chains present in the PC. They shift the shear plane of the

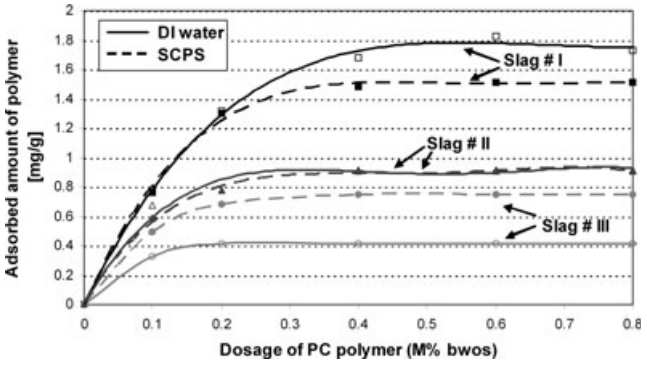

Fig. 11. Adsorption isotherms for PC polymer 45PC6 on slag samples dispersed in DI water[19] and SCPS.

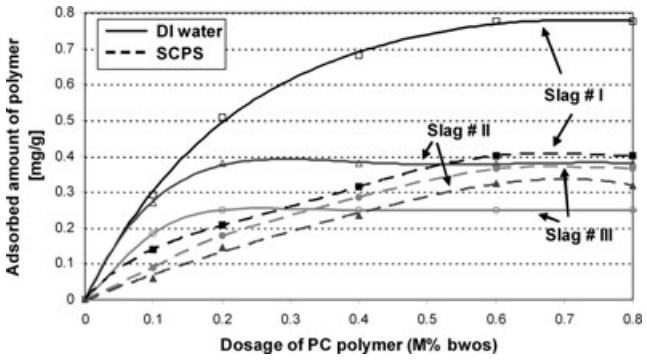

Fig. 12. Adsorption isotherms for PC polymer 45PC1.5 on slag samples dispersed in DI water[19] and SCPS.

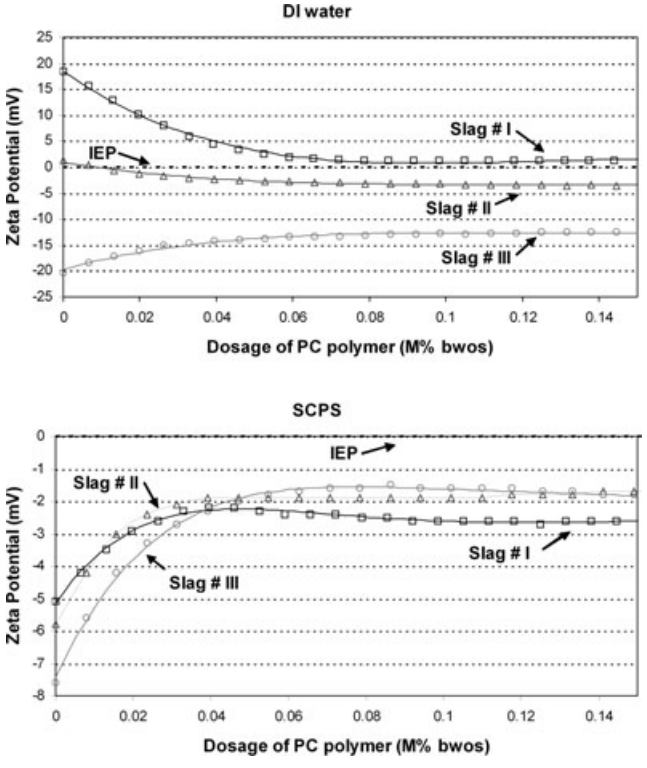

Fig. 13. Effect of dosage of PC polymer 45PC6 on zeta potential of slag dispersed in DI water[19] (top) and SCPS (bottom).

zeta potential farther away from the slag surface where the zeta potential approaches a value close to zero.[28]

IV. Conclusion

When GGBFS is dispersed in cement pore solution, strong interaction occurs between the surface of slag and the ions present in this solution. The first effect stems from adsorption of calcium ions onto the slag surface. At the high pH values existing in SCPS, slag initially exhibits a negative surface charge owed to deprotonation of silanol groups. This negatively charged surface then adsorbs calcium ions that originate from the SCPS and dissolution of the slag. This way, a layer of Ca^{2+} is formed on the slag surface, which renders its surface positively charged. The positive Ca^{2+} layer attracts sulfate ions present in the SCPS, thus forming a second layer of sulfate ions which alters the surface charge of slag to negative. Over time, further deprotonation of silanol groups on the slag surface occurs, which allows for adsorption of more calcium and sulfate ions. This effect decreases the zeta potentials of the slag slurries to more negative values, until they reach an equilibrium state.

When incorporated into concrete, varying slags can produce differences in workability. This is owed to the disparity in the surface chemistry of the slag samples which results from the dissimilar ability of individual slags to adsorb calcium ions. Slags releasing higher amounts of Ca^{2+} ions during their hydration adsorb higher quantities of PC and thus require more dosage to achieve the same fluidity as slag releasing less Ca^{2+}. This result confirms previous work which established the same relationship between the slag content present in a blended cement and the PC dosage required.

From these experiments, it is suggested that when PCs are added to blended cements containing slag, competitive adsorption between the polymers and sulfate ions for positively charged adsorption sites on the surface of slag can occur. The adsorbed amount of PC, and hence its dispersing effectiveness, mainly depend on the difference in anionic charge of the copolymer and sulfate. Here, PC polymer 45PC6 is sufficiently anionic to occupy enough adsorption sites on slag. Contrary to this, PC polymer 45PC1.5 is not sufficiently anionic to compete with SO_4^{2-}, and hence, cannot adsorb in large amount on the surface of slag. Consequently, very high dosages of this polymer are required to obtain high workability of concretes containing slag cement.

The study demonstrates that in general, the anionic charge amount of the superplasticizer and the packing density of Ca^{2+} ions adsorbed on the slag surface are the two main parameters which impact PC adsorption on slag. This way, different saturated adsorbed amounts of PC can result. Consequently, the dosages of superplasticizer required to instigate high flowability in concrete mixtures containing slag can vary significantly.

Acknowledgments

This work has been supported by a grant from the German Research Foundation (Deutsche Forschungsgemeinschaft). In addition, A. H. thanks Al-Baath University in Homs, Syria for a stipend to finance his study, and he thanks TUM graduate school for their encouragement.

References

[1]M. Moranville, "Cement Made from Blast Furnace Slag"; pp. 637–78 in *Lea's Chemistry of Cement and Concrete*, 4th edition, Edited by P. Hewlett. Elsevier Science & Technology Books, Oxford, 2004.

[2]W. Kramer, "Blast Furnace Slags and Slag Cements"; pp. 957–81 in*Proceedings of the 4th Int. Symp. on the Chemistry of Cement*, Washington, Vol. II, 1960.

[3]ACI committee 233R-95, *Ground Granulated Blast-Furnace Slag as a Cementitious Constituent in Concrete*. American Concrete Institute, Farmington Hills, Michigan, 1995.

[4]F. Schröder, "Blast Furnace Slags and Slag Cements"; pp. 149–99 in*Proceedings of the 5th Int. Symp. on the Chemistry of Cement*, Tokyo, Vol. IV, 1968.

[5]R. W. Nurse, "Slag Cements"; pp. 37–68 in *The Chemistry of Cements*, Vol.2, Edited by H. F. W. Taylor. Academic Press, London, New York, 1964.

[6]D. W. Lewis, "History of Slag Cements"; *Paper Presented at University of Alabama Slag Cement Seminar*, American Slag Association MF 186-6, April 1981.

[7]L. Jianyong and T. Pei, "Effect of Slag and Silica Fume on Mechanical Properties of High Strength Concrete," *Cem. Concr. Res.*, **27** [6] 833–7 (1997).

[8]G. J. Osborne, "Durability of Portland Blast-Furnace Slag Cement Concrete," *Cem. Con. Comp.*, **21** [1] 11–21 (1999).

[9]E. Lang, "Blast Furnace Cements"; pp. 310–25 in *Structure and Performance of Cements*, 2nd edition, Edited by J. Bensted and P. Barnes. Spon Press, London, 2002.

[10]X. Fua, W. Houa, C. Yanga, D. Li, and X. Wu, "Studies on High-Strength Slag and Fly Ash Compound Cement," *Cem. Concr. Res.*, **30** [8] 1239–43 (2000).

[11]V. M. Malhotra, "Sustainability Issues and Concrete Technology"; *Paper Presented at 7th International Symposium on Cement and Concrete (ISCC)*, Jinan, China, May 9–12, 2010.

[12]V. S. Ramachandran and V. M. Malhotra, "Superplasticizers"; pp. 410–517 in *Concrete Admixtures Handbook* 2nd edition, Edited by V. S. Ramachandran. Noyes Publications, Park Ridge, NJ, 1996.

[13]K. Yoshioka, E. Sakai, M. Daimon, and A. Kitahara, "Role of Steric Hindrance in the Performance of Superplasticizers for Concrete," *J. Am. Ceram. Soc.*, **80** [10] 2667–71 (1997).

[14]A. Ohta, T. Sugiyama, and Y. Tanaka, "Fluidizing Mechanism and Application of Polycarboxylate-Based Superplasticizers"; pp. 359–78, *5th*

CANMET/ACI International Conference on Superplasticizers and Other Chemical Admixtures in Concrete, Rome, Italy, Edited by V. M. Malhotra. ACI Publication SP-173, Farmington Hills, MI, 1997.

[15]K. Yamada, T. Takahashi, S. Hanehara, and M. Matsuhisa, "Effects of the Chemical Structure on the Properties of Polycarboxylate-Type Superplasticizer," *Cem. Concr. Res.*, **30** [2] 197–207 (2000).

[16]M. Palacios, F. Puertas, P. Bowen, and Y. F. Houst, "Effect of PCs Superplasticizers on the Rheological Properties and Hydration Process of Slag-Blended Cement Pastes," *J. Mater. Sci.*, **44**, 2714–23 (2009).

[17]M. Kumar, N. P. Singh, and S. K. Singh, "Effect of Polycarboxylate Type of Super Plasticizer on the Hydration Properties of Composite Cements," *Front. Chem. China*, **6** [1] 38–43 (2011).

[18]S. K. Agarwal, I. Masood, and S. K. Malhotra, "Compatibility of Superplasticizers with Different Cements," *Construct. Build. Mater.*, **14**, 253–9 (2000).

[19]A. Habbaba and J. Plank, "Interaction Between Polycarboxylate Superplasticizers and Amorphous Blast Furnace Slag," *J. Am. Ceram. Soc.*, **93** [9] 2857–63 (2010).

[20]J. Plank, K. Pöllman, N. Zouaoui, P. R. Andres, and C. Schaefer, "Synthesis and Performance of Methacrylic Ester Based Polycarboxylate Superplasticizers Possessing Hydroxy Terminated Poly(Ethylene Glycol) Side Chain," *Cem. Concr. Res.*, **38** [10] 1210–6 (2008).

[21]A. L. Kelzenberg, S. L. Tracy, B. J. Christiansen, J. J. Thomas, M. E. Clarage, S. Hodson, and H. M. Jennings, "Chemistry of the Aqueous Phase of Ordinary Portland Cement Pastes at Early Reaction Times," *J. Am. Ceram. Soc.*, **81** [9] 2349–59 (1998).

[22]W. Rechenberg and S. Sprung, "Composition of the Solution in the Hydration of Cement," *Cem. Concr. Res.*, **13**, 119–26 (1983).

[23]A. S. Dukhin and P. J. Goetz, "Acoustic and Electroacoustic Spectroscopy," *Langmuir*, **12**, 4336–44 (1996).

[24]S. J. Barnett, M. A. Halliwell, N. J. Crammond, C. D. Adam, and A. R. W. Jackson, "Study of Thaumasite and Ettringite Phases Formed in Sulphate/Blastfurnace Slag Slurries Using XRD Full Pattern Fitting," *Cem. Con. Comp.*, **24**, 339–46 (2002).

[25]J. Plank and B. Sachsenhauser, "Experimental Determination of the Effective Anionic Charge Density of Polycarboxylate Superplasticizers in Cement Pore Solution," *Cem. Concr. Res.*, **39** [1] 1–5 (2009).

[26]J. Plank and C. Hirsch, "Superplasticizer Adsorption on Synthetic Ettringite"; pp. 283–98 *Seventh CANMET/ACI Conference on Superplasticizers in Concrete*, Edited by V. M. Malhotra. ACI, Berlin, SP 217-19, 2003.

[27]J. Plank and B. Sachsenhauser, "Experimental Determination of the Thermodynamic Parameters Affecting the Adsorption Behaviour and Dispersion Effectiveness of PCE Superplasticizers"; pp. 87–102 *9th CANMET/ACI Conference on Superplasticizers and Other Chemical Admixtures in Concrete (Supplementary Papers)*, Edited by V. M. Malhotra. ACI, Seville, 2009.

[28]J. Plank and B. Sachsenhauser, "Impact of Molecular Structure on Zeta Potential and Adsorption Conformation of α-Allyl-ω-Methoxypolyethylene Glycol - Maleic Anhydride Superplasticizers," *J. Adv. Concr. Technol.*, **4** [2] 233–9 (2006). □

Paper 3

Synthesis and Performance of a Modified Polycarboxylate Dispersant for Concrete Possessing Enhanced Cement Compatibility

Ahmad Habbaba, Alex Lange, Johann Plank

Journal of Applied Polymer Science
published online on November 13, 2012

DOI: 10.1002/app.38742

Journal of Applied Polymer Science

Synthesis and Performance of a Modified Polycarboxylate Dispersant for Concrete Possessing Enhanced Cement Compatibility

Ahmad Habbaba, Alex Lange, Johann Plank
Technical University of Munich, Chair for Construction Chemicals, Lichtenbergstr 4, 85747 Garching, Germany
Correspondence to: J. Plank (E-mail: sekretariat@bauchemie.ch.tum.de)

ABSTRACT: It is well established that the performance of polycarboxylate (PCE) superplasticizers can be severely affected by the composition of individual cements. Here, a novel allylether/maleic anhydride (APEG)-based PCE was synthesized using allyl maleate monomer as a new, additional building block. When polymerized into the PCE main chain, this building block was found to form a cyclic lactone structure. The resulting PCE molecule was tested with respect to the dispersing force in cements possessing different phase compositions and alkali sulfate (K_2SO_4) contents. These data were compared with those from conventional APEG- and methacrylate ester (MPEG)-type PCEs. Results obtained from cement paste flowability and adsorption measurements suggest that the modified PCE disperses all cement samples well and hence is more robust against variations in cement composition. Apparently, the new building block induces a higher affinity of the polymer to the surface of cement and can form a denser polymer layer. © 2012 Wiley Periodicals, Inc. J. Appl. Polym. Sci. 000: 000–000, 2012

KEYWORDS: adsorption; rheology; plasticizer; radical polymerization

Received 30 July 2012; accepted 18 October 2012; published online
DOI: 10.1002/app.38742

INTRODUCTION

Polycarboxylate (PCE) superplasticizers are applied in the construction industry to produce highly flowable concretes such as e.g. self-compacting or high strength concrete which are characterized by a low water-to-cement ratio (w/c). Also, specially modified PCE superplasticizers can provide excellent fluidity retention over a time period of 2 h and more. Generally, PCEs are comb-shaped copolymers which consist of a negatively charged backbone holding carboxylate groups and grafted side chains commonly composed of polyethylene oxide units. The charged backbone can adsorb onto the surface of hydrating cement particles in three different ways, namely in train, loop or tail mode, while the nonadsorbed graft chains protrude from the cement surface into the pore solution.[1] The interaction between superplasticizers and cement is generally well understood.[2,3] The mechanism behind the dispersing effect of PCEs is based on steric hindrance between cement particles as well as electrostatic repulsion forces.[4–6]

It was observed that in concrete manufacturing, certain PCE molecules do not work well with specific cements, thus the flowability obtained at a given dosage of these PCEs was rather poor. Moreover, in some cases, the PCEs failed completely to provide any fluidity. This phenomenon is commonly referred to as "incompatibility" between cement and specific PCE products. Various explanations have been presented for this behavior, such as the variation in clinker composition of cement, contamination of the concrete with clay or silt, and perturbation of PCE adsorption by sulfate ions released from cement ("sulfate effect").[7] Because of these undesired effects, the usage of PCE superplasticizers in the concrete manufacturing industry has experienced some setback recently and prompted a partial revival of polycondensate-based superplasticizers.

The sulfate components present in cement can occur in four different forms: gypsum, hemihydrate ($CaSO_4 \cdot {}^1/_2H_2O$), anhydrite and alkali sulfates. Generally, sulfate has a remarkable impact on the properties of cement. Overdosing results in a false set which is owed to spontaneous crystallization of gypsum while a lack of sulfate in cements possessing a high calcium aluminate (C_3A) content may lead to a flash set during the initial stage of hydration.[8]

Previous works have clearly shown the strong influence of alkali sulfates present in cement on the performance of PCEs as a result of their rapid dissolution and thus release of sulfate ions.[7,9,10] First, some researchers found that the sulfate content present in cement can significantly impede the flowability of the slurries containing PCE.[9,10] Opposite to this trend it was demonstrated that a high dosage of K_2SO_4 may in fact enhance the workability retention ("slump loss behavior") of certain PCEs.[10]

Consequently, some researchers believe that an optimum content of alkali sulfate exists for PCE performance.[11] As mechanistic explanation, it is presented that higher sulfate concentrations existing in cement paste cause lower adsorption of PCE.[12] Other researchers reported evidence that the side chain of PCE comb polymers might become compressed when elevated contents of sulfate ions are present in the cement pore solution. The corresponding shrinkage of the PCE molecule decreases the steric hindrance effect.[9]

Here, we report on the impact of different cement compositions and sulfate concentrations on the workability of concrete achieved by a specifically designed polycarboxylate molecule. First, its tolerance against three different cement samples possessing distinctly different tricalcium aluminate (C_3A) contents was compared. Second, the behavior in the presence of increased amounts (0–2 wt %) of free dissolved sulfates (added as K_2SO_4) was probed utilizing the "mini slump" test. Additionally, adsorption isotherms were obtained to assess whether this PCE and sulfate actually involve in competitive adsorption. From this data it was aimed to propose a model explaining the difference in cement compatibility between conventional PCE and the novel PCE molecule which incorporates a new structural feature.

MATERIALS AND METHODS

Cement Samples

Three different cement samples (CEM I 32.5 R from HeidelbergCement, Rohrdorf plant/Germany; CEM I 42.5 R from HeidelbergCement, Geseke plant/Germany; and CEM I 52.5 R from Holcim, Lägerdorf plant/Germany), all ordinary Portland cements, were used in this work. Table I lists their phase compositions as determined by quantitative X-ray diffraction (XRD) analysis using *Rietveld* refinement and thermogravimetry. D8 advance instrument from Bruker-AXS (Karlsruhe/Germany) was used in the XRD analysis while thermogravimetry was performed on a STA 409 PC apparatus from NETZSCH, Selb/Germany. Specific surface area and particle size distribution (d_{50} value) were determined using a *Blaine* instrument (Toni Technik, Berlin/Germany) and a laser granulometer (Cilas 1064, Marseille/France), respectively.

Table I. Phase Compositions and Properties of the Cement Samples Employed in the Study

Phase	CEM I 32.5R wt %	CEM I 42.5R wt %	CEM I 52.5R wt %
C_3S	60.4	67.2	70.3
C_2S	11.9	14.0	12.0
C_3A	9.3	8.4	1.1
C_4AF	7.3	2.7	12.5
Free lime	1.9	0.1	0.5
Periklas	2.0	0.0	0.0
Anhydrite	3.1	2.4	0.3
Hemihydrite	1.3	0.0	1.8
Gypsum	0.0	0.0	0.2
Calcite	2.6	3.8	0.6
Quartz	0.3	0.8	0.0
K_2O	0.9	0.7	0.4
Na_2O	0.3	0.2	0.2
Spec. surface area (Blaine) ($cm^2\ g^{-1}$)	3 040	3 300	4 700
d_{50} value (μm)	16.16	10.82	6.80
water/cement ratio (w/c)[a]	0.48	0.55	0.505

[a]Value to obtain a paste spread of 18 ± 0.5 cm.

Chemicals

K_2SO_4 powder, maleic anhydride, allyl alcohol, and benzoyl peroxide, all analytically pure grade, were purchased from Merck KGaA, Darmstadt/Germany. The allyl ether macromonomer α-allyl-ω-methoxy polyethylene glycol ($n_{EO} = 34$) was obtained from NOF CORPORATION, Tokyo, Japan.

Polycarboxylate Samples

Five PCE superplasticizers were synthesized and tested. As first polymer, the novel PCE copolymer was prepared from α-allyl-ω-methoxypolyethylene glycol ether macromonomer, maleic anhydride, and allyl maleate as a new building block.

A typical synthesis is carried out following the principal process described in a patent application.[13] First, the building block is synthesized by reacting 6.25 g (64 mmol) of maleic anhydride with 3.72 g (64 mmol) of allyl alcohol at 60°C for 1 h. Note that it is critical to avoid any molar excess of allyl alcohol, for the reason explained below. During the reaction, the maleic anhydride will melt and form a homogeneous reaction product with the allyl alcohol which is allyl maleate with a purity of about 96%. The synthesis method described here inevitably produces a small amount of diallyl maleate (~2%) which can act as a crosslinking agent during subsequent PCE synthesis which makes the polymer ineffective as cement dispersant. Therefore, higher concentrations of diallyl maleate must be avoided, and the best way is to react maleic anhydride with a slight substoichiometric amount of allyl alcohol. To further purify the allyl maleate, it was distilled under vacuum (3 h Pa) to yield a colorless, nearly odorless liquid. The allyl maleate should be stored in a cool, dark place and should be consumed rapidly as it was found to undergo self polymerization.

Second, synthesis of the novel PCE is carried out by mixing 100 g (64 mmol) of allylether macromonomer ($n_{EO} = 34$), 6.25 (64 mmol) g of maleic anhydride and 10.0 g (64 mmol) of purified allyl maleate. This mixture is heated to 90°C and the reaction vessel is flushed with an inert gas, preferably nitrogen. While stirring, 2.00 g of benzoyl peroxide are added as powder continuously over a time period of 90 min. The quality of the resulting polymer greatly depends on accurate and uninterrupted addition of this radical initiator. After complete addition of the benzoyl peroxide, the mixture is heated to 100°C and is stirred for another 90 min. The viscosity of the mixture will gradually increase, but remains stirrable over the whole reaction period. During the polymerization process, the color of the reaction mixture will change to yellowish. At the end, ~120 mL of deionized water are added to the reaction mixture while it is still hot to yield a polycarboxylate solution of ~50 wt % solid content. The solution can be neutralized with 30 wt % aqueous NaOH which will produce the

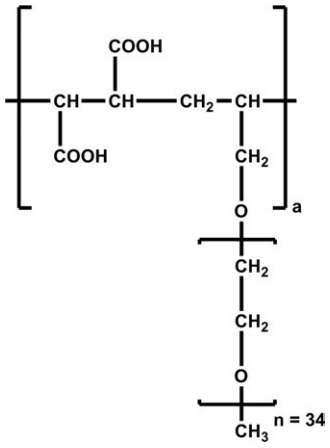

Figure 1. Chemical structure of the synthesized APEG-based PCE sample.

sodium salt of the PCE. This polymer was designated as modified PCE (*m*34APEG).

For comparison, the same APEG-type PCE as above, but in the absence of the building block allyl maleate was prepared following the description as before. This reference polymer was designated as 34APEG. The chemical structure of this type of PCE polymer which is strictly tactical because allyl ether does not homopolymerize is displayed in Figure 1.

For further comparison, three more PCEs (*x*MPEG*y*) based on methacrylic acid-*co*-*ω*-methoxy poly(ethylene glycol) (MPEG) methacrylate ester were prepared. This kind of PCE is among the most commonly used PCE products which are applied in concrete. Their general chemical structure is shown in Figure 2. There, "*x*" refers to the number of ethylene oxide units (n_{EO}) present in the side chain of the PCE comb polymers and was 25 or 45, respectively, whereas "*y*" refers to the molar ratio of methacrylic acid to MPEG methacrylate ester which was 6 : 1, 3 : 1, and 1.5 : 1, respectively. Aqueous radical copolymerization was utilized to synthesize these copolymers. The initiator used was sodium peroxodisulfate, and methallyl sulfonic acid was employed as a chain transfer agent. Details of the synthesis process have been disclosed before.[14]

After copolymerization, polymer solutions were generally neutralized with sodium hydroxide and dialyzed using a 6000–8000 Da cellulose cut-off membrane (Spectra/Pro, Spectrum Laboratories, Rancho Dominguez, CA). After concentration under vacuum in a rotary evaporator ("Rotovap" Laborota 4003 from Heidolph Instruments GmbH & Co. KG in Schwabach/Germany), viscous polymer solutions possessing solid contents of ~40 wt % were obtained.

All copolymers were characterized using Waters 2695 gel permeation chromatography (GPC) separation module equipped with a refractory index detector (2414 module, Waters, Eschborn/Germany) and a Dawn EOS 3 angle static light scattering detector (Wyatt Technology, Clinton, SC). A d_n/d_c of 0.135 mL g^{-1} (value for poly(ethylene oxide)) was utilized to determine molar masses.[15] Ultrahydrogel columns 500, 250, 120 (Waters, Eschborn/Germany) with an operating range (PEO/PEG) of M_W between 100 and 1,000,000 Da were used. Eluent was 0.1*N* $NaNO_3$ at pH = 12 adjusted with NaOH.

Cement Pore Solution

The term "pore solution" (PS) generally describes the aqueous phase loaded with electrolytes which exists between cement particles when cement is dispersed in water at a specific water-to-solids ratio. Here, the pore solution was gained via vacuum filtration of the cement paste prepared from CEM I 32.5 R (w/c = 0.48) in the absence or the presence of 1 wt % (w/c = 0.5) or 2 wt % (w/c = 0.55) of K_2SO_4, respectively.

Anionic Charge Amounts of PCE Samples

The anionic charge amounts of the copolymers were determined by polyelectrolyte titration using a particle charge detector PCD 03 pH (BTG Mütek GmbH, Herrsching/Germany). The charge detector consists of a PTFE cylinder with an oscillating PTFE piston in the center. The polyanionic polymer adsorbs onto the Teflon surface, while the counter ions are being separated from the polymer when the piston is moving. This creates a streaming current, which is measured by two Pt electrodes inside the Teflon cylinder. The anionic charges were determined by titrating the PCEs dissolved in cement pore solutions using 0.001*N* poly(diallyldimethylammoniumchloride), PolyDADMAC as cationic counter-polyelectrolyte.

Mini Slump Test

Flowability of pastes obtained by dispersion of the neat cement samples or of cement plus K_2SO_4 was determined utilizing a "mini slump test" according to DIN EN 1015. The test was carried out as follows: Over a period of 1 min, 300 g of cement were filled into a porcelain cup which contained the specific amount of DI water. The w/c ratio was 0.3 for the cement compatibility test (Cement Compatibility section), while for all other tests the ratios provided in Table I were used to obtain a spread of 18 ± 0.5 cm. The mixture was allowed to soak for 1 min, stirred manually with a spoon for 2 min. Immediately after stirring, the slurry was poured into a Vicat cone (height 40 mm, top diameter 70 mm, bottom diameter 80 mm) placed on a glass plate, filled to the brim and the cone was removed vertically. The resulting diameter (spread) of the paste represents the flow value of the slurry. The spread was measured twice; the second measurement being perpendicular to the first one, and an average was obtained to give the slump value. Each test was repeated three times, and the average of the paste flow diameter was reported as the slump flow

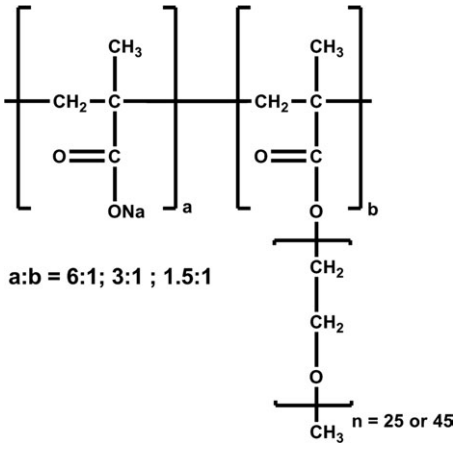

Figure 2. Chemical structure of the synthesized MPEG-based PCE samples.

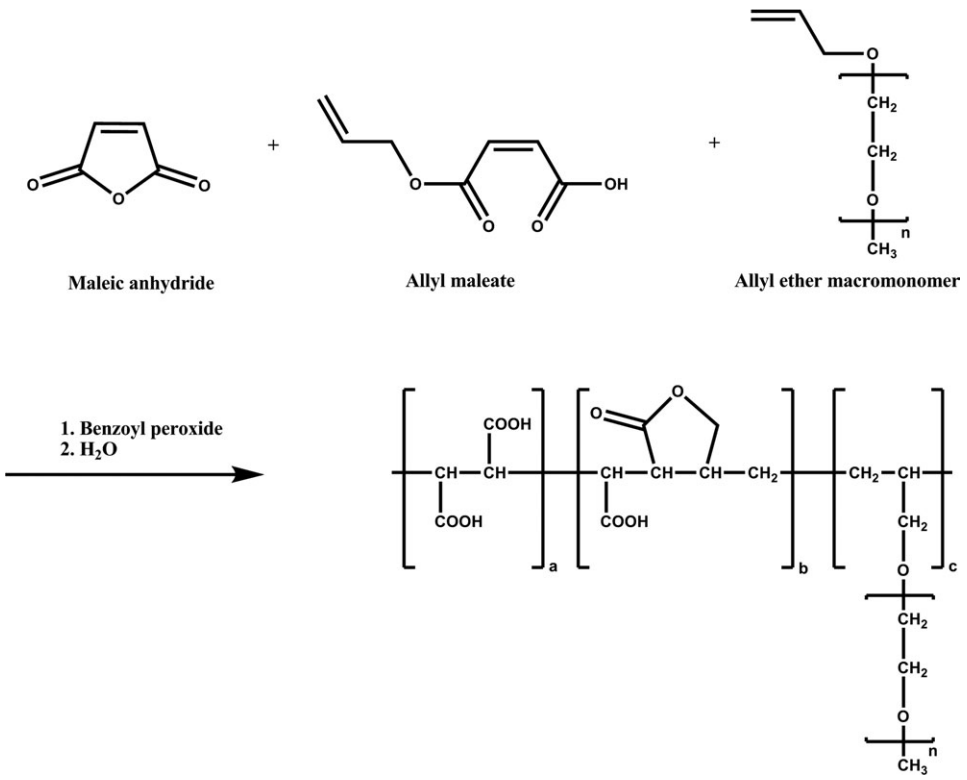

Scheme 1. Reaction sequence leading to the formation of modified PCE polymer *m*34APEG.

value. The margin of error was ±3%. Using this test protocol, the PCE dosages required to reach a spread of 26 ± 0.5 cm were determined.

Adsorption of PCE Samples

The adsorbed amounts of the PCEs on cement were determined according to the depletion method. Different dosages of copolymer were added to the slurries of the cement sample CEM I 32.5 R blended with different amounts of K_2SO_4 (w/c = 0.5 and 0.55 for cement blended with 1 and 2 wt % sulfate, respectively). The pastes were filled into 50 mL centrifuge tubes, shaken for 2 min at 2400 rpm in a wobbler (VWR International, Darmstadt/Germany) and centrifuged for 10 min at 8500 rpm in a centrifuge (Heraeus International, Osterode/Germany). For quantification of the organic carbon content in the supernatant, a High TOC II apparatus from Elementar (Hanau/Germany) was used. Centrifugates were diluted at 20 : 1 (v/v) with 0.1*N* HCl to remove inorganic carbonates and to prevent the dissolution of carbon dioxide in the alkaline solution. The samples were oxidized in a glass tube at 1000°C on a platinum catalyst using synthetic air, the exhaust gas was dried over phosphorous pentoxide and the carbon dioxide was determined in a NDIR cell. The amount of organic carbon present in the sample was calculated based on the values obtained for monopotassium phthalate which was used as calibration standard. The adsorbed amounts of individual PCEs were obtained by subtracting the concentration of PCE found in the centrifugate from the initial PCE concentration existing prior to contact with cement. All measurements were repeated three times and averaged.

Hydrodynamic Radius of PCE Molecules

Different polymer solutions were prepared by dissolving 1 g of PCE powder in 100 mL of cement pore solution (see Cement Pore Solution section), and the average particle sizes of individual PCE molecules were determined by dynamic light scattering measurement using a Horiba LB-550 instrument (HORIBA, Kyoto/Japan). Each sample was measured four times, and the average was reported as the hydrodynamic radius of PCE.

Other Instruments

For ^{1}H NMR analysis, a 250 MHz spectrometer from Bruker BioSpin, Karlsruhe/Germany was utilized while IR was conducted using a Vertex 70 FTIR—ATR instrument from Bruker Optics, Karlsruhe/Germany. Quantification of sulfate concentration contained in cement pore solutions was performed on an ICS-2000 ion chromatograph from Dionex, Sunnyvale, CA.

RESULTS AND DISCUSSION

Synthesis and Chemical Structure of the Modified PCE

The novel type of PCE was synthesized by free radical copolymerization in bulk from allyl ether macromonomer, maleic anhydride, and allyl maleate at a molar of ratio 1 : 1 : 1. The sequence of reactions occurring in the synthesis is described in Scheme 1.

Surprisingly, it was found that allyl maleate which presents a potential crosslinking agent for PCE does not much increase the molecular weight and viscosity of the aqueous *m*34APEG solution. Also, in the ^{1}H NMR spectrum of the purified terpolymer, only traces of protons characteristic for the allyl C=C double bond were detected (Figure 3). These observations prompted the idea that during the copolymerization process, the allyl maleate building block undergoes cyclization to a five-membered heterocyclus, as is shown in Scheme 1. Such ring formation has

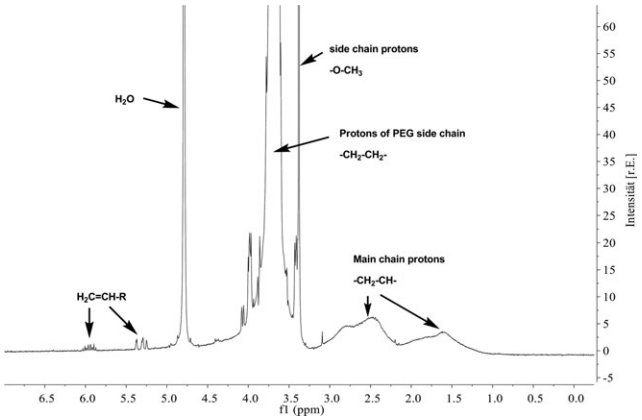

Figure 3. ^{1}H NMR spectrum of the purified *m*34APEG copolymer, measured in D_2O.

been reported before for unconjugated dienes.[16] Further evidence for the formation of a lactone ring was provided by FT-IR spectroscopy. There, a signal at ~1760 cm^{-1} which is characteristic for the C=O absorption in a five-membered lactone ring appeared (Figure 4). For comparison, in γ-butyro lactone, the same group produces an absorption at 1770 cm^{-1}.[17] Another indirect proof for cyclization lies in the fact that when the reaction products of acrylic or itaconic acid with allyl alcohol are used in the PCE synthesis, the resulting terpolymers exhibit significantly higher M_w than the nonmodified reference polymer, as a result of crosslinking plausibly induced by the unreacted C=C double bond present in allyl acrylate or allyl itaconate which apparently did not undergo cyclization. Also, in these copolymers, no IR absorption characteristic for a lactone CO groups was found. These observations signify that an α-olefinic proton is required to undergo this reaction, and such proton is only available in maleic anhydride. To conclude, with the lactone cycle the newly synthesized PCE possesses a specific structural feature which clearly distinguishes it from conventional PCE molecules.

Next, the characteristic molecular properties of *m*34APEG sample were compared with those of the non-modified reference polymer. The results are exhibited in Table II. According to this data, it is evident that the modified and nonmodified PCE samples possess very comparable properties with respect to molar masses, polydispersity and hydrodynamic radius. The differences lie in their specific anionic charge amounts, as is shown in

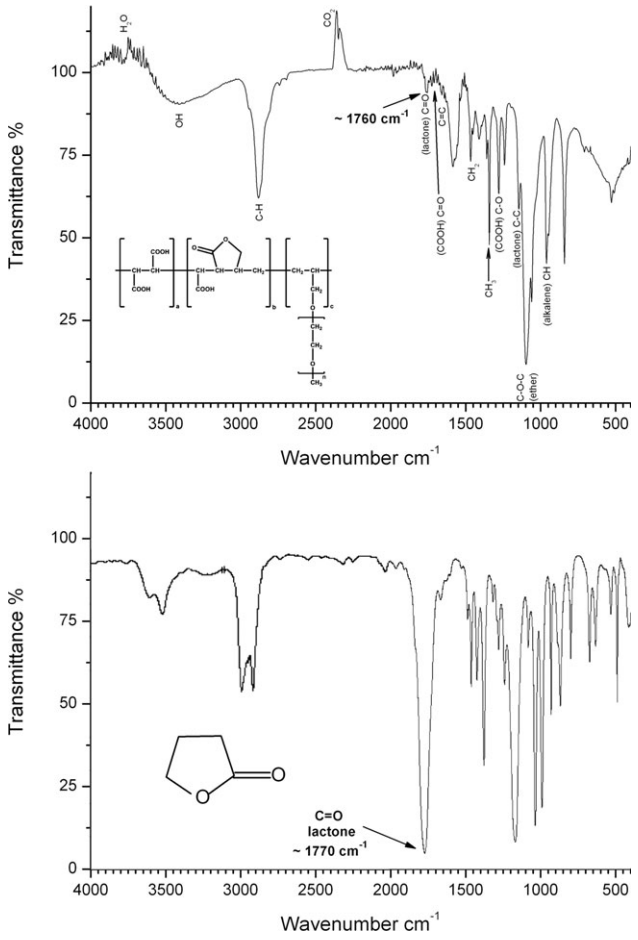

Figure 4. FT IR spectra of modified PCE polymer *m*34APEG containing the allyl maleate building block (top) and of γ-butyro lactone17 (bottom).

Table II. There, it becomes evident that *m*34APEG possesses a higher anionic charge than 34APEG, as a result of incorporation of the charged building block.

Cement Compatibility

In the following, the dispersion ability of this new PCE molecule was compared with those from PCEs possessing conventional structures. To probe the robustness against variations in cement compositions, namely the tricalcium aluminate (C_3A) content, distinctly different cement samples were selected and tested. Here, a w/c ratio of 0.3 was chosen for all cement pastes

Table II. Characteristic Properties of the Synthesized PCE Comb Polymers

Copolymer	Side chain n_{EO}	Molar masses		Polydispersity index (M_W/M_n)	Hydrodynamic radius $R_{h(avg)}$ (nm)	Spec. anionic charge in CPS[a] (μeq g^{-1})
		M_W (g mol^{-1})	M_n (g mol^{-1})			
*m*34APEG	34	78,430	24,830	3.2	7.0	195
34APEG	34	63,100	22,900	2.8	6.2	140
25MPEG3	25	67,590	28,290	2.4	6.0	1100
45MPEG1.5	45	196,300	51,900	3.8	8.7	145
45MPEG6	45	163,100	45,570	3.6	10.2	910

[a]CPS = cement pore solution gained from cement sample CEM I 32.5 R.

to challenge the polymer's ability to disperse under particularly difficult conditions. The results are shown in Figure 5.

The data suggests that sample CEM I 32.5R is particularly difficult to disperse by PCE, plausibly because of a combination of high C_3A and free lime content (Table I). All nonmodified PCE samples 34APEG and 25MPEG3 (the latter was chosen as an example for MPEG-type PCEs; the two other MPEG samples produced similar results) require substantially higher dosages than the modified PCE sample *m*34APEG. We attribute its superior behavior to incorporation of the new building block allyl maleate which apparently renders the PCE molecule more robust against high contents of C_3A and free lime.

In practical concrete manufacturing, the robustness of the modified PCE presents a huge advantage because it allows to switch cement suppliers without the need of reformulating the entire mix design. This way, extensive lab testing can be avoided.

Tolerance to Sulfate

Sulfates are contained in every Portland cement, both as alkali sulfates originating from the combustion of sulfurous fuel which produces SO_3, and from the addition of calcium sulfates for set control of cement. Depending on the manufacturer, significant variations in the sulfate contents of individual cement samples can occur, whereby high sulfate concentrations can severely impede the effectiveness of PCE polymers ("sulfate effect").[10]

In the literature, two mechanisms are discussed to explain the negative effect of sulfate on PCEs: First, competitive adsorption between sulfate and PCE, whereby the highly anionic sulfate ions preferably adsorb onto cement and occupy most of the surface sites on hydrates available for adsorption. This way, PCE is prevented from adsorbing in sufficient amount on cement. The second mechanism involves shrinkage of the PCE molecule, which leads to a more coiled conformation that cannot adsorb as easily on cement.[9]

According to that, we studied the behavior of our PCEs in two steps: at first, the impact of sulfate on the workability of the PCEs in cement paste was determined utilizing mini slump tests. Second, the effect of sulfate on the adsorbed amounts of the PCEs was studied. For these tests, the "difficult" cement sample CEM I 32.5 R (w/c = 0.48) was used. To this cement, 1 wt % (w/c = 0.5) or 2 wt % (w/c = 0.55) of K_2SO_4, respectively were added to generate an elevated sulfate content in cement. Utilizing ion chromatography, the sulfate concentrations as follows were determined in the pore solutions: (a) neat cement: 12.8 g L^{-1}; (b) cement + 1 wt % K_2SO_4: 20.8 g L^{-1}; (c) cement + 2 wt % K_2SO_4: 23.6 g L^{-1} of SO_4^{2-}.

Impact on Workability. The following experiments were carried out using the CEM I 32.5 R sample, a cement which was demonstrated before to possess high "incompatibility" with conventional PCEs, as a result of its high C_3A and free lime content (Figure 5). The initial spread of this cement paste (w/c = 0.48) was 18 ± 0.5 cm. To achieve the target flow of 26 ± 0.5 cm, the required dosages of the PCE samples were 0.095; 0.11; 0.10; 0.18, and 0.21 % bwoc (by weight of cement) for *m*34APEG, 34APEG, 25MPEG3, 45MPEG6, and 45MPEG1.5, respectively.

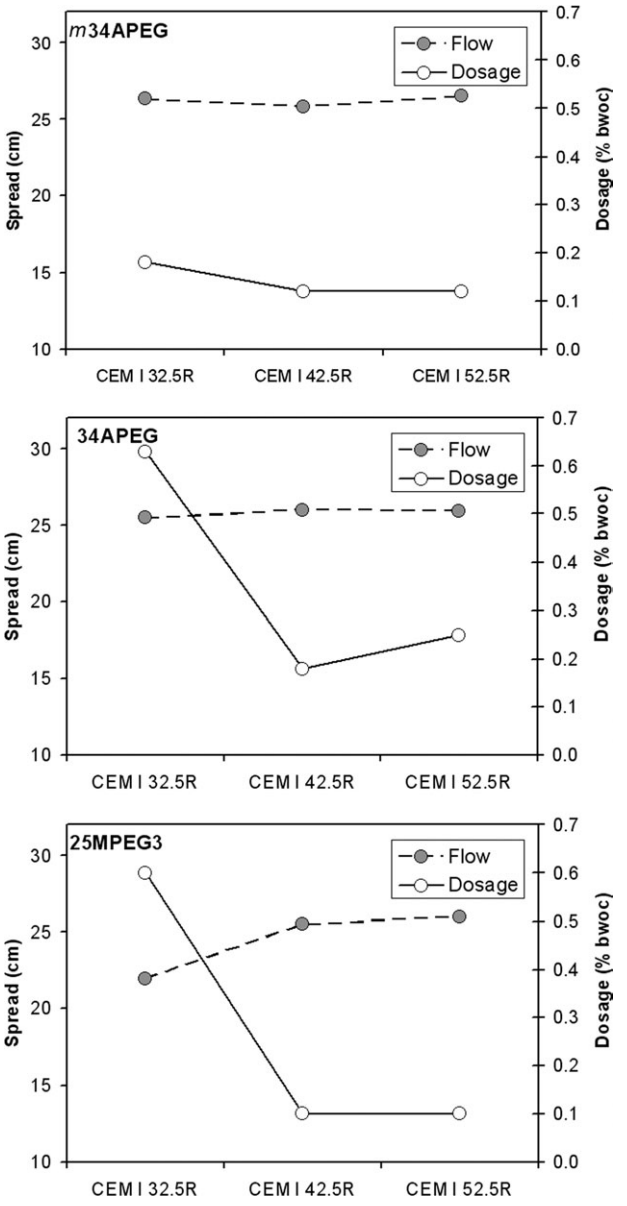

Figure 5. Dispersing ability of PCE polymers *m*34APEG, 34APEG, and 25MPEG3 in pastes (w/c = 0.3) prepared from different cement samples.

At these dosages, the influence of K_2SO_4 on the dispersing effectiveness of the PCEs in the cement slurries was determined. Up to 2 % bwoc of K_2SO_4 were added as solid to the freshly mixed cement paste and worked into the slurry by stirring for 5 min before measurements were taken. The results are presented in Figure 6.

It was found that the modified PCE sample *m*34APEG exhibits the highest robustness against sulfate, while its reference polymer 34APEG shows a particularly weak tolerance against K_2SO_4. All MPEG-type PCE samples behave comparably with sulfate, their dispersion power is affected, but less than for the nonmodified APEG polymer 34APEG.

Again, the test results demonstrate that the new building block allyl maleate renders a PCE polymer with enhanced cement

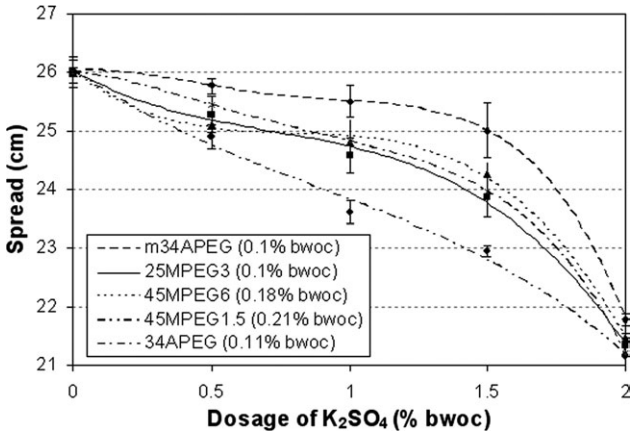

Figure 6. Effect of K_2SO_4 addition on the fluidity of cement pastes (CEM I 32.5 R, w/c = 0.48) holding different PCE samples.

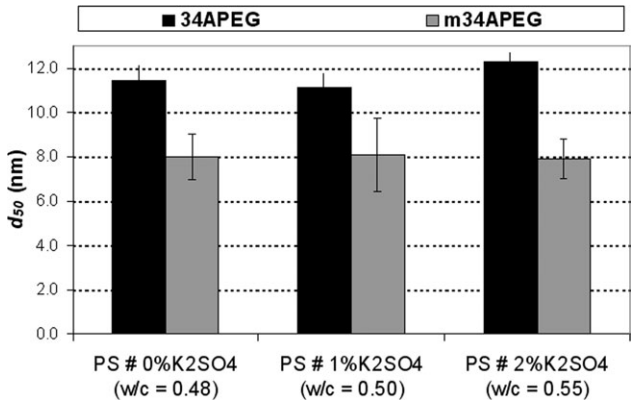

Figure 8. Hydrodynamic radius of PCE samples 34APEG and *m*34APEG, measured in filtrates of CEM I 32.5 R pastes at increased K_2SO_4 additions.

compatibility, here with respect to variation in the sulfate content.

Mechanism for Sulfate Tolerance. To understand the mechanism underlying the robustness in presence of sulfate, adsorbed amounts of the modified PCE on cement as a function of the K_2SO_4 amount added were determined. The results are shown in Figure 7.

Normally, the dispersing effectiveness of a superplasticizer directly correlates with the adsorbed amount of polymer. Consequently, adsorption of a sulfate tolerant PCE polymer can be expected to be quite independent of the sulfate concentration. Here, for *m*34APEG PCE it was found indeed that its adsorbed amounts are not much affected by different K_2SO_4 additions. This result instigates that the novel terpolymer possesses such high affinity to the surface of cement that even in competition with highly anionic sulfate ions, its adsorption still can take place. We attribute this enhanced affinity to its specific chemical structure as well as the higher anionic charge compared to 34APEG, as was shown in Table II.

In earlier literature, it was postulated that PCE molecules can shrink as a result of elevated sulfate content and thus become less effective.[9] This mechanism could provide another potential explanation for the increased sulfate tolerance of the novel PCE polymer. To investigate, the steric size (hydrodynamic radius, R_h) of *m*34APEG in the pore solutions of the cement/K_2SO_4 blends was determined. This experiment provides information on whether the PCE molecule is indeed compressed by dissolved sulfate ions and attains a coiled conformation. The results are presented in Figure 8.

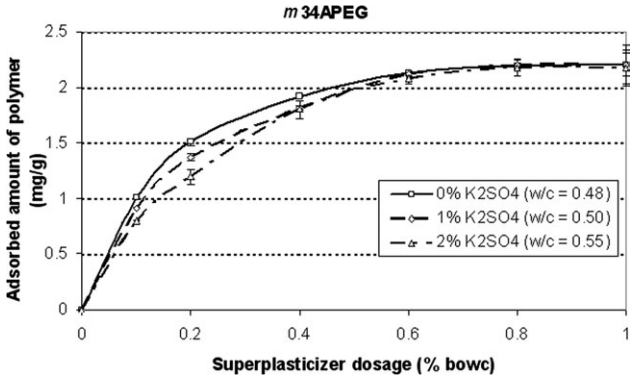

Figure 7. Adsorption isotherms for PCE polymer *m*34APEG on CEM I 32.5 R at 0–2% bwoc K_2SO_4 addition.

Obviously, the hydrodynamic radius of *m*34APEG remains stable at ~8 nm and is independent of the K_2SO_4 amount present. This clarifies that the molecule is not shrunk by dissolved sulfate ions. Thus, the sulfate concentration present in the pore solution has no influence on the steric size of this PCE polymer.

As a comparison, the steric size of the reference polymer 34APEG was measured. Again, it was found that its radius was independent of the sulfate concentration. This way, it was demonstrated that for the two APEG-type PCE molecules tested here, sulfate induced coiling of the macromolecules is not occurring. More important, however, is the observation that nonmodified 34APEG generally possesses a significantly larger steric size (d_{50} = 12 nm, Figure 8), compared to *m*34APEG (~8 nm). This instigates that upon adsorption, the modified PCE polymer can form a much denser polymer layer on the surface of cement, and thus can develop a considerably stronger dispersion force, in particular as it carries a higher anionic charge than 34APEG.

CONCLUSIONS

The experiments demonstrate that a PCE polymer containing a five-membered lactone ring as a novel building block exhibits improved cement compatibility, because it is less affected by high C_3A, free lime and sulfate concentrations occurring in different cement samples.

During the hydration process of cement, sulfate ions are originated from dissolving calcium sulfates and alkali sulfates which can significantly perturb the dispersing performance of specific PCE molecules as a result of decreased adsorption. From the experiments conducted it is suggested that in the presence of sulfates, the PCE polymer containing the lactone ring is

performing more robust than conventional PCE polymers. This property is attributed to its higher anionic charge and its smaller steric size which allows the formation of a more densely packed polymer layer on the surface of cement particles.

While the favorable behavior of the novel PCE polymer with sulfate anions can be explained, its high tolerance toward cements containing large amounts of C_3A and free lime was not clarified. Further studies are necessary to uncover the reason behind the negative effects of this combination on conventional PCE polymers.

ACKNOWLEDGMENTS

A. H. thanks Al-Baath University in Homs, Syria for a stipend to finance his study, and he warmly thanks TUM graduate school for their encouragement.

REFERENCES

1. Houst, Y. F.; Bowen, P.; Perche, F.; Kauppi, A.; Borget, P.; Galmiche, L.; Le Meins, J. F.; Lafuma, F.; Flatt, R. J.; Schober, I.; Banfill, P. F. G.; Swift, D. S.; Myrvold, B. O.; Petersen, B. G.; Reknes, K. *Cem. Concr. Res.* **2008**, *38*, 1197.
2. Ohta, A.; Sugiyama, T.; Tanaka, Y. In 5th International Conference on Superplasticizers and Other Chemical Admixtures in Concrete, Rome, Italy, SP-173, Malhotra, V. M., Ed.; CANMET/ACI, **1997**; p 359.
3. Yoshioka, K.; Sakai, E.; Daimon, M.; Kitahara, A. *J. Am. Ceram. Soc.* **1997**, *80*, 2667.
4. Sakai, E.; Kang, J. K.; Daimon, M. In 6th International Conference on Superplasticizers and Other Chemical Admixtures in Concrete, Farmington Hills, MI, USA, SP-195, Malhotra, V. M., Ed.; CANMET/ACI, **2000**; p 75.
5. Plank, J.; Hirsch, C. *Cem. Concr. Res.* **2007**, *37*, 537.
6. Blask, O.; Honert, D. In 7th International Conference on Superplasticizers and Other Chemical Admixtures in Concrete, Berlin, Germany, SP-217, Malhotra, V. M., Ed.; CANMET/ACI, **2003**; p 87.
7. Magarotto, R.; Torresan, I.; Zeminian, N. In Proceeding of the 11th International Congress on the Chemistry of Cement: Cement's Contribution to development in the 21st Century, Vol. 2, Durban, South Africa, May 11–16, Grieve, G., Owens, G., Eds.; **2003**; p 569.
8. Hanehara, S.; Yamada, K. *Cem. Concr. Res.* **1999**, *29*, 1159.
9. Yamada, K.; Ogawa, S.; Hanehara, S. *Cem. Concr. Res.* **2001**, *31*, 375.
10. Magarotto, R.; Moratti, F.; Zeminian, N. In 8th International Conference on Superplasticizers and Other Chemical Admixtures in Concrete, Sorrento, Italy, SP-239-15, Mallhotra, V. M., Ed.; CANMET/ACI, **2006**; p 215.
11. Jiang, S. P.; Kim, B. G.; Aitcin, P. C. *Cem. Concr. Res.* **1999**, *29*, 71.
12. Yoshioka, K.; Tazawa, E.; Kawai, K.; Enohata, T. *Cem. Concr. Res.* **2002**, *32*, 1507.
13. Plank, J.; Lange, A. EU Patent 22,002,354, **2012**.
14. Plank, J.; Pöllman, K.; Zouaoui, N.; Andres, P. R.; Schaefer, C. *Cem. Concr. Res.* **2008**, *38*, 1210.
15. Teresa, M.; Laguna, R.; Medrano, R.; Plana, M. P.; Tarazona, M. P. *J. Chromatogr. A* **2001**, *919*, 13.
16. Odian, G. Principles of Polymerization, 4th ed.; Wiley: New York, **2004**; p 832.
17. Available at: http://riodb01.ibase.aist.go.jp.eaccess.ub.tum.de/sdbs/cgi-bin/direct_frame_top.cgi, accessed on July 18, **2012**.

Paper 4

SYNERGISTIC AND ANTAGONISTIC EFFECT OF SO_4^{2-} ON DISPERSING POWER OF PC

Ahmad Habbaba, Nadia Zouaoui, Johann Plank

ACI Material Journal (American Concrete Institute)

Accepted on December 14, 2012

SYNERGISTIC AND ANTAGONISTIC EFFECT OF SO_4^{2-} ON DISPERSING POWER OF PC

Ahmad Habbaba, Nadia Zouaoui, Johann Plank*

Chair for Construction Chemicals, Technische Universität München, 85747 Garching, Germany

Biography:

ACI member **Ahmad Habbaba** is a senior Ph.D. student at the chair for construction chemicals, Technische Universität München, Germany. He studied chemistry and received his BS, MS and Diploma degree from Aleppo University (Syria). His research interests include interaction of admixtures with cement in concrete.

Nadia Zouaoui currently is a marketing manager for laboratory equipment. In 2009, she finished her Ph.D. at Technische Universität München on the topic "Impact of the molecular architecture of methacrylic acid-based polycarboxylates on their dispersion properties in $CaSO_4$ and Portland cement-based systems".

Johann Plank is full Professor at the Institute of Inorganic Chemistry of Technische Universität München, Germany. Since 2001, he holds the Chair for Construction Chemicals there. His research interests include cement chemistry, concrete admixtures, organic-inorganic composite and nano materials, concrete, dry-mix mortars and oil well cementing.

ABSTRACT

The dispersing performance of polycarboxylate (PC) superplasticizers can be strongly enhanced or impeded by sulfate ions present in cement pore solution. Here, two PCs based on methacrylic acid–*co*–ω–methoxy poly(ethylene glycol) methacrylate ester were tested in an inert model suspension based on $CaCO_3$ which contained different amounts of potassium sulfate. It was found that the dispersing effectiveness of highly anionic PCs is positively affected by sulfate, stemming from concomitant adsorption of both PC and sulfate. Contrary, sulfate negatively impacts performance of PCs possessing low anionic character as a consequence of competitive adsorption between PC and sulfate.

Keywords: Adsorption, Superplasticizer, Fluidity, Polycarboxylate, Zeta potential.

INTRODUCTION

Normally, PC-based superplasticizers are applied in the construction industry to produce highly flowable and/or high strength concrete possessing a low water to cement ratio. Some PC superplasticizers also show fluidity retention over time. Commonly, PCs are comb-shaped copolymers which consist of a negatively charged backbone holding carboxylate groups, and grafted side chains mainly composed of polyethylene oxide units. The charged backbone adsorbs onto the surface of the hydrated cement particles whereby three different conformations are possible (train, loop or tail), while the non-adsorbed graft chains protrude from the cement surface into the pore solution[1]. Owed to this mechanism, PC polymers possessing high specific anionic charge density adsorb in higher amounts on cement than PC molecules exhibiting lower anionic charge. The interaction between superplasticizers and cement is generally well understood[1-3]. The mechanism behind the dispersing effect of PCs is based on steric hindrance as well as electrostatic repulsion forces between the cement particles[4-7].

Usually, cement contains sulfate compounds which can occur in four different forms: gypsum, hemi-hydrate, anhydrite and alkali sulfates. The concentration of free dissolved sulfate ions present in cement pore solution is time-dependent and is impacted by the content of alkali sulfates, the fineness and kind of interground calcium sulfates, of temperature[8,9] and by the adsorption of specific polymers on the calcium sulfates[10]. Many researchers have empirically studied the dispersion behavior of PCs depending on the availability of sulfate ions in pore solution[4] while other authors pointed to the fact that low sulfate concentrations may lead to the formation of organo-mineral phases as a result of PC-C_3A interaction[11].

Several studies reported that a high concentration of free dissolved sulfate present in the pore solution can severely impact the dispersion performance of certain PCs[12-14]. This negative effect was explained by a model which includes sulfate-induced shrinkage of the PC molecule. It was

assumed that such coiled PC cannot adsorb as well as in the stretched conformation which exists when the sulfate concentration is low[15]. Other authors pointed out that competitive adsorption between PC and sulfate ions may play a more dominate role in the negative effect on cement dispersion[16,17].

All previous researches focused on the negative effect of sulfate ions on the dispersing performance of PC polymers in cement, while positive effects such as *e.g.* enhanced flowability of the concrete never were reported. In our works, however, we repeatedly noticed that specific PC molecules seemed to perform exceptionally well in their dispersing effectiveness with certain cements. Further investigation revealed that this phenomenon always occurred when a PC possessing high anionic charge amount was added to a cement paste containing a high concentration of free dissolved sulfate. So far, no explanation for this highly desirable effect was published.

At first, we attempted to investigate the mechanism underlying this positive effect in cement paste. But there, any analysis of sulfate migration from the pore solution to the surface of cement turned out to be impossible, because of the overwhelmingly high total concentration of SO_4^{2-} in the pore solution. Any depletion of sulfate e.g. by adsorption on cement would be so minor that it is essentially non-detectable. To escape this dilemma, we chose to conduct this study in a model inert system, namely a calcium carbonate (limestone) suspension. We deemed this acceptable because in cement paste, the two PC polymers studied exhibited similar trends with respect to their dispersing ability than in $CaCO_3$ suspension, *i.e.* polymer 45PC6 was a more effective dispersant than 45PC1.5. Compared to cement, the $CaCO_3$ system allows controlling and analyzing precisely the sulfate concentrations in the dissolved and adsorbed state. Moreover, no hydration process takes place, which can alter the ion concentrations in the pore solution or the surface chemistry of the solids particles.

In our study, we first investigated the impact of sulfate ions on the workability of aqueous $CaCO_3$ slurries containing two differently composed polycarboxylate-based superplasticizers. Next, the surface charge of limestone dispersed in water was determined via zeta potential measurement, followed by adsorption studies for PC and sulfate on $CaCO_3$ particles employing TOC measurements for PC and ion chromatography for SO_4^{2-} analysis. From this data, a model was derived which can explain the structure-related differences in the behavior of PCs in presence of various sulfate concentrations.

RESEARCH SIGNIFICANCE

Previous studies on the interaction between polycarboxylates and sulfate ions only focused on the negative impact of sulfate on dispersing performance of PC, while positive effects were overlooked. Here, it is shown that specific PC molecules in fact can benefit from the presence of higher sulfate concentrations in cement pore solution. The mechanism underlying this improvement in dispersing performance of specific PCs is concomitant adsorption of PC/SO_4^{2-}. Utilizing this synergistic effect, a more economical superplasticizer can be formulated by addition of controlled amounts of sulfate to the liquid admixture. Also, PC molecules which are negatively impacted by sulfate were identified.

EXPERIMENTAL INVESTIGATION

Materials

Limestone

Limestone powder "SCHAEFER Precal 18" (Schäfer Kalk GmbH & Co KG, Diez, Germany) with a density of 2.69 g/cm^3 (167.93 lb/ft^3) and an average particle size (d_{50} value) of 12.58 µm (49.5 × 10^{-5} in) was employed. Its purity was 98.4 % calcite (Q-XRD using *Rietveld* refinement). The specific surface area of the nearly spherical particles was found at 2,830 cm^2/g (339.1 gal/lb) (BET, N_2), and 2,688 cm^2/g (322.1 gal/lb) (Blaine method). All experiments with the limestone suspension

were performed at a water-to-$CaCO_3$ ratio of 0.413. When suspended in DI water, this calcium carbonate suspension exhibited a pH value of ~ 9.

Polycarboxylate samples

Two methacrylic acid–*co*–ω–methoxy poly(ethylene glycol) (MPEG) methacrylate ester based superplasticizers denominated as 45PC1.5 and 45PC6, resp. were synthesized and used in this work. Their general chemical structure is shown in **Fig. 1**. The number "45" in front of PC refers to the number of ethylene oxide units (n_{EO}) present in the side chains of the PC comb polymers, whereas the number behind PC refers to the molar ratio between methacrylic acid and MPEG methacrylate ester which either was 1.5:1 or 6:1. The copolymers were synthesized via free radical copolymerization in aqueous solution using sodium peroxodisulfate as initiator and methallyl sulfonic acid as chain transfer agent. Details of the synthesis process have been disclosed before[18]. After copolymerization, the polymer solutions were neutralized with sodium hydroxide and dialyzed using a 6,000 – 8,000 Da cellulose cut-off membrane (Spectra/Pro, Spectrum Laboratories Inc., Rancho Dominguez, CA, USA).

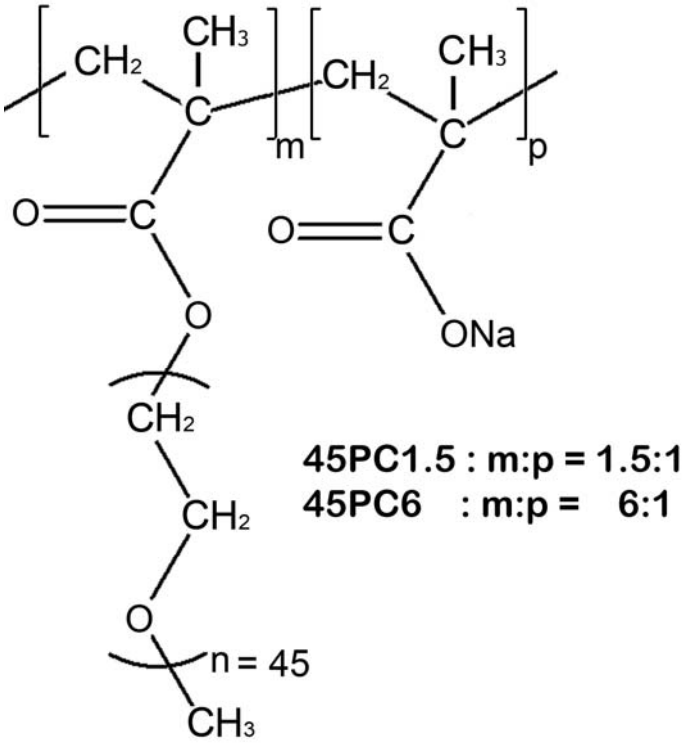

Fig. 1 – Chemical structure of the polycarboxylate copolymer samples

The copolymers were characterized using a Waters 2695 gel permeation chromatography (GPC) separation module equipped with a refractory index detector (2414 module, Waters, Eschborn, Germany) and a Dawn EOS 3 angle static light scattering detector (Wyatt Technology, Clinton, USA). A *dn*/*dc* of 0.135 mL/g (0.016 gal/lb) (value for polyethylene oxide) was utilized to determine molar masses[19]. Ultrahydrogel columns 500, 250, 120 (Waters, Eschborn, Germany) with an operating range (PEO/PEG) of M_W between 100 and 1,000,000 Da were employed. Eluent was 0.1 N $NaNO_3$ at pH=12 adjusted with NaOH. The data on properties of the PC samples obtained from GPC analysis is presented in **Table 1**.

Table 1 – Characteristic properties of the synthesized PC comb polymers

Copolymer	Molar ratio methacrylic acid:ester	Side chain n_{EO}	Molar masses M_W (g/mol)*	Molar masses M_n (g/mol)*	Polydispersity index (M_W/M_n)	Hydrodynamic radius $R_{h(avg)}$ (nm)**
45PC1.5	1.5	45	196,300	51,900	3.8	8.7
45PC6	6.0	45	222,300	52,340	4.2	10.4

*conversion factor: 1 g/mol = 0.035 oz/mol
**conversion factor: 1 nm = 3.937×10^{-8} in

K_2SO_4

K_2SO_4 powder, analytically pure grade (purchased from Merck KGaA, Darmstadt, Germany) was employed in the tests.

Methods

Mini slump test

Flowability of aqueous $CaCO_3$ pastes was determined utilizing a "mini slump test" according to DIN EN 1015. The test was carried out as follows: Over one minute, 300 g (10.58 oz) of limestone powder were filled into a porcelain casserole which contained 123.9 mL (4.19 fl oz) of DI water (w/s = 0.413 to obtain a target flow of 18 ± 0.5 cm (7.1 ± 0.2 in)), then left to soak for another minute and stirred again manually with a spoon for two minutes. Immediately after the stirring, the

paste was poured into a Vicat cone (height 40 mm (1.57 in), top diameter 70 mm (2.76 in), bottom diameter 80 mm (3.15 in)) placed on a glass plate filled to the brim and the cone was vertically removed. The resulting diameter of the paste represents the flow value of the slurry. This spread was measured twice; the second measurement being perpendicular to the first and averaged. Each test was performed three times, and the average of the paste flow diameters was reported as the slump flow value. The margin of error was ± 3%. When aqueous PC solutions were employed, then the amount of the water contained in the PC solution was subtracted from the volume of mixing water, to maintain a constant w/s ratio of 0.413.

Adsorption of PC and SO_4^{2-}

The adsorbed amounts of PC and sulfate on $CaCO_3$ were determined according to the depletion method. Certain dosages of either copolymer and/or K_2SO_4 were added to the $CaCO_3$ slurry, then filled into 50 mL (1.69 fl oz) centrifuge tubes, shaken for 2 min at 2,400 rpm in a wobbler (VWR International, Darmstadt, Germany) to equilibrate and centrifuged for 10 min at 8,500 rpm (Heraeus International, Osterode, Germany). Centrifugates were diluted 20:1 (v/v) with 0.1 N HCl to remove inorganic carbonates and to prevent sorption of carbon dioxide by the alkaline solution. The adsorbed amount of PC was obtained by subtracting the concentration of PC found in the centrifugate from the initial PC concentration existing prior to contact with limestone. Unadsorbed PC concentration was quantified using a High TOC II apparatus from Elementar (Hanau, Germany) which can determine the organic carbon content present in the supernatant.

To determine the concentration of sulfate in the pore solution, ion chromatography (instrument ICS-2000 from Dionex, Sunnyvale, CA, USA) was utilized. For quantification, a calibration curve employing different sulfate concentrations was developed. The adsorbed amount of SO_4^{2-} was determined by subtracting the amount of sulfate found in the pore solution from the initial amount added. All measurements were repeated three times and averaged.

Zeta potential

Electrokinetic properties were measured using a Model DT-1200 Electroacoustic Spectrometer (Dispersion Technology, Inc., Bedford Hills, NY, USA). The highly solids loaded $CaCO_3$ suspension requires an electroacoustic instrument to be able to measure in undiluted condition.

EXPERIMENTAL RESULTS AND DISCUSSION

To understand the fundamental interaction between the polycarboxylates and calcium carbonate, it is necessary to first study the surface chemistry of $CaCO_3$ particles in water. The main target here was to understand the electrical surface charge of the limestone dispersed in DI water, and to investigate the effect of sulfate ions on this charge by using zeta potential measurements.

Zeta potential of $CaCO_3$ dispersed in DI water

Zeta potential is the potential at the shear plane between the suspended solid particles and the liquid phase[20]. When dispersed in DI water, the surface charge of the limestone sample was positive (+ 40 mV). Such highly positively charged surface can attract any negatively charged molecule or anion present in the pore solution for adsorption.

To investigate the effect of SO_4^{2-} ions on the surface charge of the calcium carbonate particles, increased amounts of sulfate anions were titrated dropwise as 1 M K_2SO_4 solution to the $CaCO_3$ suspension. There, a strong decrease in zeta potential was found as a result of increasing SO_4^{2-} concentration (**Fig. 2**). At only ~ 0.15 mg SO_4^{2-}/g $CaCO_3$ (~ 1.05 gr SO_4^{2-}/lb $CaCO_3$) added, charge reversal from positive to negative occurred, supposedly as a result of increased sulfate adsorption on the $CaCO_3$ surface. After addition of 1.0 mg SO_4^{2-}/g (7.1 gr SO_4^{2-}/lb $CaCO_3$) $CaCO_3$, the surface charge of calcium carbonate attained a constant value of - 11.6 mV, thus indicating that the surface of limestone now is saturated with SO_4^{2-} ions and in equilibrium condition. Thus, no further decrease in the zeta potential value was observed when more sulfates was added. This experiment

demonstrates that the positively charged surface of $CaCO_3$ not only attracts anionic polymers, but can also be occupied by small inorganic anions such as sulfate.

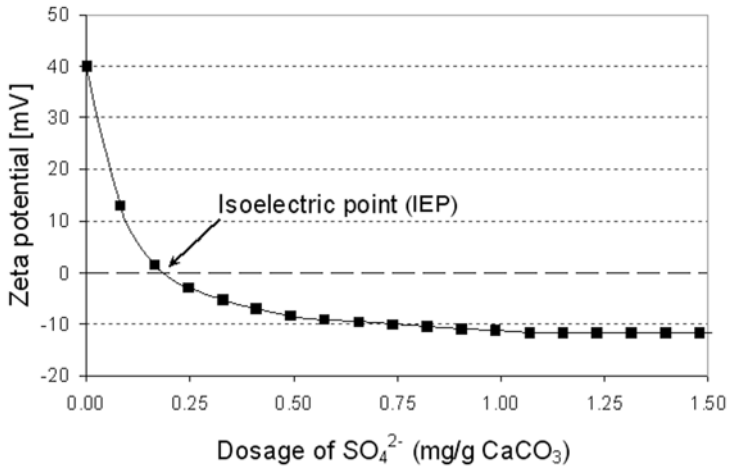

Fig. 2 – Zeta potential of $CaCO_3$ dispersed in DI water (w/s = 0.413) as a function of SO_4^{2-} ion concentration (conversion factor: 1 mg/g = 7.015 gr/lb)

Impact of sulfate on the dispersing power of PC

The initial spread of the limestone slurry employing the mini slump test was set at 18.3 cm (7.2 in) which corresponds to a w/s ratio of 0.413. No significant change in the spread was detected when 1.0 % by weight of solid (bwos) of K_2SO_4 was added to the slurry.

Whereas, addition of 0.05 % bwos of 45PC1.5 (no sulfate present) increased the spread of the slurry to 27.9 cm (11 in), thus confirming high efficiency of this PC. Even better performance was obtained from 45PC6 which required a dosage of only 0.03 % bwos to achieve a spread of 26.3 cm (10.4 in) (**Fig. 3** and **4**). Next, the influence of K_2SO_4 on the dispersing effectiveness of both PCs in the calcium carbonate slurry was studied as follows: 0.05 % bwos of 45PC1.5 or 0.03 % bwos of 45PC6 were mixed into the $CaCO_3$ suspension over 1 min, then soaked unagitated for another minute, followed by stirring for 2 min. After that, 1 % bwos of K_2SO_4 was added to the suspension and stirring continued for another 2 min. The final mixture was poured into a Vicat cone and its spread was measured.

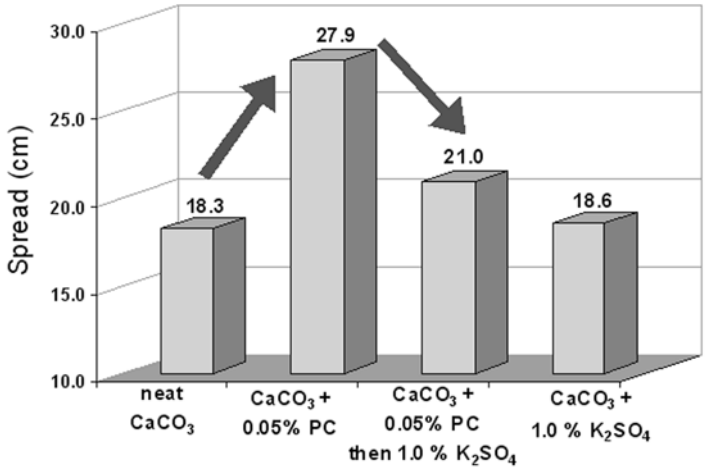

Fig. 3 – Effect of K_2SO_4 addition on the flowability of $CaCO_3$ slurry (w/s = 0.413) containing PC polymer 45PC1.5 (conversion factor: 1 cm = 0.394 in)

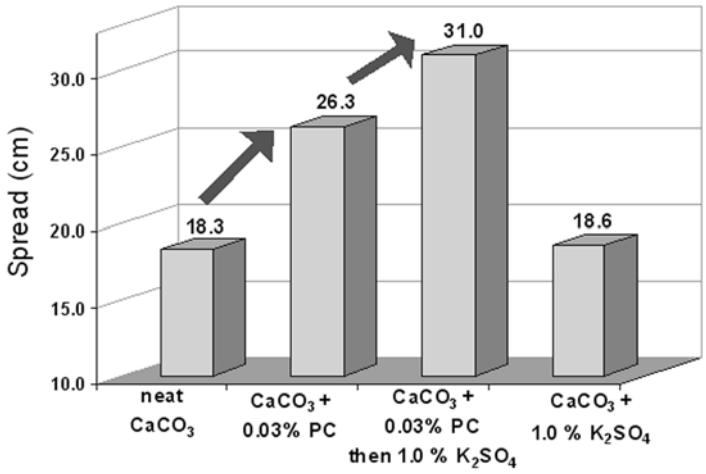

Fig. 4 – Effect of K_2SO_4 addition on the flowability of $CaCO_3$ slurry (w/s = 0.413) containing PC polymer 45PC6 (conversion factor: 1 cm = 0.394 in)

For the polymer 45PC1.5, a strong reduction in flowability from 27.9 cm (11 in) spread (no sulfate present) to 21.0 cm (8.3 in) (1 % K_2SO_4 added) was observed, indicating that the dispersing power of this kind of PC is severely impeded by elevated sulfate concentrations (**Fig. 3**). This behavior is in agreement with previous reports which describe a negative effect of sulfate on PC performance[12, 13, 15].

Contrary to 45PC1.5, addition of 1.0 % bwos of K_2SO_4 to the $CaCO_3$ slurry containing 0.03 % bwos of 45PC6 improved its fluidity substantially from 26.3 cm (10.4 in) (no sulfate present) to

31.0 cm (12.2 in) (**Fig. 4**), thus indicating a very beneficial synergistic effect between this PC and sulfate. In fact, in the presence of 1 % K_2SO_4 a dosage of only 0.018 % of 45PC6 were required to achieve the same spread (26.1 cm (10.3 in)) as with 0.03 % dosage in absence of sulfate. This demonstrates that such kind of PC can indeed benefit from the presence of high amounts of sulfate. To explain the reason behind this behavior, the adsorbed amounts of both PC and sulfate ions on $CaCO_3$ were determined.

Effect of K_2SO_4 on adsorption of PC samples

Normally, the dispersing effectiveness of superplasticizers correlates with their adsorbed amounts. The higher the adsorbed amount, the better is the fluidity of the paste. Thus, the adsorbed amounts of the PCs on $CaCO_3$ dispersed in DI water were determined for each copolymer by adding 0.05 % of 45PC1.5 and 0.03 % of 45PC6 respectively to individual limestone slurries (w/s = 0.413). After centrifugation, the residual PC contents were determined. The results are shown in **Fig. 5** and **6**, resp.

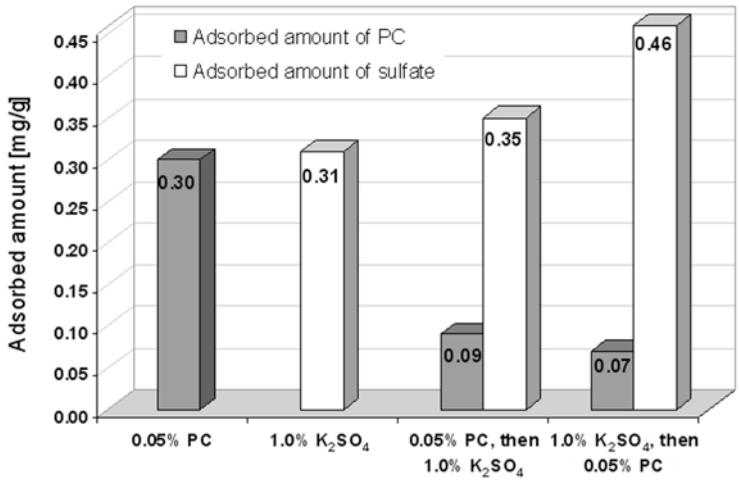

Fig. 5 – Effect of K_2SO_4 on the adsorbed amount of 45PC1.5 on $CaCO_3$ (w/s = 0.413) (conversion factor: 1 mg/g = 7.015 gr/lb)

For PC polymer 45PC1.5, a considerable impact of K_2SO_4 ions on its adsorption was observed. When 1.0 % bwos of potassium sulfate were added to the limestone slurry containing 0.05 % bwos

45PC1.5, then the adsorbed amount of this PC decreased from 0.3 mg/g $CaCO_3$ (2.1 gr/lb $CaCO_3$) to only 0.09 mg/g (0.63 gr/lb $CaCO_3$) (**Fig. 5**). In contrast to this PC, no significant change in the adsorption of 45PC6 was observed in the presence of 1.0 % bwos of K_2SO_4 (**Fig.6**).

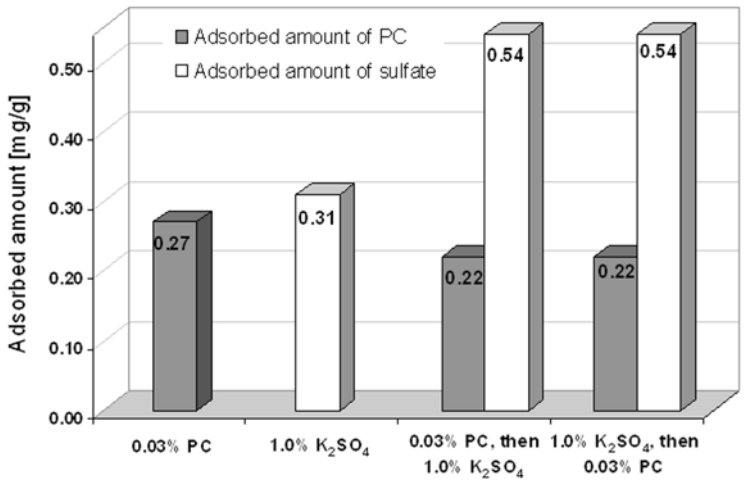

Fig. 6 – Effect of K_2SO_4 on the adsorbed amount of 45PC6 on $CaCO_3$ (w/s = 0.413) (conversion factor: 1 mg/g = 7.015 gr/lb)

On the other hand, ion chromatography revealed that when 1 % of K_2SO_4 is added to the $CaCO_3$ slurry (no PC present), then 0.31 mg SO_4^{2-}/g $CaCO_3$ (2.17 gr SO_4^{2-}/lb $CaCO_3$) adsorb on the calcium carbonate surface, as was already suggested by the zeta potential measurements displayed in **Fig. 2**. Thus, it is confirmed that sulfate indeed can occupy mineral surfaces such as in $CaCO_3$ if they are positively charged.

When 45PC1.5 is present in the K_2SO_4 treated $CaCO_3$ slurry, then adsorption of SO_4^{2-} ions on calcium carbonate is not much affected by this PC. It increases slightly from 0.31 to 0.35 mg/g $CaCO_3$ (2.17 to 2.46 gr/lb $CaCO_3$), but this change is practically within the accuracy of the analysis. Whereas, in the presence of 45PC6 sulfate adsorption increased substantially to 0.54 mg/g $CaCO_3$ (3.79 gr/lb $CaCO_3$), while the adsorbed amount of this PC decreased only slightly from 0.27 to 0.22 mg/g $CaCO_3$ (1.89 to 1.54 gr/lb $CaCO_3$).

To investigate whether the order of addition for PC and K_2SO_4 influences the results, an additional experiment was performed whereby at first 1.0 % of K_2SO_4 was added, and this was followed after 2 min of stirring by addition of 0.05 % bwos of 45PC1.5. The result is displayed in **Fig. 5**. According to this, from the tendency practically the same results were obtained, independent of the order of addition of PC and sulfate. Again, a high amount of sulfate and a low amount of PC adsorb. A similar effect was observed for the combination of 45PC6 with K_2SO_4 (results not shown in **Fig. 6**), i.e. the order of addition did not influence the adsorbed amount of PC and sulfate. Consequently, this experiment demonstrates that a different order of addition cannot mitigate the negative effect of SO_4^{2-} on PC polymers possessing low anionic character. Instead, adsorption of PC and sulfate presents a dynamic process whereby a final equilibrium is attained which may involve partial desorption of already adsorbed species by anions possessing higher charge density.

Mechanistic model

When dispersed in water, the limestone particles start to agglomerate due to Van der Waals attractive forces which normally occur at inter-particle distances in the range of 5 to 7 nm (19.7×10^{-8} to 27.6×10^{-8} in)[21]. Addition of anionic PC polymers and/or sulfate to the calcium carbonate slurry allows overcoming these forces as a result of adsorption, which therefore improves fluidity. Based on the above results, the impact of sulfate on the PC admixtures can be explained mechanistically as follows:

Addition of sulfate: The initially positively charged surface of $CaCO_3$ can attract SO_4^{2-} for adsorption, forming a very thin negative layer covering the surface. This layer produces some electrostatic repulsion between the particles. However, because of the very low thickness of this layer, the distances between particles are not large enough to overcome the Van der Waals attractive forces which hence will persist and cause agglomeration of the particles. Therefore, in spite of 0.31 mg SO_4^{2-}/g $CaCO_3$ (2.17 gr SO_4^{2-}/lb $CaCO_3$) adsorbed, no significant change was observed in the rheological properties of the limestone slurry.

Addition of PC: As is well established, the negatively charged PC polymers adsorb on positive mineral surfaces such as from limestone, thus generating a steric hindrance between the particles. Owed to the far extending side chain of PC, this repulsive force at the solid-liquid interface is strong enough to overcome the attractive Van de Waals inter-particle forces. Hence, addition of PC can improve the fluidity of the $CaCO_3$ slurry.

Addition of 45PC1.5 in presence of sulfate: Apparently, sulfate ions compete with this less anionic PC for adsorption sites on the surface of $CaCO_3$ and can replace a considerable amount of 45PC1.5 (as is shown in **Fig. 5**, the adsorbed amount of 45PC1.5 decreased from 0.3 mg/g to 0.09 mg/g (2.1 to 0.63 gr/lb) in presence of sulfate). Such polymer can only adsorb on surface sites which are not occupied by sulfate, causing only weak steric repulsion between the limestone particles. This concept is schematically illustrated in **Fig. 7**. Obviously, this type of PC possessing low anionic charge density is not able to compete well with sulfate for adsorption sites. As a consequence, its dispersing performance is severely impeded by sulfate, and only low fluidity is achieved.

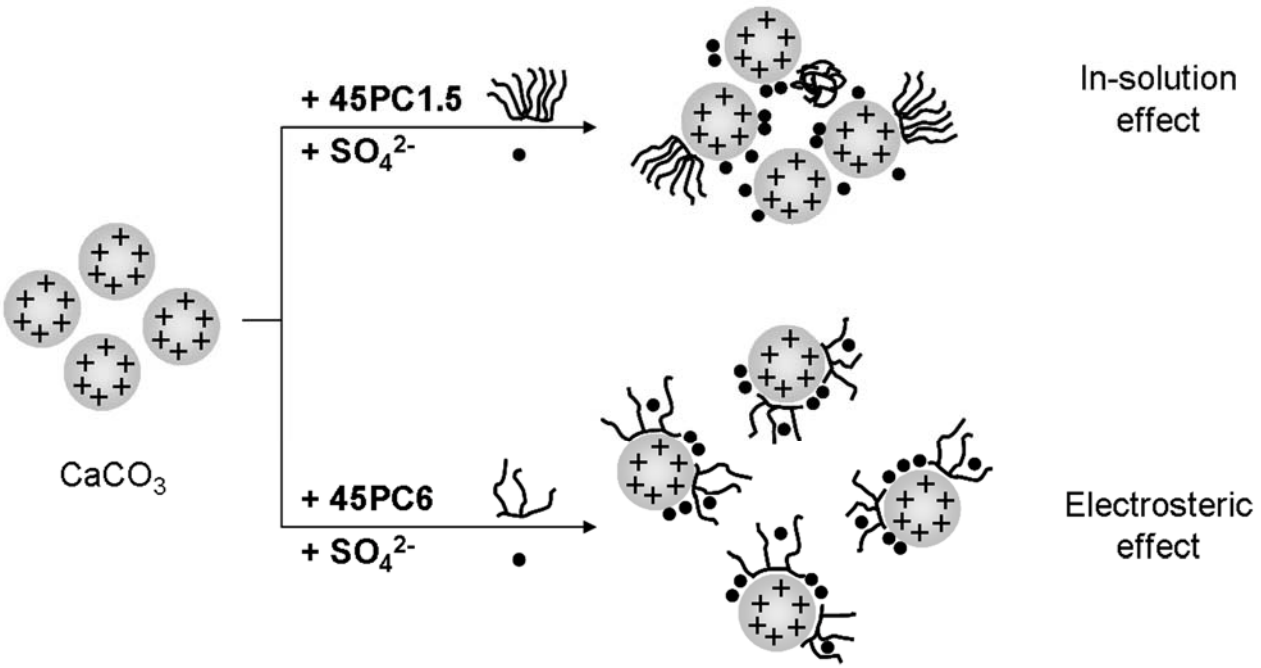

Fig. 7 – Schematic representation of the adsorption behavior of the two PC samples on $CaCO_3$ in the presence of sulfate, illustrating the electrosteric and in-solution effect (size of ions/atoms not to scale)

Addition of 45PC6 in presence of sulfate: Here, sulfate does not much impact adsorption of the polymer. Conversely, the adsorbed amount of sulfate ions increased in this case. Obviously, polymer 45PC6 is sufficiently anionic to occupy enough adsorption sites on the surface of $CaCO_3$ particles, thus causing a strong steric repulsion which is seconded by increased electrostatic repulsion as a consequence of substantial sulfate adsorption. Apparently, here concomitant adsorption of both PC and sulfate occurs whereby the small sulfate anions fill the interstitial space existing between the cylindrical volume spaces occupied by the PC comb polymer (**Fig. 7**). As a consequence of this synergistic effect between PC and SO_4^{2-}, fluidity of the $CaCO_3$ slurry increased from 26.3 cm to 31 cm (10.4 in to 12.2 in) when both 45PC6 and sulfate were present.

CONCLUSIONS

During the hydration of cement, sulfate ions originating from calcium sulfates and alkali sulfates such as K_2SO_4 dissolve into the pore solution. They can significantly affect the dispersing performance of PC admixtures. In this study we found that the fluidity of a $CaCO_3$ paste can either significantly decrease or increase, depending on the anionic charge character of the PC. Thus, sulfate can play a positive or negative role for the dispersing effectiveness of PC. Our experiments demonstrate that a negative impact can occur for PC polymers possessing low anionic charge. Their adsorbed amount decreases in the presence of sulfate, which decreases the fluidity of the slurry. In case of sufficiently anionic charged PC, sulfate anions cannot prevent its adsorption. To the contrary, an additional amount of sulfate will adsorb in the interstitial spaces between the large macro molecules, thus enhancing dispersion by a supplementary electrostatic effect. Plausibly, this interplay between PC molecules and sulfate will be similar in cement-based systems such as concrete.

The main finding of this study was that the dispersing performance of highly anionic PCs (e.g. 45PC6) can be improved by the addition of controlled amounts of sulfate salts to the liquid admixture. Utilizing this effect, a more economical superplasticizer could be attained.

ACKNOWLEDGMENTS

A. H. likes to thank Al-Baath University in Homs, Syria for a stipend to finance this study.

REFERENCES

1. Yamada, K.; Takahashi, T.; Hanehara, S., and Matsuhisa, M., "Effects of the chemical structure on the properties of polycarboxylate-type superplasticizer", *Cem. Concr. Res.*, V. 30, No. 2, 2000, pp. 197-207.

2. Yoshioka, K.; Sakai, E.; Daimon, M., and Kitahara, A., "Role of steric hindrance in the performance of superplasticizers for concrete", *J. Am. Ceram. Soc.*, V. 80, 1997, pp. 2667-2671.

3. Ohta, A.; Sugiyama, T., and Tanaka, Y., "Fluidizing mechanism and application of polycarboxylate-based superplasticizers" in: Malhotra, V. M., editor, 5th International Conference on Superplasticizers and Other Chemical Admixtures in Concrete, Rome, Italy, SP-173, *CANMET/ACI*, 1997, pp. 359 –378.

4. Ramachandran, V. S., and Malhotra, V. M., "Superplasticizers", in: Ramachandran, V. S., editor, Concrete Admixtures Handbook, 2nd ed, New Jersey, USA, *Noyes publications*, 1996, pp. 410-517.

5. Sakai, E.; Kang, J. K., and Daimon, M., "Action mechanisms of comb-type superplasticizers containing grafted polyethylene oxide chains", in: Malhotra, V. M. editor, 6th International Conference on Superplasticizers and Other Chemical Admixtures in Concrete, Farmington Hills, MI, USA, SP-195, *CANMET/ACI*, 2000, pp. 75-90.

6. Plank, J., and Hirsch, Ch., "Impact of zeta potential of early cement hydration phases on superplasticizer adsorption", *Cem. Concr. Res.*, V. 37, 2007, pp. 537-542.

7. Blask, O., and Honert, D., "The electrostatic potential of highly filled cement suspensions containing various superplasticizers", in: Malhotra, V. M., editor, 7th International Conference on Superplasticizers and Other Chemical Admixtures in Concrete, Berlin, Germany, SP-217, *CANMET/ACI*, 2003, pp. 87-101.

8. Khalil, S. M., "Ward M A. Influence of SO_3 and C_3A on the early reaction rates of Portland cement in the presence of calcium lignosulfonate", *Am. Ceram. Soc. Bull.*, V. 57, 1978, pp.1116–1122.

9. Tuthill, L. H.; Adams, R. F.; Bailyey, S. N., and Smith, R. W., "A case of abnormally slow hardening concrete for tunnel lining", *J. Am. Concr. Inst*., V. 57, 1961, pp. 1091–1110.

10. Dodson, V. H., and Hayden, T. D., "Another look at the Portland cement/chemical admixture incompatibility problem", *Cem. Concr. Aggreg*., V. 11, 1989, pp. 52–56.

11. Flatt, R. J., and Houst, Y. F., "A simplified view on chemical effects perturbing the action of superplasticizers", *Cem. Concr. Res.*, V. 31, 2001, pp. 1169–1176.

12. Magarotto, R.; Moratti, F., and Zeminian, N., "Influence of sulfates content in cement on the performances of superplasticizes", in: Mallhotra V M, editor. 8th International Conference on Superplasticizers and Other Chemical Admixtures in Concrete, Sorrento, Italy, SP-239-15, *CANMET/ACI*, 2006, pp. 215-229.

13. Magarotto, R.; Torresan, I., and Zeminian, N., "Effect of alkaline sulfates on performance of superplasticizers" in: Grieve, G., and Owens, G., editors, Proceeding of the 11th International Congress on the Chemistry of Cement: Cement's Contribution to development in the 21st Century. Vol. 2. Durban, South Africa, May 11 – 16, 2003, pp. 569-580.

14. Haehnel, C.; Lambois-Burger, H.; Guillot, L., and Borgarello, E., "Interaction between cements and superplasticizers", Proceedings of the 12th International Congress on the Chemistry of Cement, Montreal, Canada, July 8-13, 2007, pp. 1-14.

15. Yamada, K.; Ogawa, S., and Hanehara, S., "Controlling of the adsorption and dispersing force of polycarboxylate-type superplasticizer by sulfate ion concentration in aqueous phase", *Cem. Concr. Res.*, V. 31, 2001, pp. 375-383.

16. Flatt, R. J.; Zimmermann, J.; Hampel, C.; Kurz, C.; Schober, I.; Plassard, C., and Lesniewska, E., "The role of adsorption energy in the sulphate-polycarboxylate competition", in: Holland, T. C.; Gupta, P. R., and Malhotra, V. M., editors, 9th International Conference on Superplasticizers and

Other Chemical Admixtures in Concrete, Detroit, MI, USA, SP-262-12, *CANMET/ACI*, 2009, pp. 153–1648.

17. Zimmermann, J.; Hampel, C.; Kurz, C.; Frunz, L., and Flatt, R. J., "Effect of polymer structure on the sulphate-polycarboxylate competition", in: Holland, T. C.; Gupta, P. R., and Malhotra, V. M., editors, 9th International Conference on Superplasticizers and Other Chemical Admixtures in Concrete, Detroit, MI, USA, SP-262-12, *CANMET/ACI*, 2009, pp. 165-176.

18. Plank, J.; Pöllman, K.; Zouaoui, N.; Andres, P. R., and Schaefer, C., "Synthesis and performance of methacrylic ester based polycarboxylate superplasticizers possessing hydroxy terminated poly(ethylene glycol) side chain", *Cem. Concr. Res.*, V. 38, No. 10, 2008, pp. 1210-1216.

19. Teresa, M.; Laguna, R.; Medrano, R.; Plana, M. P., and Tarazona, M. P., "Polymer characterization by size-exclusion chromatography with multiple detection", *J. Chromatogr. A.*, V. 919, No. 1, 2001, pp. 13-19.

20. Nägele E., "The zeta potential of cement", *Cem. Conc.r Res.*, V. 15, No. 3, 1985, pp. 453-462.

21. Cheung, J.; Jeknavorian, A.; Roberts, L., and Silva, D., "Impact of admixtures on the hydration kinetics of Portland cement", *Cem. Concr. Res.*, V. 12, No. 41, 2011, pp. 1309–1289.

Paper 5

Formation of Organo-Mineral Phases from Superplasticizers: Can It Explain the Differences Occasionally Observed at Early and Delayed Addition of These Admixtures?

A. Habbaba, Z. Dai, J. Plank

Journal of Cement and Concrete Research
Submitted on November 12, 2012 (under review)

Formation of Organo-Mineral Phases from Superplasticizers: Can It Explain the Differences Occasionally Observed at Early and Delayed Addition of These Admixtures?

A. Habbaba, Z. Dai, J. Plank*

Technische Universität München, Chair for Construction Chemicals, 85747 Garching, Germany

* Corresponding author address: Technische Universität München, Chair for Construction Chemicals, Lichtenbergstr. 4, 85747 Garching, Germany. Tel: +49 89 289 13151, Fax: +49 89 289 13152
E-mail address: sekretariat@bauchemie.ch.tum.de

Abstract

Most superplasticizers (SPs) exhibit significantly higher dispersing performance when added to an already mixed concrete (delayed mode) instead of addition with the mixing water (early addition). Here, the specific parameters which determine this effect were investigated. At first, the tendency of four polycarboxylates and BNS to intercalate into C_3A hydrates was correlated with the flow values of pastes prepared from six different commercial cements at early and delayed addition. It was found that the contents of alkalisulfates and C_3A present in the cement samples play the key role. For cements exhibiting a low alkalisulfate/C_3A molar ratio (0.04 – 1.29), huge differences in paste flow at early and delayed addition were observed, presumably because of chemisorption (intercalation) of the SP into C_3A hydrates. While at high alkalisulfate/C_3A molar ratios (~ 2), AF_t (ettringite) is formed predominantly, and SP intercalation is impossible. Consequently, similar flow values are attained at early and delayed addition.

Keywords

Portland Cement (D); Sulfate (D); Polymers (D); Dispersion (A); Organo-mineral phase.

1. Introduction

Modern concrete technology requires high performance admixtures in order to fulfill the demands of excellent workability and high compressive strength after hardening [1]. Superplasticizers (SPs), either based on polycondensate or polycarboxylate ether (PCE) chemistry, allow to produce a highly flowable concrete and/or to reduce the water/cement ratio of concrete, resulting in higher compressive strength and improved durability. For those applications, it is essential to profoundly understand the interactions occurring between the SPs and the mineral components formed during cement hydration. It is generally accepted that high water reduction and high fluidity of concrete containing SP is attributed to the polymer molecules adsorbing onto the surface of cement hydrate phases [2, 3]. In this way, a polymer layer exercising an electrostatic and/or steric effect between the cement particles is formed [4, 5]. As a result, interparticle friction is reduced and flowability of the dispersion is achieved.

Numerous studies conclude that Portland cement possessing a high C_3A content interacts particularly strong with SPs [2-4, 6-8]. Especially for high performance concrete where the effectiveness of the SP plays a most critical role, this interaction with C_3A has led to the recommendation to only use Portland cement with low content of C_3A (< 3 wt.%).

The hydration of C_3A and tetracalcium alumoferrite (C_4AF) present in cement produces hydrocalumite-type layered double hydroxides (LDHs) which can intercalate various anions in between their cationic main layers. For example, the layered phases C_2AH_8 and C_4AH_{13} are formed by intercalation of OH^- anions [9]. They are metastable compounds which within minutes or hours convert to the cubic phase katoite, C_3AH_6, the thermodynamically most stable modification of the calcium aluminate hydrates at room temperature. Sulfate which is commonly present in any ordinary Portland cement (OPC), *e.g.* in the form of gypsum, to control its setting behavior, may intercalate into the layered calcium aluminate hydrates as

well, resulting in $[Ca_4Al_2(OH)_{12}](SO_4)\bullet 6H_2O$ (AF_m or monosulfoaluminate) [10]. Some years ago it has been found that also anionic polymers which are applied as concrete admixtures can intercalate into the lamellar calcium aluminate hydrates. From the group of SPs, β-naphthalene sulfonate formaldehyde condensate (BNS) was the first for which intercalation was reported [11]. Recently, we could demonstrate the formation of calcium aluminum layered double hydroxides incorporating PCE superplasticizers (Ca-Al-PCE-LDHs). They were obtained by rehydration of C_3A in aqueous PCE solution [12, 13]. According to this study, the ability of PCEs to intercalate increases with higher anionic charge density and shorter side chain. PCEs possessing side chains containing up to 45 ethylene oxide units (EOUs) were found to intercalate easily whereas a PCE with 111 EOUs hardly intercalates. Besides the steric size of PCE, sulfate is another factor determining the extent of PCE intercalation. At high SO_3/C_3A ratios in cement (*e.g.* > 2), sulfate, because of its higher specific anionic charge density in comparison to PCE, will occupy the interlamellar space and thus prevent intercalation of the polymer. Thus, in this study PCE intercalation was found to occur only at SO_3/C_3A ratios at or below 1 [14]. Note that here SO_3 stands for the total amount of SO_3 contained in a cement sample (the sum of SO_3 from calcium and alkali sulfates). The conformation of intercalated PCE molecules was investigated by another group [15]. They found that the side chains of PCE comb polymers form blobs (half - spheres) which are filling the interlayer space.

Another effect well known in concrete technology is that some SPs show great differences in their performance, depending on the time of addition to concrete. Typically, delayed addition (*i.e.* SP addition to an already mixed concrete) produces higher concrete flowability than early addition (*i.e.* SP addition in the mixing water). It has been observed that this effect occurs only for combinations of certain SPs and cements, that it can be more or less pronounced, and it may not show at all. No conclusive experimental data has been presented so far to explain

this phenomenon. In a brilliant article published in 2001, *Flatt* and *Houst* presented numerous data from concrete testing which suggest that interaction of SPs with hydrating cement not only involves surface adsorption, but may include as well the formation of organo-mineral phases resulting from SP intercalation into lamellar calcium aluminate hydrates [16]. According to them, chemical absorption of SPs occurring during the very first seconds of cement hydration could explain the difference in SP performance at early and delayed addition. The authors also point out that sulfate may play a key role in this process.

Obviously, if SPs are intercalated, then they are no longer available for the superplasticizing effect which requires surface adsorption on the cement grains. In such case, a higher dosage of SP will be required to compensate the polymer lost by chemical absorption.

The aim of our study was to correlate experimental data on the intercalation ability of SPs with their fluidizing effect upon early and delayed addition to cement paste. For this purpose, we selected six commercial cements possessing different contents of C_3A, total SO_3 and alkali SO_3. We then tested the spread flow values of those cement pastes after immediate and delayed addition of four PCE samples possessing various side chain lengths. A BNS polycondensate was chosen for comparison. It was hoped that the different intercalation tendency of these SPs as determined in a previous study could provide a mechanistic explanation for the differences in their dispersing performance observed at different times of addition. Furthermore, the chemical composition of the cement samples was correlated with the flow behaviors.

2. Materials and Methods

2.1. Cement samples

Six commercial cement samples obtained from different sources in Germany (**Table 1**) were used. Their phase composition is shown in **Table 2**. The phase contents were determined by

X-ray diffraction (XRD) using *Rietveld* refinement (Bruker D8 advance instrument, Bruker-AXS, Karlsruhe, Germany). Only the contents of gypsum and hemihydrate were determined by differential scanning calorimetry (DSC 200 F3, Netzsch, Selb, Germany) using the pure phases for calibration. The content of alkali sulfates was calculated as difference between the total SO_3 content contained in the cement sample as obtained from X-ray fluorescence (XRF instrument Axios from PANalytical, Philips, Eindhoven, the Netherlands) and the cumulated SO_3 content present in gypsum, hemihydrate and anhydrite as obtained by TG/XRD analysis. The molar ratios of SO_3/C_3A were established from the total SO_3 content of the cement samples and the C_3A content determined by *Rietveld* analysis.

Table 1: Type and source of the commercial cement samples used in the study

Cement sample	Type	Producer
# 1	CEM I 52.5 R	Schwenk Cement KG, Heidenheim plant
# 2	CEM I 32.5 R	HeidelbergCement, Rohrdorf plant
# 3	CEM I 52.5 N	HeidelbergCement, Geseke plant
# 4	CEM I 32.5 N-LH/HS	Schwenk Cement KG, Allmendingen plant
# 5	CEM I 52.5 R HS/LA	Holcim, Lägerdorf plant
# 6	CEM I 52.5 N-HS-LA	HeidelbergCement, Paderborn plant

The selected cements represent differences in the C_3A contents varying from as low as 1.1 M-% up to 9.3 M-%, as well as in the alkali sulfate contents (expressed as SO_3) ranging from 0.1 M-% to 1.23 M-%. The total SO_3/C_3A molar ratios vary between 0.94 (sample # 3) and 7.23 (sample # 6).

2.2 Superplasticizer samples

The superplasticizers used were different methacrylic acid – ω –methoxy poly(ethylene glycol) methacrylate ester copolymers with side chain lengths of 8.5; 17; 45 and 111 ethylene oxide units (EOUs), respectively, and a molar ratio of methacrylic acid : methacrylate ester of 6:1. Synthesis and characteristic properties (molar masses, polydispersity index, etc.) of these

polymers were described in a previous work [12]. Moreover, a BNS polycondensate (Melcret® 500 F, a commercial product from BASF Construction Polymers GmbH, Trostberg / Germany) was tested as well. The chemical structures of the SPs are presented in **Fig. 1**.

Table 2: Phase compositions of the six commercial cement samples studied

Phase (M-%)	Cement sample					
	# 1	**# 2**	**# 3**	**# 4**	**# 5**	**# 6**
Alite	68.1	60.4	67.2	45.1	70.3	58.0
Belite	14.6	11.1	14.0	26.2	12.0	16.4
C_3A cubic	7.3	3.4	8.4	1.9	0.6	1.4
C_3A orthorhombic	1.2	5.9	0.0	0.0	0.5	0.0
C_4AF	3.9	7.3	2.7	17.1	12.5	15.3
Calcite	0.0	2.6	3.8	1.6	0.6	0.0
Periklase	0.0	2.0	0.0	0.0	0.0	0.0
Gypsum	0.0	0.0	0.0	0.3	0.2	0.9
Hemihydrate	3.1	1.3	0.0	1.5	1.8	0.4
Anhydrite	1.8	3.1	2.4	3.6	0.3	3.1
Dolomite	0.0	0.6	0.0	0.0	0.0	0.0
Lime	0.0	1.2	0.1	0.0	0.0	0.4
Quartz	0.0	0.3	0.8	0.1	0.0	0.0
Total SO_3	2.60	2.90	2.35	3.40	1.93	3.00
Alkali SO_3	0.10	0.70	1.23	0.72	0.68	0.85
Total SO_3/C_3A [m. r.][a]	1.05	1.04	0.94	6.04	5.90	7.23
Alkali SO_3/C_3A [m. r.][a]	0.04	0.25	0.50	1.29	2.09	2.05
w/c ratio[b]	0.57	0.56	0.55	0.44	0.47	0.53

[a] m. r. = molar ratio
[b] required to obtain a paste spread of 18±0.5 cm in 'mini slump' test

2.3 Paste flow tests

For all cements, pastes were prepared at the specific w/c ratios producing a flow value (spread) of 18 ± 0.5 cm (*mini slump test*). As early addition, SP was added to the mixing water. The SP dosage was chosen to produce a flow value of 26 ± 0.5 cm. In a typical experiment, cement powder was poured into the mixing water and let to soak for 2 min without agitation. Then the blend was mixed manually for 2 min to obtain a well-dispersed paste. Thereafter, the paste was poured into a Vicat cone (top diameter 6 cm, bottom diameter 7 cm, height 4 cm). The cone then was removed and the diameter of the spread cement paste was measured. Testing was carried out at a temperature of 23 ± 1 °C. Generally, the amount

of water introduced from addition of the SP solution was subtracted from the amount of mixing water to maintain a constant w/c ratio for each cement sample. The SP dosage in the mix is expressed on a dry mass basis (% by weight of cement, bwoc). As delayed addition, the SP was added to the cement paste which has been stirred before for 2 min and was left to rest for one minute. At this point, the SP solution was added and then mixed manually into the paste for two minutes before the spread value was taken. In all preparations, the SP dosages were set to provide a spread flow of the cement paste of 26 ± 0.5 cm under early addition condition. The same dosages were applied at delayed addition.

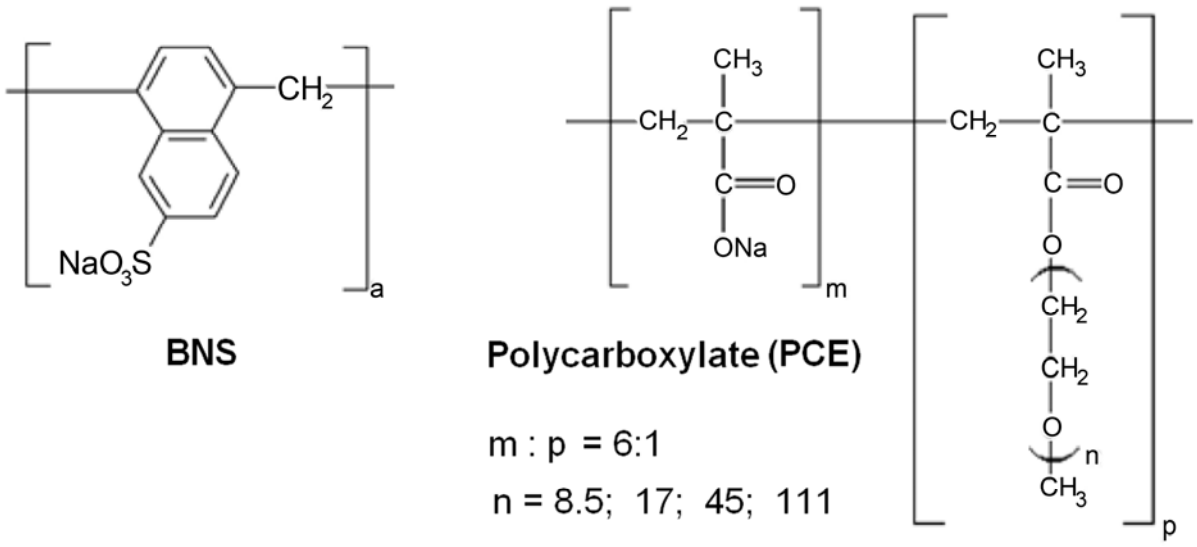

Fig. 1. Chemical structures of the BNS and the polycarboxylate samples used

3. Results and Discussion

Previous studies investigating cement and superplasticizer compatibility were focused on the interference of sulfates with SP [17]. There, it was shown that sulfate can impede the adsorption of PCE and thus reduce its dispersing ability, while no attention has been given to the possibility of PCE intercalation which is also controlled by sulfate. In recent work, however, we established that besides the side chain length of PCE, the molar ratio of total sulfate/C_3A present in cement determines whether intercalation will occur or not [14]. As an

example, the XRD patterns of PCE sample 45PC6 as a function of sulfate/C_3A ratio are shown in **Fig. 2** [18]. At a sulfate/C_3A ratio of 1 and higher, no PCE intercalation was observed. There, the divalent sulfate anion which has a higher tendency to intercalate than the PCE molecules present in sufficient quantity to occupy the entire interlayer space of the calcium aluminate hydrates. Thus, chemisorption of PCE is prevented by sulfate anions.

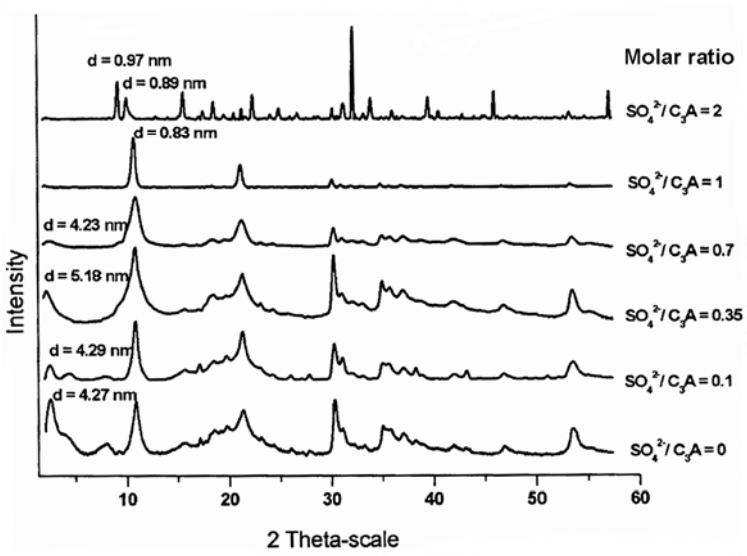

Fig. 2. XRD patterns of C_3A rehydrated in the presence of PCE sample 45PC6 at various sulfate concentrations

Here, it was attempted to establish a correlation between the paste flow at early and delayed PCE addition and the intercalation tendency of the PCEs as evidenced in the XRD patterns of our previous work [18].

For this purpose, the spread flow values of pastes prepared from the six different cements holding the four different PCE samples and a BNS were determined and the values for early and delayed addition were compared. Generally, SP dosages were set to give a flow value of 26 ± 0.5 cm at early addition. The results are shown in **Figures 3 - 8**.

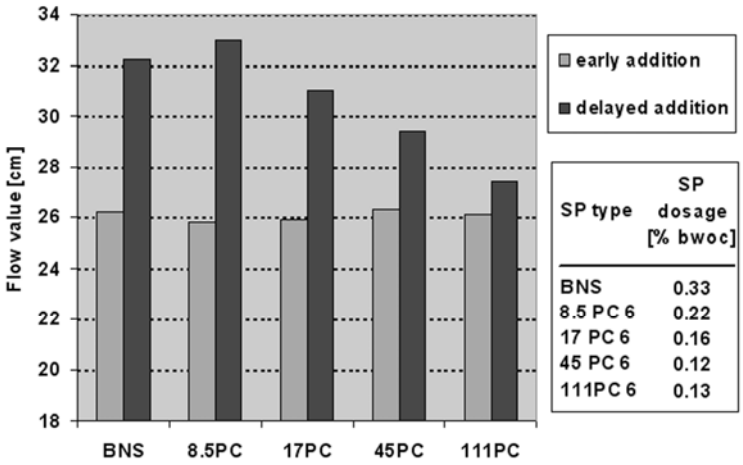

Fig. 3. Flow values of pastes prepared from cement sample # 1 (w/c = 0.57) at early and delayed addition of SP samples

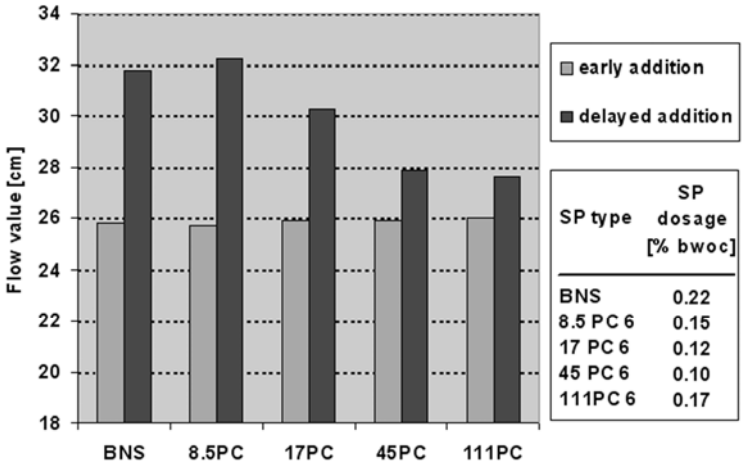

Fig. 4. Flow values of pastes prepared from cement sample # 2 (w/c = 0.56) at early and delayed addition of SP samples

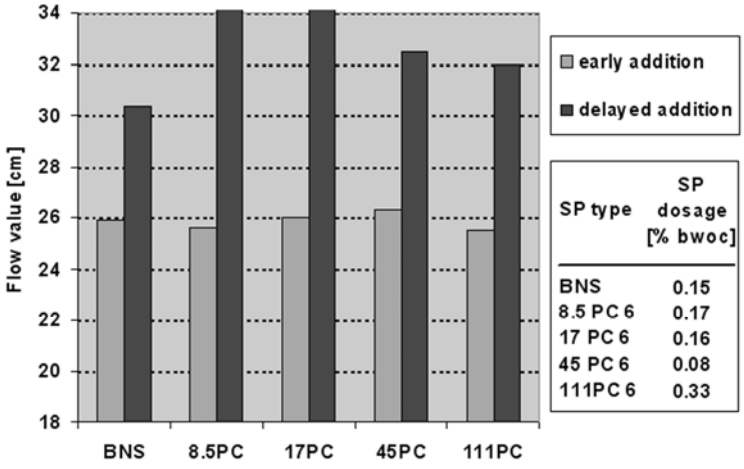

Fig. 5. Flow values of pastes prepared from cement sample # 3 (w/c = 0.55) at early and delayed addition of SP samples

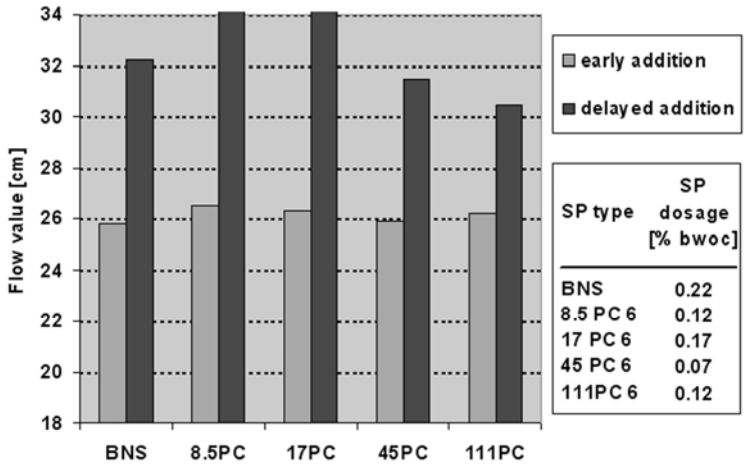

Fig. 6. Flow values of pastes prepared from cement sample # 4 (w/c = 0.44) at early and delayed addition of SP samples

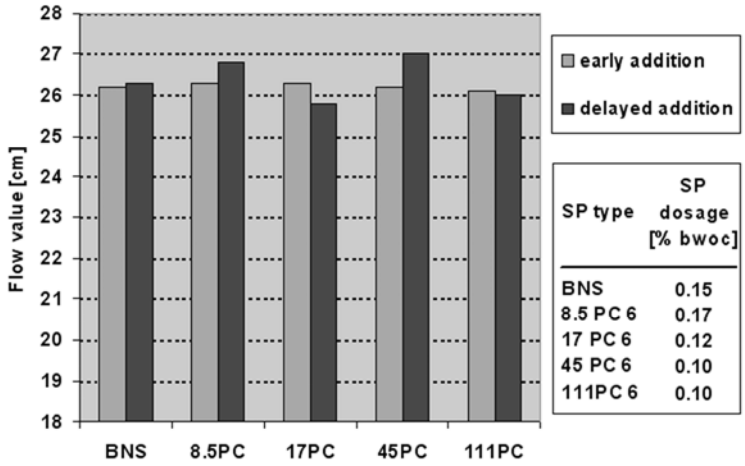

Fig. 7. Flow values of pastes prepared from cement sample # 5 (w/c = 0.47) at early and delayed addition of SP samples

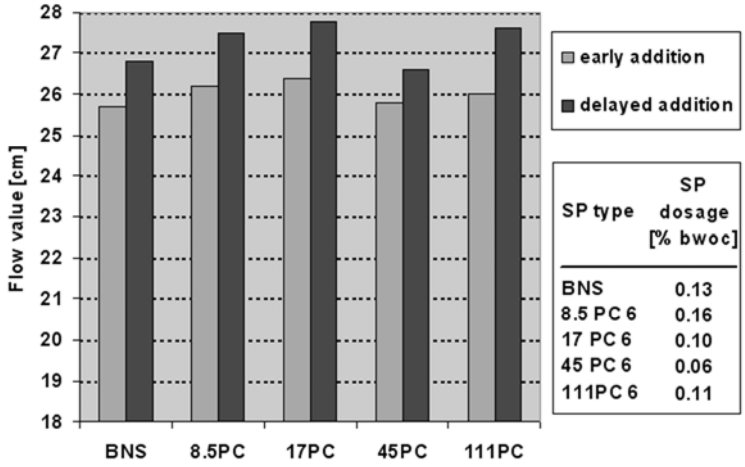

Fig. 8. Flow values of pastes prepared from cement sample # 6 (w/c = 0.53) at early and delayed addition of SP samples

From the six cement samples, four (samples # 1 – 4) exhibit a strong influence of the addition time on the flow value (**Fig. 3 – 6**) while for cement samples # 5 and 6, practically no such significant difference was found (**Fig. 7** and **8**). Generally, the polycondensate-based BNS superplasticizer did not behave much different than the PCEs.

For those cement samples where a huge difference in paste flow values was observed after early and delayed addition, it became obvious that the effect decreases with increasing side chain length of PCE. For example, at a graft chain length of 8.5 EOUs only, delayed addition consistently produces a much higher flow value than at early addition (**Fig. 3 – 6**). With increasing side chain length of PCE, the differential in flow value at early and delayed addition stepwise becomes less, and 111PC6 which possesses a particularly long side chain made of 111 EOUs exhibits the least difference of all PCE samples. This behavior perfectly correlates with the intercalation tendency of the PCEs as established in our previous study [14]. There, it was demonstrated that 111PC6 molecules do not intercalate much into the interlayer space of C–A–H phases, presumably because of their excessive steric size. While PCEs containing short side chains exhibit a high affinity towards the cationic $[Ca_2Al(OH)_6]^+$ sheets present in the AF_m layered structure. Hence, the observations made here in the 'mini slump' tests provide evidence that intercalation (chemisorption) may play a critical role for the effects at early and delayed addition.

Opposite to this trend, however, cement samples # 5 and 6 did not produce much difference between their flow values at early and delayed addition. Also, no differences in the behavior of individual SPs (be it PCE or BNS) were observed (**Fig. 7** and **8**). This observation suggests that with these cements, intercalation of the SPs generally does not occur; no matter whether the SP is present at the very beginning of cement hydration or later on.

In their previous paper, *Flatt* and *Houst* theorized that in systems where the concentration of free dissolved sulfate is low at the beginning of cement hydration and the SP is present in the mixing water, then the SP is immediately trapped by instantaneously formed C–A–H in the form of organo-mineral phases, thus depleting the SP from the pore solution and resulting in poor cement dispersion. However, when performing delayed SP addition, less polymer might be consumed because after several munities of mixing and hydration, enough sulfates have been dissolved to occupy the interlayer space of C–A–H phases, and monosulfo aluminate (AF_m) is formed.

To probe the applicability of this model to our experiments, at first the total SO_3 contents of all six cement samples utilized in this study were considered (**Table 2**). There, no correlation with the behavior of the six cement samples at early and delayed addition was observed. Next, the molar ratios between total SO_3 and C_3A, and the alkali sulfate content present in the cements were looked at (**Table 2**). Again, it was found that they do not match with the paste flow data shown in **Fig. 3** – **8**. Consequently, these parameters cannot explain the differences observed at early and delayed addition. Interestingly, however, a clear correlation exists between the molar ratio of alkali sulfate and C_3A (**Table 2**). At low molar ratios (0.04 – 1.29 for cement samples # 1 – 4), considerable differences between early and delayed addition occur. Apparently, in these systems the amount of alkali sulfate which chemisorbs instantaneously when water is added to cement, is insufficient to form enough monosulfo aluminate. There, instead of sulfate, the SP can occupy the interlayer space of C–A–H phases and then is consumed in a chemical reaction. Whereas when an excess amount of alkali sulfates relative to C_3A is available as is the case for cement samples # 5 and 6 (alkali SO_3/C_3A ratio is ~ 2), then sulfate immediately converts C_3A into monosulfo aluminate (AF_m) or even ettringite (AF_t). In such situation, the SP cannot undergo a chemical reaction with C–A–H phases and thus remains available for surface adsorption on cement hydrates which

produces high cement dispersion. Under those conditions, SP generally interacts with cement by surface adsorption only, independent of the time of addition. This model can explain why here no difference in dispersing effectiveness is observed. Another conclusion from these experiments is the alkali sulfates apparently dissolve much faster than the calcium sulfates. Therefore, they and not the calcium sulfates determine whether an SP can intercalate or not.

4. Conclusion

Significant differences in the dispersing ability of several polycarboxylates and a BNS superplasticizer at early and delayed addition were observed for cements possessing different compositions. It was found that the molar ratio between alkali sulfate and C_3A determined whether a cement sample exhibits much or no significant difference between early and delayed addition of SP. Generally, the effectiveness of an SP is independent of its addition time when a cement possessing a high molar ratio of alkali sulfate/C_3A content (~ 2) is utilized. Another observation was that for PCE based superplasticizers, the effect of different addition time is less pronounced when polymers possessing longer side chains are applied.

Based upon these findings it is proposed that at high alkali sulfate concentrations relative to C_3A, sulfates are the anionic species which incorporates into the C–A–H structure within the very first seconds of cement hydration. While when insufficient amounts of alkali sulfate are present, then SP molecules are used up to fill the interlayer space of the very early C–A–H crystals.

To summarize, the effects occurring at early and delayed addition between SPs and cement are mainly controlled by the alkali sulfates, and much less by the calcium sulfates. The effect seems to be independent of the chemical type of superplasticizer.

References

[1] V. S. Ramachandran, V. M. Malhotra, Superplasticizers, in: V. S. Ramachandran (ed.), Concrete Admixtures Handbook' 2nd ed., Noyes Publications, New Jersey, USA, 1996, pp. 410-517.

[2] E. Sakai, K. Yamada, A. Ohta, Molecular Structure and Dispersion-Adsorption Mechanisms of Comb-Type Superplasticizers Used in Japan, J. Adv. Concr. Techn. 1 (2003) 16-25.

[3] J. Plank, C. Hirsch, Superplasticizer Adsorption on Synthetic Ettringite, in: V. M. Malhotra (Ed.), Seventh CANMET/ACI Conference on Superplasticizers and Other Chemical Admixtures in Concrete, ACI, SP-217, 2003, pp. 283-298.

[4] M. Kinoshita, T. Nawa, M. lida, and H. Ichiboji, Effect of Chemical Structure on Fluidizing Mechanism of Concrete Superplasticizer Containing Polyethylene Oxide Graft Chains, in: V. M. Malhotra (Ed.), 6th CANMET/ACI International Conference on Superplasticizers and other Chemical Admixtures in Concrete, SP-195, Nice, France, 2000, pp. 163-180.

[5] A. Ohta, T. Sugiyama and Y. Tanaka, Fluidizing mechanism and application of polycarboxylate-based superplasticizers, in: V. M. Malhotra (Ed.), 5th CANMET/ACI Conference on Superplasticizers in Concrete, SP-173, 1997, pp. 359-378.

[6] P.-C. Aitcin, C. Jolicoeur, J. G. MacGregor, Superplasticizers: How they work and why they occasionally don't, Concr. Int. 16 (1994) 45-52.

[7] H. Uchikawa, D. Sawaki, S. Hanehara, Influence of kind and added timing of the organic admixture on the composition, structure and property of fresh cement paste, Cem. Concr. Res. 25 (1995) 353-364.

[8] M. Y. A. Mollah, W. J. Adams, R. Schennach, D. L. Cocke, A review of cement-superplasticizer interactions and their models, Adv. Cem. Res. 12 (2000) 153-161.

[9] H.F.W. Taylor, Cement chemistry, 2nd ed., Section: Hydrated aluminate, ferrite and sulfate phases, Thomas Telford, London, U.K., 1997, pp. 157 – 185.

[10] B. A. Clark and P. W. Brown, The Formation of Calcium Sulfoaluminate Hydrate Compounds: Part II, Cem. Concr. Res. 30 (2000) 233–240.

[11] V. Fernon, A. Vichot, N. Le Goanvic, P. Colombet, F. Corazza and U. Costa, Interaction between portland cement hydrates and polynaphthalene sulfonates, in: V. M. Malhotra (Ed.), Fifth CANMET/ACI Conference on Superplasticizers in Concrete, ACI, SP-173, 1997, pp. 225-248.

[12] J. Plank, Z. Dai, P. R. Andres, Preparation and characterisation of new Ca-Al-polycarboxylate layered double hydroxides, Mater. Lett. 60 (2006) 3614-3617.

[13] J. Plank, H. Keller, P. R. Andres, Z. Dai, Novel organo-mineral phases obtained by intercalation of maleic anhydride – allyl ether copolymers into layered calcium aluminium hydrates, Inorg. Chim. Acta. 359 (2006) 4901-4908.

[14] J. Plank, Z. Dai, H. Keller, F. von Hoessle, W. Seidl, Fundamental mechanisms for polycarboxylate intercalation into C_3A hydrate phases and the role of sulfate present in cement, Cem. Concr. Res. 40 (1) (2010) 45 – 57.

[15] C. Giraudeau, J.-B. d'Espinose de Lacaillerie, Z. Souguir, A. Nonat, R. Flatt, Surface and intercalation chemistry of polycarboxylate copolymers in cementitious systems, J. Am. Ceram. Soc. 92 (2009) 2471–2488.

[16] R.J. Flatt, Y.F. Houst, A simplified view on chemical effects perturbing the action of superplasticizers, Cem. Concr. Res. 31 (2001) 1169–1176.

[17] K. Yamada, S. Ogawa, S. Hanehara, Controlling of the adsorption and dispersing force of polycarboxylate-type superplasticizer by sulfate ion concentration in aqueous phase, Cem. Concr. Res. 31 (2001) 375–383.

[18] Dai, Z., Technische Universität München, Chair for Construction Chemicals, unpublished results (2006).

Paper 6

Surface chemistry of ground granulated blast furnace slag in cement pore solution: Understanding the behavior of slag in blended cements containing polycarboxylate superplasticizers

A. Habbaba, J. Plank

Proceedings of the XIII ICCC International Congress on the Chemistry of Cement
Abstract book p. 407, Madrid/Spain 2011

Surface chemistry of ground granulated blast furnace slag in cement pore solution: Understanding the behavior of slag in blended cements containing polycarboxylate superplasticizers

Habbaba A, Plank J*
Technische Universität München, Lehrstuhl für Bauchemie, Lichtenbergstr. 4, 85747 Garching b. München, Germany

Abstract
Ground granulated blast furnace slag produced in iron-making is an amorphous, vitreous material which is widely used in blended cements. Here, the surface chemistry of slag dispersed in water and synthetic cement pore solution was studied in absence and presence of anionic dispersants. Three different slag samples possessing different oxide compositions and two polycarboxylate dispersants based on methacrylic acid–co–ω-methoxy poly(ethylene glycol) methacrylate ester were investigated. When suspended in deionized water, all slag samples released different amounts of Ca^{2+}, K^{+}, Na^{+} and OH^{-} ions, thus producing pore solutions possessing high pH values (12 - 12.6). This dissolution process lasts for approximately 2 h until equilibrium is achieved.
Cement pore solution strongly impacts the surface charge and hence adsorption capability of the slags, as was evidenced by their electrokinetic properties. Zeta potential measurements of the slag suspensions revealed that when dispersed in alkaline solution, all slags initially possess a highly negative surface charge resulting from deprotonated silanol groups. The initially negatively charged slag adsorbs considerable amounts of Ca^{2+} ions on its surface until saturation is achieved. Through this mechanism, slag attains a layer of Ca^{2+} ions on its surface which results in a positive zeta potential. In cement pore solution where sulfate anions are present, the zeta potential becomes negative due to adsorption of sulfate ions onto the positively charged layer of calcium ions. Consequently, the surface charge of slags dispersed in cement pore solution is always negative.
Polycarboxylate superplasticizers effectively disperse slag suspensions. The effect differs between slag samples, depending on their composition. Effectiveness is particularly strong for PCs possessing high anionic charge amount. Their dispersion mechanism is based on adsorption onto the positively charged layer of Ca^{2+} ions present on the surface of slag. Typically, Langmuir – type adsorption isotherms are observed for polycarboxylates. Adsorption of PC occurs through desorption of sulfate ions from the layer of adsorbed Ca^{2+} ions. This effect is commonly referred to as competitive adsorption. The study demonstrates that when blended into cement, slag is not inert to anionic superplasticizers. Instead, competition occurs between cement and slag for the dispersant.

Originality
Ground granulated blast furnace slag (GGBFS) belongs to the group of supplementary cementitious materials (SCMs) which are commonly blended with clinker to produce Portland composite cements (e.g. CEM II and CEM III). The interaction between superplasticizers and cement is generally well understood. However, the effects of superplasticizers on SCMs such as slag are less known. Most research studies on this topic focus on the interaction between superplasticizers and the entire system of blended cements including SCMs, but do not differentiate between the individual components which are present there. Therefore, in our study we focussed on slag as single component and determined the specific interaction between polycarboxylate and slag.
First, the electrical surface charge developed by GGBFS when suspended in water was determined using a zeta potential instrument. Next, interaction between PC and GGBFS was studied by adsorption and zeta potential measurements performed in slag and cement pore solutions. Based on these results, a model for the electrochemical double layer existing on GGBFS surface in water and cement pore solution was developed. Finally, the relationship between the surface properties of slag and the dispersing performance obtained from the PCs is presented.

Chief contributions
Slag cements allow to build high strength and durable concrete structures similar to those achieved with ordinary Portland cement. However, the dosage of superplasticizer used in concrete mixtures containing slag cement or granulated blast furnace slag can vary significantly. The reason for this effect is not yet understood well. Most studies in this field ignored a potential interaction between superplasticizer and slag. They considered slag to be an inert material relative to superplasticizers.
The results of this work demonstrate that strong interaction between PC and the surface of slag can occur, and that in blended cements, PC will interact with both Portland cement and slag. Consequently, slag is not inert towards PC, and higher or lower PC dosages compared to pure CEM I - based systems have to be considered when formulating concretes containing slag. The ratios of specific surface area and positive surface charge between cement and slag will determine the distribution of adsorbed PC polymer between those two components.

Keywords: *Slag, blended cements, polycarboxylate, adsorption, zeta potential.*

* **Corresponding author: Email sekretariat@bauchemie.ch.tum.de; Tel +49 89 289 13151, Fax +49 89 289 13152**

1. Introduction

Slag is a by-product obtained in iron making from iron ore, coke (carbon-rich fuel resulting from the burning of coal), and a flux (limestone or dolomite) (Moranville, 2004). At the end of the smelting process, lime will have combined with components present in the iron ore and coke, forming molten blast furnace slag floating on top of the liquid iron. The slag is then separated from the liquid metal and cooled. There are several different ways by which slag can be cooled, the most common being air-cooling and water-cooling. This produces a glassy, granular product which is then dried and ground into a fine powder which is known as "ground granulated blast furnace slag" (GGBFS). Blast furnace slag consists essentially of silicates and alumosilicates of calcium and other bases (ACI committee 1995). GGBFS is used as a supplementary cementitious material (SCM), either by premixing the slag with Portland cement clinker to produce a blended cement during the cement production process, or by adding the slag as a mineral admixture to concrete containing Portland cement (Lewis, 1981). Slag cements allow to build high strength and durable concrete structures similar to those achieved with ordinary Portland cement (OPC) (Osborne, 1999).
Superplasticizers are used in the manufacture of concrete to improve its flow properties, and/or to reduce the water to cement ratio (w/c) in order to reach high strength and durability. The interaction between superplasticizers and cement is generally well understood (Yoshioka *et al*., 1997). However, the effects of superplasticizers on SCMs such as GGBFS are less known. Here, we report on the interaction between polycarboxylate-based superplasticizers (PCs) and GGBFS. First, the electrical surface charge developed by GGBFS suspended in water, $CaCl_2$ solution and synthetic cement pore solution (SCPS) was determined using a zeta potential instrument. Next, interaction between PC and GGBFS was studied via both adsorption and zeta potential measurements. Based on these results, a model for the electrochemical double layer existing on GGBFS surface in cement pore solution was developed. Finally, the relationship between the surface properties of slag and the dispersing performance of the PCs is presented.

2. Materials

2.1. Ground granulated blast furnace slag samples

Three GGBFS samples from different sources in Germany (slag # I from Schwenk cement company, Karlstadt, slag # II from Holcim's Salzgitter plant, Salzgitter, and slag # III from Holcim's Hansa Bremen plant, Bremen) were used in this study. Their physical properties are shown in Table 1. Their chemical compositions were published in previous work (Habbaba *et al.*, 2010).

2.2. Polycarboxylate samples

Two methacrylic acid–co–ω–methoxy poly(ethylene glycol) (MPEG) methacrylate ester based superplasticizers denominated as 45PC1.5 and 45PC6 were synthesized by aqueous free radical polymerization for this work (Plank *et al.,* 2008). Their general chemical structure is shown in Figure 1. 45 refers to the number of ethylene oxide units (n_{EO}) present in the side chain of the PC comb polymers, whereas the number after PC refers to the molar ratio between methacrylic acid and MPEG methacrylate ester (1.5 or 6) Their molecular weights (M_w) were 196,300 g/mol for 45PC1.5 and 222,300 g/mol for 45PC6 (GPC method).

2.3. Synthetic cement pore solution

In aqueous cement pastes, Ca^{2+} ions exist in the pore solution as a result of hydrolysis and dissolution of the calcium silicates (Moranville, 2004). Other ions such as K^+, Na^+ and SO_4^{2-} are also present. The concentrations of these ions vary with w/c ratio and the type of cement used. In this work, an SCPS possessing an ion composition similar to that produced by OPC at a w/c ratio of 0.5 was used. Its ion contents were 0.4 g/L Ca^{2+}, 7.1 g/L K^+, 2.25 g/L Na^+ and 8.29 g/L SO_4^{2-} (Rechenberg *et al*., 1983).

Table 1: Physical properties and w/s ratios of the GGBFS samples.

Property	Slag		
	# I	# II	# III
water/slag ratio	0.55	0.52	0.46
SCPS/slag ratio	0.59	0.53	0.505
d_{50} value [µm]	9.53	10.19	9.25
Density [g/cm^3]	2.86	2.91	2.91
Specific surface area (Blaine) [cm^2/g]	4,000	3,480	4,080

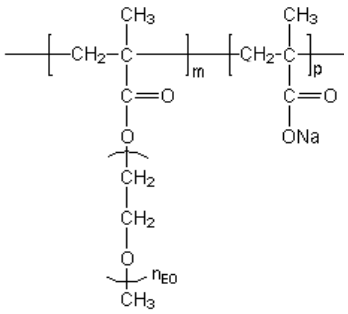

Figure 1: Chemical structure of the synthesized polycarboxylate copolymers.

2.4. Methods

Rheological properties of slag samples dispersed in SCPS were determined using a 'mini slump' test according to DIN EN 1015. Water-to-slag and SCPS-to-slag ratios required to obtain a target slump flow of 18±0.5 cm were determined as shown in Table 1.

Zeta potential was measured using Model DT-1200 Electroacoustic Spectrometer (Dispersion Technology, Inc. NY, USA). The highly solids loaded suspensions used in this work require an electroacoustic instrument to obtain zeta potential values which are representative of the conditions in actual concrete (Dukhin *et al.*, 1996). Zeta potential of the slurry was recorded as a function of polycarboxylate concentration.

Anionic charge amount of the copolymers used was determined by polyelectrolyte titration using a particle charge detector PCD 03 pH (BTG Mütek GmbH, Herrsching, Germany). Details of this instrument have been described before (Plank *et al.*, 2009a). The anionic charges were determined by titrating PC dissolved in slag pore solution (SPS) and in SCPS with cationic poly(diallyldimethylammonium chloride).

The adsorbed amount of PC on slag surface was determined according to the depletion method. Consumption (depletion) of the copolymer from the liquid phase solely was the result of surface adsorption. No intercalation, coprecipitation or micellization of PC into slag hydrates had occurred. Those chemical interactions were observed for cement (Flatt *et al.*, 2001; Plank *et al*., 2010). Different dosages of copolymer were added to the slag suspension. A High TOC II apparatus (Elementar, Hanau, Germany) was used to quantify organic carbon in filtrate samples. Adsorbed amount of PC is obtained by subtracting the concentration of PC found in the centrifugate from the initial PC concentration added to the slag paste.

3. Results and Discussions

3.1. Zeta potential of slag dispersed in water, $CaCl_2$ solution and SCPS

When dispersed in water, the initial surface charge of the GGBFS samples was found to be positive or negative, ranging from -20 mV for slag # III to an almost neutral value (+1 mV) for slag # II, and a positive one (+17 mV) for slag # I. The final surface charge mainly depends on the concentration of calcium ions released from the slag into the pore solution (Habbaba *et al.*, 2010).

To determine the sole effect of calcium ions on slag surface charge in the absence of sulfate ions, time-dependent zeta potential measurements were taken for all slag samples dispersed in a $CaCl_2$ solution containing 0.4 g/L Ca^{2+} (this value corresponds to the concentration of calcium ions present in cement pore solution). A significant effect of calcium ions was observed, compared to the aqueous system (Figure 2). All zeta potential values increased over time until a stable state was attained after approximately two hours. The final zeta potential values for slags # I, II and III were +32, +14 and +4 mV respectively (Figure 2).

When the slag samples were dispersed in sulfate containing SCPS, the initial zeta potential values decreased to negative values for all three samples (-5, -5.5 and -7 mV for slags # I, II and III respectively). This effect can be attributed to the adsorption of sulfate ions. Over time, the surface charges then decreased further and stabilized after ~ 3 h (Figure 2).

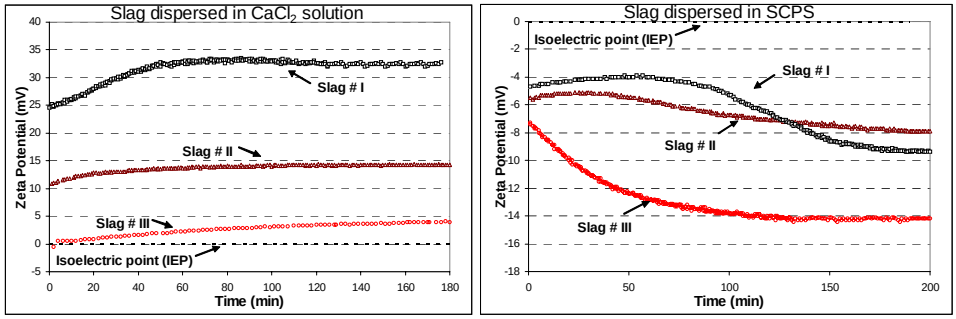

Figure 2: Time-dependent zeta potentials of slag samples dispersed in $CaCl_2$ solution (left) and in SCPS (right); w/s ratios as in Table 1.

3.2. Ion concentrations in slag pore solution and SCPS

When slag was dispersed in water, its filtrate (which is called slag pore solution, SPS) contained dissolved Ca^{2+} ions at concentrations of 0.35, 0.2 and 0.1 mg/L for slags # I, II and III, respectively (Habbaba *et al.*, 2010). These Ca^{2+} concentrations correlate well with the obtained zeta potential values: the higher the Ca^{2+} concentration, the more positive is the zeta potential of the slag sample. Hence, the positive surface charge is the result of adsorption of calcium ions dissolved from slag which then form a Ca^{2+} layer on the slag surface.

When dispersed in SCPS, additional amounts of calcium ions adsorb on slag, thus increasing the density of the calcium layer on the slag surface further. This effect can be tracked by the depletion of Ca^{2+} ions from SCPS, and an increase of the positive surface charge of slag.

Such consumption of Ca^{2+} ions from SCPS was observed when slags # I and II were dispersed in SCPS (Ca^{2+} concentration in SCPS decreased from 400 to 300 mg/L). The initial charge of the slag suspensions increased from +17 to +25 mV for slag # I, and from +1 to +10 mV in slag # II. Slag # III consumed about double the amount of Ca^{2+} (Ca^{2+} concentration in SCPS decreased to 150 mg/L). Accordingly, the initial surface charge of this slag increased by ~20 mV.

Consumption of sulfate ions by slag dispersed in SCPS was determined by utilizing ion chromatography, ICS-2000 (Dionex, Sunnyvale, CA, USA). There, no consumption of SO_4^{2-} ions from SCPS was observed (SO_4^{2-} concentrations in SCPS before and after addition of slag # I were 8.29 and 8.27 mg/L, respectively).

3.3. Anionic charge amount of polycarboxylate samples

The dispersing power of PCs is generally correlated to their anionic charge amount, which is affected by the pH value and the presence of significant amounts of electrolytes (especially Ca^{2+}). Table 2 shows the anionic charge amounts of the PCs used in this study under different conditions.

The anionic charge amounts of the PCs increase with increasing methacrylic acid content in the polymer (Plank *et al.*, 2009a). Accordingly, the anionic charge amount of sample 45PC6 is considerably higher than that of 45PC1.5. It is also evident that in the filtrate from the aqueous suspension of slag # III (SPS # III) which contains the lowest concentration of Ca^{2+} ions, both polymers exhibit the highest anionic charge amount.

3.4. Effect of PC on rheological properties of slag suspensions

'Mini slump' tests according to DIN EN 1015 were utilized to investigate the rheological properties of slag suspensions in the presence of PCs. The dosages of superplasticizer required to obtain a target

slump flow of 26±0.5 cm were determined. For slags dispersed in water, lower dosages of 45PC6 (0.01 – 0.06 % bwos) were required to attain the same spread as when 45PC1.5 was used (0.06 – 0.11 % bwos). This result is owed to the higher anionic charge amount of 45PC6. In case of slag samples dispersed in SCPS, similar dosages of 45PC6 were required to achieve the target spread. However, the dosages of 45PC1.5 were extremely high (0.65 – 0.8 % bwos). Obviously, 45PC1.5 which is a polycarboxylate typically used in ready-mix concrete is not a suitable dispersant for cementitious slag systems. To clarify the mechanism behind this effect, adsorption of 45PC1.5 and 45PC6 on slag was compared.

Table 2: Anionic charge amount of PC samples measured in SPS and SCPS.

Pore solution	Anionic charge amount of PC polymer [µeq/g]	
	45PC1.5	45PC6
SCPS	175	1,200
SPS # I*	298	1,235
SPS # II*	306	1,261
SPS # III*	460	1,437

* filtrates of aqueous slag suspensions (w/s ratios as in Table 1)

3.5. Adsorption of PC on slag dispersed in water and SCPS

First, adsorbed amounts of 45PC6 in both slag-water and slag-SCPS systems were measured using the TOC method. In both systems, the adsorbed amount of 45PC6 increases with dosage until it reaches a saturation point (Figure 3) which is lowest for slag # III and highest for slag # I.
Apparently, the main difference between both slags dispersed in water and SCPS is the total adsorbed amount of polymer. The anionic charge amount of PC and the positive surface charge arising from adsorption of Ca^{2+} ions on slag are the two main parameters determining the amount of the copolymer adsorbed on slag. When slag # I is dispersed in water or SCPS the final surface charges of slag are comparable (~ +32 mV). Whereas, the anionic charge amount of this PC is lower in SCPS than in SPS (Table 2). This results in a lower adsorbed amount of 45PC6 on slag # I dispersed in SCPS, compared to that in SPS (1.8 versus 1.51 mg/g). For slag # II, due to different anionic charge amounts of 45PC6 in each solution, PC adsorption should be lower in SCPS than in SPS. However, the higher adsorbed amount of calcium ions on the surface of slag # II in SCPS instigates a greater affinity for PC, thus resulting in similar amounts of PC adsorbed in both systems (~ 0.91 mg/g).

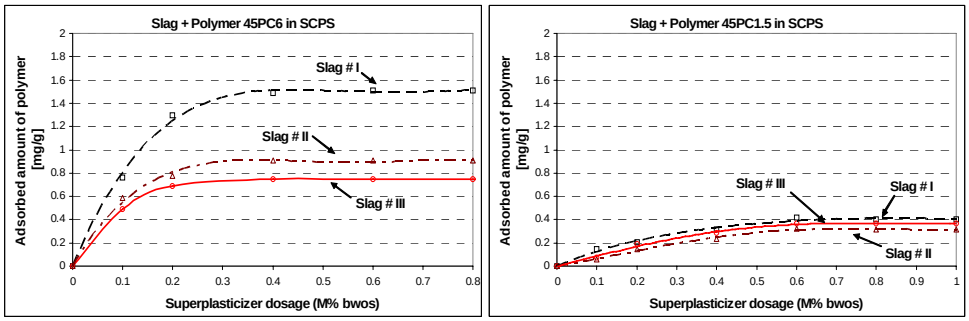

Figure 3: Adsorption isotherms for polycarboxylates 45PC6 (left) and 45PC1.5 (right) on the slag samples dispersed in SCPS.

In general, the amounts of 45PC6 adsorbed on the slag samples dispersed in SCPS follow the order: Slag # I > II > III. This trend correlates well with the positive surface charge of the individual slag samples. In other words, the packing density of the layer of adsorbed Ca^{2+} ions determines the quantity of adsorbed polymer, which levels out at the point of saturation.
Compared to 45PC6, adsorption of 45PC1.5 on slag was much lower (~ 0.45 mg/g at point of saturation) (Figure 3). Surprisingly, similar adsorbed amounts were found for all three slag samples.

This instigates that adsorption of this type of PC mainly is driven by a gain in entropy, and not by electrostatic attraction forces (Plank *et al*., 2009b). This low adsorption explains why 45PC1.5 is not an effective dispersant for slag suspensions (section 3.4.).

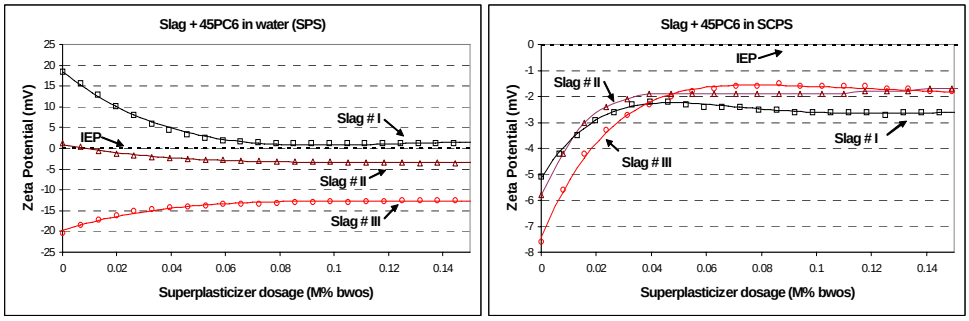

Figure 4: The effect of polycarboxylate 45PC6 on the zeta potential of slag dispersed in water (left) and in SCPS (right).

3.6. Effect of PC on zeta potential of slag suspensions

For all slag pastes, a shift in zeta potential values towards the isoelectric point occurs when 45PC6 is added, thus confirming adsorption of the PC onto the slag surface (Figure 4). The more negative zeta potential values from slag # III in SPS in presence of PC is due to the lower adsorbed amount of PC. Generally, the shift in zeta potential instigated by adsorption of superplasticizer can be attributed to the steric effect of the polyethylene oxide (PEO) side chains present in the PC. They shift the shear plane of the zeta potential farther away from the slag surface. For 45PC6 which represents a comb polymer possessing very long side chains, the development of zeta potential in all three slag suspensions is illustrated in Figure 5.

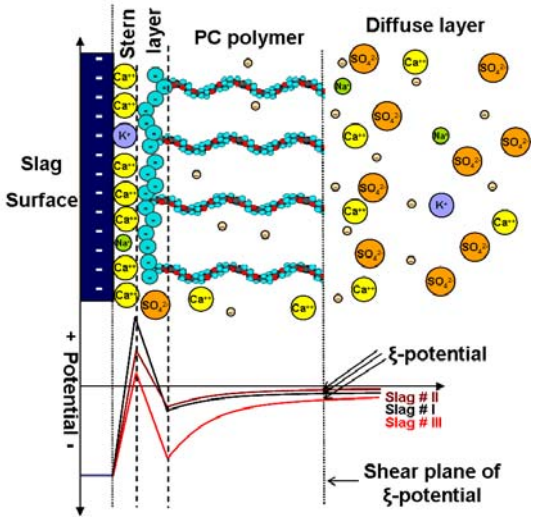

Figure 5: Schematic representation of the electrochemical double layer existing on the surface of slag dispersed in SCPS, illustrating the steric effect of the side chain of adsorbed 45PC6 polymer on the zeta potential value (size of ions/atoms not to scale).

4. Conclusions

When GGBFS is dispersed in cement pore solution, strong interaction occurs between the slag surface and the ions present in SCPS. The main effect comes from adsorption of calcium ions onto the slag surface. At high pH in SCPS, slag initially exhibits a negative surface charge owed to deprotonation of silanol groups. This negatively charged surface then adsorbs calcium ions present in SCPS, which

originate from the dissolution of cement and slag itself. This way, a layer of Ca^{2+} is formed on the slag surface, rendering the surface positively charged. Over time, further deprotonation of silanol groups on the slag surface occurs, allowing adsorption of more calcium ions until a state of equilibrium is attained.

When incorporated into concrete, different slags can give rise to varying workability. This is owed to the differences in the surface chemistry of the slag samples, which result from the different abilities of individual slags to adsorb calcium ions.

When PCs are added to blended cements containing slag, competitive adsorption between the copolymer and sulfate ions for adsorption sites on the surface of slag occurs. The adsorbed amount of PC, and hence its dispersing effectiveness, mainly depends on the difference in anionic charge amount of the copolymer and sulfate. Here, 45PC6 is sufficiently anionic to prevent adsorption of sulfate ions on the slag surface. Contrary to this, 45PC1.5 which is much less anionic can not achieve this. Thus, 45PC1.5 adsorbs insignificantly on the surface of slag. Consequently, very high dosages of this polymer are required to obtain high workability of concretes containing slag.

The saturated adsorbed amounts found for 45PC6 on slag (0.75 – 1.51 mg/g) are comparable to those typical for Portland cement. Therefore, when PC is added to a concrete containing GGBFS, competitive adsorption of the superplasticizer between the surfaces of cement and slag will occur. In the equilibrium state, the relative adsorbed amounts of PC on each surface are determined by the relative values of the positive surface charge of the two components, and their respective surface areas.

In general, the anionic charge amount of the superplasticizer and the packing density of Ca^{2+} ions on the slag surface are the main two parameters which impact PC adsorption on slag. This way, different saturated adsorbed amounts of PC can result. Consequently, the dosage of superplasticizer required to instigate high flowability in concrete mixtures containing slag can vary significantly.

5. References

- ACI committee 233R-95, 1995. Ground Granulated Blast- Furnace Slag as a Cementitious Constituent in Concrete. *American Concrete Institute*, Farmington Hills, Michigan.
- Dukhin, A. S. and Goetz, P. J., 1996. Acoustic and Electroacoustic Spectroscopy. *Langmuir*, 12, 4336-4344.
- Flatt, R.J. and Houst, Y.F., 2001. A simplified view on chemical effects perturbing the action of superplasticizers. *Cem. Concr. Res.*, 31, 1169-1176.
- Habbaba, A. and Plank, J., 2010. Interaction between polycarboxylate superplasticizers and amorphous blast furnace slag. *J. Am. Ceram. Soc.*, 93 (9), 2857-2863.
- Lewis, D. W. 1981. History of slag cements. Paper presented at University of Alabama Slag Cement Seminar, *American Slag Association MF 186-6*, April.
- Moranville, M., 2004. Cement made from blast furnace slag, pp 637-678 in: *Lea's Chemistry of Cement and Concrete*, 4th ed, Peter Hewlett. Oxford: Elsevier Science & Technology Books.
- Osborne, G. J., 1999. Durability of Portland blast-furnace slag cement concrete. *Cem. Con. Comp.*, 21, 11-21.
- Plank, J., Dai, Z., Keller, H., von Hoessle, F. and Seidl, W., 2010. Fundamental mechanisms for polycarboxylate intercalation into C_3A hydrate phases and the role of sulfate present in cement. *Cem. Concr. Res.*, 40, 45-47.
- Plank, J., Pöllmann, K., Zouaoui N., Andres, P. R. and Schaefer, C., 2008. Synthesis and performance of methacrylic ester based polycarboxylate superplasticizers possessing hydroxy terminated poly(ethylene glycol) side chains. *Cem. Concr. Res.*, 38, 1210-1216.
- Plank, J. and Sachsenhauser, B., 2009. Experimental determination of the effective anionic charge density of polycarboxylate superplasticizers in cement pore solution. *Cem. Concr. Res.*, 39, 1-5.
- Plank, J. and Sachsenhauser, B., 2009. Experimental determination of the thermodynamic parameters affecting the adsorption behaviour and dispersion effectiveness of PCE superplasticizers. V. M. Malhotra (Ed.) 9th *CANMET/ACI Conference* on superplasticizers and other chemical admixtures in concrete (supplementary papers), ACI, Seville, 87-102.
- Rechenberg, W. and Sprung, S., 1983. Composition of the solution in the hydration of cement. *Cem. Concr. Res*. 13, 119–126.
- Yoshioka, K., Sakai, E., Daimon, M. and Kitahara, A., 1997. Role of steric hindrance in the performance of superplasticizers for concrete. *J. Am. Ceram. Soc.*, 80, 2667-2671.

Paper 7

Interaction between Polycarboxylate Superplasticizers and Amorphous Ground Granulated Blast Furnace Slag

A. Habbaba, J. Plank

GDCh-Monographie, 42 (2010) 152 – 159

Interaction between Polycarboxylate Superplasticizers and Amorphous Ground Granulated Blast Furnace Slag

Habbaba, A., Garching/D; Plank, J., Garching/D;

TU München, Lehrstuhl für Bauchemie, Lichtenbergstr. 4, 85747 Garching b. München

ABSTRACT

The surface chemistry of slag dispersed in water and its behavior in cement paste were studied in the absence and presence of anionic dispersants. Three different slag samples and two polycarboxylate superplasticizers based on methacrylic acid–*co*–ω-methoxy poly(ethylene glycol) methacrylate ester were investigated. Electrokinetic properties of slag suspensions were determined via zeta potential measurement, revealing that initially negatively charged slag adsorbs considerable amounts of Ca^{2+} ions onto its surface until the point of saturation is reached. This process renders the surface of slag to be strongly positively charged in cement pore solution where a high concentration of Ca^{2+} ions is present. This positively charged layer of adsorbed Ca^{2+} ions in turn acts as an anchoring site for anionic polycarboxylate dispersants giving rise to a Langmuir – type adsorption isotherm as the dispersant adsorbs onto the surface. This study demonstrates that when blended into cement, slag is not inert with respect to these anionic superplasticizers. Instead, competitive adsorption occurs between cement and slag, which has an impact on the dosages of superplasticizers necessary to disperse CEM II / CEM III cements.

1 INTRODUCTION

Slag is an amorphous by-product of various metal refining processes. The slag obtained from iron making derives from impurities contained in the iron ore, coke, limestone and other compounds. In the production of iron, slags are generated at three different stages of processing and are classified as: blast furnace slag, electric arc furnace slag and ladle slag /1/. Blast furnace slag is obtained by quenching molten iron slag floating on top of the molten iron in a blast furnace (1400 - 1600 ºC) with water or steam. This produces a glassy, granular product which is then dried and ground into fine powder, thus known as "ground granulated blast furnace slag" (GGBFS).

GGBFS belongs to the group of supplementary cementitious materials (SCMs) which are commonly blended with Portland cement clinker to produce Portland composite cements (*e.g.* CEM II and CEM III cements). Slag cements allow to build high strength and durable concrete structures similar to those achieved with ordinary Portland cement (OPC) /2/.

The aim of using superplasticizers in concrete is to improve its flow properties, and/or to reduce the water to cement ratio (w/c) in order to reach high strength and durability. The interaction between superplasticizers and cement is generally

well understood /3/, however, the effects of superplasticizers on SCMs (such as GGBFS) are less known. Here, we report on the interaction between polycarboxylate-based superplasticizers (PCs) and GGBFS. First, the electrical surface charges developed by GGBFS suspended in water, $CaCl_2$ solution and synthetic cement pore solution (SCPS) were determined using a zeta potential instrument. Next, interaction between PC and GGBFS was studied via both adsorption and zeta potential measurements. Based on these results, a model for the electrochemical double layer existing on GGBFS surface in cement pore solution was developed. Finally, the relationship between the surface properties of slag and the dispersing performance of the PCs will be presented.

2 Materials

2.1 Blast furnace slag

Three GGBFS samples from different sources in Germany (slag # I from Schwenk cement company, slag # II from Holcim's Salzgitter plant, and slag # III from Holcim's Hansa Bremen plant) were used in this study. According to X-ray fluorescence analysis (XFA), the slag samples contain huge contents of CaO ranging from 42.8 % in slag # I, 38.6 % in slag # III, to 36.4 % in slag # II. The slags also contain huge amount of SiO_2: 35.9 %, 36.3 % and 38.6 % for slag # I, II and III respectively. Al_2O_3 contents were comparable in all slag samples (~ 11.5 %). Slag # II exhibits a particularly high content of MgO (11.5 %) compared to slags # I and III (~ 6.4 %). Other oxides such as TiO_2, Fe_2O_3, Mn_3O_4, and SrO are present in less amounts (up to 0.8 %).
Water-to-slag and SCPC-to-slag ratios required to obtain a target flow of 18±0.5 cm were determined in a mini slump test according to DIN EN 1015 (Table I).

2.2 Polycarboxylates

Two methacrylic acid–*co*–ω-methoxy poly(ethylene glycol) (MPEG) methacrylate ester based superplasticizers denominated as 45PC1.5 and 45PC6 were used in this work. Their general chemical structure is shown in Fig. 1. 45 refers to the number of ethylene oxide (EO) units (n_{EO}) present in the side chains of the PC comb polymers, whereas the number after PC refers to the molar ratio between methacrylic acid and MPEG methacrylate ester (1.5 or 6).

2.3 Synthetic pore solution

In aqueous cement slurries, Ca^{2+} ions exist in the cement pore solution as a result of hydrolysis and dissolution of the calcium silicates /1/. Other ions such as K^+, Na^+, and SO_4^{2-} are also present. The concentrations of these ions vary with the type of cement used and the w/c ratio. In this work, a SCPS possessing similar ions composition to that produced by OPC was used. Its ion contents are 0.4 g/L Ca^{2+}, 7.1 g/L K^+, 2.25 g/L Na^+ and 8.29 g/L SO_4^{2-}.

Table I. Physical properties and w/s ratios of the GGBFS samples.

	Slag		
	# I	# II	# III
water/slag	0.55	0.52	0.46
SCPS/slag	0.59	0.53	0.505
d_{50} [µm]	9.53	10.19	9.25
Density [g/cm^3]	2.86	2.91	2.91
Blaine [cm^2/g]	4,000	3,480	4,080

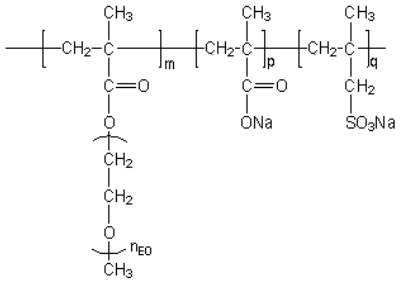

Fig. 1. Chemical structure of the synthesized polycarboxylate copolymers.

3 Results and discussion

3.1 Zeta potential of slag dispersed in water, $CaCl_2$ solution and SCPS

As a first step, the zeta potentials of the three slags dispersed in distilled water were measured over time. Their initial zeta potentials ranged from -20 mV for slag # III to an almost neutral value (+1 mV) for slag # II, and a positive one (+17 mV) for slag # I. It thus becomes obvious that the surface charge of slag is highly dependent on the chemical composition of each slag sample. Measurement of time-dependent zeta potential over a period of ~2 hours revealed that the zeta potential values of all slag samples increase to either less negative (-15 mV for slag # III) or more positive values (+32 and +9 mV for slags # I and II respectively).

Next, time-dependent zeta potential measurements were taken for all slag samples dispersed in a $CaCl_2$ solution containing 0.4 g/L Ca^{2+} (this value corresponds to the concentration of calcium ions present in SCPS). This experiment was necessary to study the sole impact of calcium ions on the surface charge of GGBFS, particularly in the absence of sulfate ions. A significant effect of calcium ions was observed in this system comparing to that in water (Fig. 2). The initial zeta potential values for slags # I, II and III increased to +25, +10 and -0.5 mV respectively. All zeta potential values increased over time until a stable state was attained after approximately 2 h (Fig. 2). The final zeta potential values for slags # I, II and III are +34, +14 and +4 mV resp.

When the slag samples were dispersed in SCPS, negative initial zeta potential values were observed for all three samples (Fig. 2), which decreased over time and stabilized after ~ 2 h. This effect is owed to the presence of sulfate ions in SCPS which adsorb on slag, thus giving its initial surface charge values of -5, -5.5 and -7 mV for slag # I, II and III respectively.

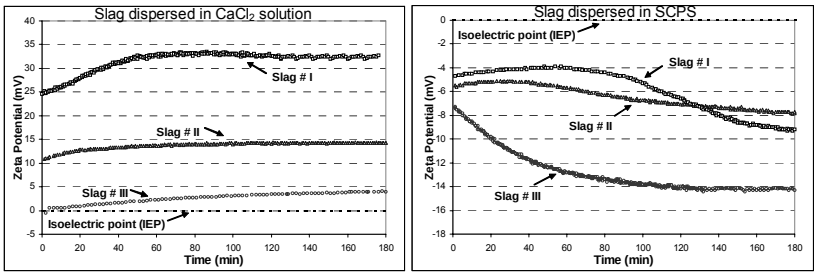

Fig. 2. Time-dependent zeta potentials of slag samples dispersed in $CaCl_2$ solution (left) and in SCPS (right), (w/s ratios as in Table I).

3.2 Time-dependent ion concentrations in slag pore solution and SCPS

When slag was dispersed in water, its filtrate (which is called slag pore solution (SPS)) contained dissolved Ca^{2+} ions at concentrations of 0.35, 0.2 and 0.1 mg/L for slags # I, II and III, respectively (determined by using AAS measurements).
In SCPS, Ca^{2+} ions are depleted in the presence of slags (Fig. 3). This confirms the results from Fig. 2 (left) where slags are shown to adsorb Ca^{2+} ions until their surfaces are in equilibrium with the aqueous medium. In order to show the sole effect of Ca^{2+} ions, zeta potential values for slag dispersed in $CaCl_2$ solution instead of SCPS was used subsequent explanation.
Slags # I and II consume almost the same amounts of calcium from SCPS, thus increasing their initial zeta potential from +17 to +25 mV for slag # I dispersed in water and $CaCl_2$ solution respectively, and from +1 to +10 mV for slag # II. Slag # III consumed about double the amount of Ca^{2+}. Accordingly, its initial zeta potential increases from -20 to -0.5 mV.

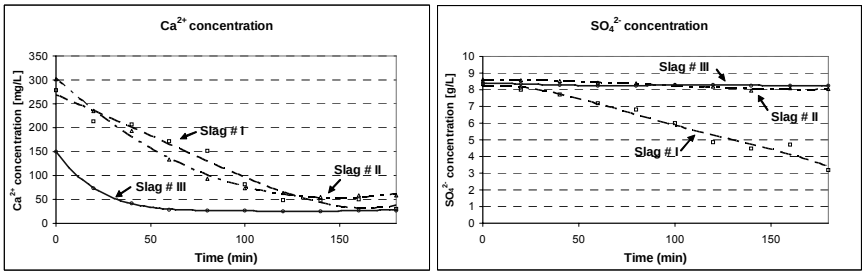

Fig. 3. Time-dependent evolution of Ca^{2+} (left) and SO_4^{2-} (right) concentration in the filtrate of slag samples suspended in SCPS (w/s ratios: as in table I).

Repeating the same experiment for sulfate ions, slag # I consumed a significant amount of SO_4^{2-} ions from SCPS (which was determined by utilizing ionic chromatography), while slags # II and III adsorbed only a minor amount (Fig. 3). This could imply that adsorption was the sole mode of uptake for slags # II and III, whilst both adsorption and formation of ettringite occurred in slag # I /4/.

3.3. Anionic charge amount of polycarboxylate samples

The dispersing power of PC is generally correlated to their anionic charge amount, which is affected by the pH value and the presence of significant amounts of electrolytes (especially Ca^{2+}). Table II shows the anionic charge amounts for the PCs used in this study at different conditions.
The anionic charge amounts of the PCs increase with increasing methacrylic acid content in the polymer /5/. Accordingly, the anionic charge amount of sample 45PC6 is considerably higher than that of 45PC1.5. It is also evident that in the filtrate from the aqueous suspension of slag # III (SPS # III) which contains the lowest concentration of Ca^{2+} ions, both polymers exhibit the highest anionic charge amount.

Table II. Anionic charge amount of PC samples measured SPS and SCPS.

Sample	Anionic charge amount of PC polymer [µeq/g]	
	45PC1.5	45PC6
SPS # I*	298	1,235
SPS # II*	306	1,261
SPS # III*	460	1,437
SCPS	175	1,200

* filtrate of aqueous slag suspensions (w/s ratios as in Table I)

3.4 Effect of PC on rheological properties of slag suspension

Mini slump tests according to DIN EN 1015 were utilized to investigate the rheological properties of slag suspensions in the presence of PCs. The dosages of superplasticizer required to obtain a target slump flow of 26±0.5 cm were determined. For slags dispersed in water, lower dosages of 45PC6 (0.01 – 0.06 % bwos) were required to attain the same spread as when 45PC1.5 was used (0.06 – 0.11 % bwos). This result is owed to the higher anionic charge amount of 45PC6. In case of slag samples dispersed in SCPS, similar dosages of 45PC6 were required to achieve the target spread, but the dosages of 45PC1.5 were extremely high (0.65 – 0.8 % bwos). Obviously, 45PC1.5 is not a suitable dispersant for cementitious slag systems. Thus, in further steps to clarify the mechanism, adsorption of 45PC6 on slag was determined.

3.5. Adsorption of PC on slag in water and SCPS

Adsorbed amounts of 45PC6 in both slag-water and slag-SCPS systems were measured using the TOC method. In both systems, the adsorbed amount of 45PC6 increases with dosage until it reaches the saturation point (Fig. 4), lowest for slag # III and highest for slag # I.

Apparently, the main difference between both slags dispersed in water and SCPS is the total adsorbed amount of the copolymer. The anionic charge amount of PC and the surface charge of each individual slag sample are the two main parameters determining the amount of the copolymer adsorbed on slag. In slag # I sample, the final surface charges of slag dispersed in water or SCPS are comparable (~ +32 mV), whereas the anionic charge amount of PC in SCPS is lower than in SPS # I (Table II). This leads to a decreased adsorbed amount of PC on slag # I dispersed in SCPS compared to that in water (1.8 versus 1.51 mg/g). In the case of slag # II, the adsorption of PC should be lower in SCPS than in water, due to the anionic charge amount of PC in each respective system. However, due to the simultaneously higher adsorption of calcium ions onto the surface of slag # II in SCPS, resulting in greater affinity for PC, the amount of PC adsorbed on both systems remained similar (~0.91 mg/g). Higher adsorption of calcium ions occurs in case of slag # III dispersed in SCPS than in water. The consequence of this process can be clearly observed by an increased adsorbed amount of the copolymer (0.75 mg/g) in SCPS comparing to the water-slag system (0.41 mg/g). Whereas the decreased anionic charge of PC in SCPS had no noticeable effect on the adsorbed amount of PC.

In general, the amounts of 45PC6 adsorbed on the slag samples dispersed in SCPS follow the order: Slag # I > II > III, which is related essentially to the positive surface charge of the individual slag samples. In other words, the packing density of the layer of adsorbed Ca^{2+} ions determines the quantity of adsorbed polymer, which levels out at the point of saturation. While the anionic charge of PC has only little effect on the adsorbed amount.

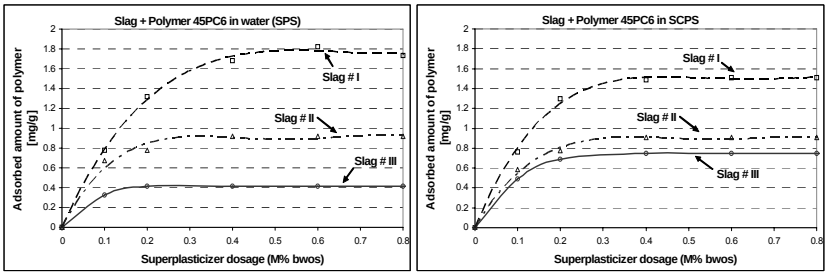

Fig. 4. Adsorption isotherms for 45PC6 on the slag samples dispersed in water (left) and PS (right).

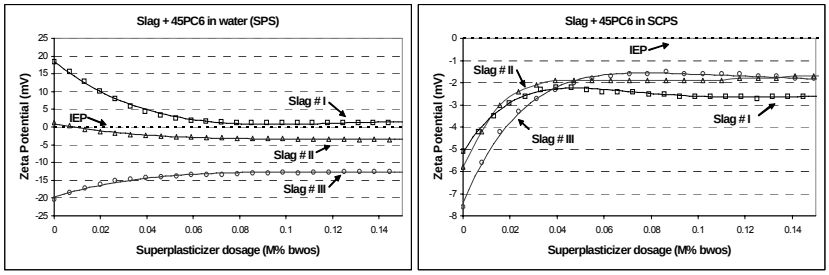

Fig. 5. The effect of 45PC6 on the zeta potential of slag dispersed in water (left) and in SCPS (right).

3.6 PCs' effect on zeta potential of slag suspensions

For all slag samples slurries, a shift in zeta potential towards the isoelectric point occurs when PC is added, thus confirming the adsorption of 45PC6 copolymer onto the slag surface (Fig. 5). The more negative zeta potential values from slag # III in SPS in presence of PC is due to the low adsorbed amount of PC. Generally, the shift in the zeta potential after the adsorption of superplasticizer here can be attributed to the steric effect of the PEO side chains present in the PCs. The PEO side chains shift the shear plane of the zeta potential farther away from the slag surface, lowering the potential in the diffuse layer. For comb polymers possessing very long side chains as is the case in 45PC6, the principle zeta potential curves are illustrated for all three slag samples in Fig. 6.

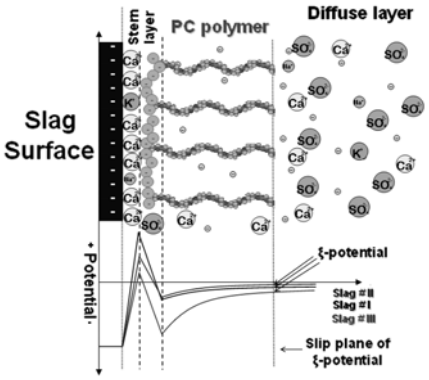

Fig. 6. Schematic representation of the electrochemical double layer existing on the surface of slag dispersed in SCPS, illustrating the steric effect of the side chain of adsorbed 45PC6 polymer on the zeta potential value (size of ions/atoms not to scale).

4 Conclusions

When GGBFS is dispersed in SCPS, an interaction occurs between the slag surface and the ions present in SCPS. The main effect comes from the adsorption of calcium and sulfate ions onto the slag surface, forming an electrochemical double layer. At high pH in the SCPS, the SiO_2 based surface of slag exhibits a negative charge owed to the deprotonation of the silanol groups. This negative surface then adsorbs calcium ions from SCPS originating from the dissolution of cement and some which are released during dissolution of the slag itself. This creates a layer of Ca^{2+} on the slag surface, rendering the surface positively charged. The positive Ca^{2+} layer can attract sulfate ions present in the SCPS, forming a second layer of sulfate ions, which alters the surface charge of slag from positive to negative. Further deprotonation of silanol group on the slag surface occurs, allowing more adsorption of calcium and sulfate ions over time. This effect decreases the zeta potentials of the slag slurries until they reach an equilibrium state.

When PCs are added to slag slurries, competitive adsorption occurs between the copolymer and the sulfate ions present in SCPS. The outcome mainly depends on the difference in anionic charge amounts of the copolymer and sulfate. Here, 45PC6 is strong enough to replace the sulfate ions from the outer layer of the slag surface. This is owed to the high anionic charge amount of 45PC6.

The saturated adsorbed amounts of 45PC6 on slag found in this work (0.75 – 1.51 mg/g) can be compared to those measured for Portland cement. Therefore, it should be clear that by adding PC to a slag-cement paste or to a concrete containing GGBFS, competitive adsorption of the superplasticizer will occur between the surfaces of cement and slag. In the equilibrium state, the relative adsorbed amounts of a PC on each surface are determined by the relative values of the positive surface charge of the two components, and their respective surface areas.

References

/1/ M. Moranville: 'Cement made from Blast furnace slag', pp 637-678 in: “Lea's Chemistry of Cement and Concrete”, 4th edition, Peter Hewlett, *Elsevier Science & Technology Books* (2004).

/2/ G. J. Osborne: “Durability of Portland blast-furnace slag cement concrete”, Cem. Con. Comp., 21 (1999) 11-21.

/3/ K. Yoshioka, E. Sakai, M. Daimon and A. Kitahara: "Role of steric hindrance in the performance of superplasticizers for concrete", J. Am. Ceram. Soc., 80 (1997) 2667-2671.

/4/ S.J. Barnett, M.A. Halliwell, N.J. Crammond, C.D. Adam and A.R.W. Jackson: “Study of thaumasite and ettringite phases formed in sulphate/ blastfurnace slag slurries using XRD full pattern fitting”. Cem. Con. Comp., 24 (2002) 339-346.

/5/ J. Plank and B. Sachsenhauser: “Experimental determination of the effective anionic charge density of polycarboxylate superplasticizers in cement pore solution”. Cem. Concr. Res., 39 (2009) 1-5.

Paper 8

Wechselwirkung von Polycarboxylat-basierten Fließmitteln mit Hüttensandmehlen

J. Plank, A. Habbaba, R. Sieber

17. ibausil, Tagungsband 1, Bauhaus-Universität Weimar (2009)

369-374

J. Plank, A. Habbaba, R. Sieber

Wechselwirkung von Polycarboxylat-basierten Fließmitteln mit Hüttensandmehlen

Einleitung

Die Wechselwirkung zwischen Zement und Zusatzmitteln wie z.B. Fließmitteln wurde mehrfach untersucht und wird weitgehend verstanden. Deutlich weniger Kenntnisse liegen über die Wirkung von Fließmitteln mit Zementzumahlstoffen wie z.B. Hüttensanden, Flugaschen, Kalksteinmehlen, Mikrosilika sowie anderen latent hydraulischen Stoffen vor. Wiederholt wurde von Unverträglichkeiten Polycarboxylat-basierter Fließmittel mit Zementen berichtet. In einigen Fällen stellte sich als Ursache dafür die Verwendung von Zementzumahlstoffen heraus. Um die Wirksamkeit von Fließmitteln in Hüttensand-enthaltenden CEM II- und CEM III-Zementen besser zu verstehen, wurden hier die spezifischen Wechselwirkungen zwischen einem Polycarboxylat-Fließmittel und drei verschiedenen Hüttensandmehlen analysiert. Die Untersuchungen erfolgten mittels Adsorptions- und Zeta-Potential-Messungen. Ziel war herauszufinden, ob das Fließmittel auf Hüttensand adsorbiert und somit eine mögliche Konkurrenz zwischen Hüttensand und Zement um das Fließmittel vorliegt.

Materialien und Methoden

Als Fließmittel wurde ein am Lehrstuhl für Bauchemie synthetisiertes Polycarboxylat (Bezeichnung: 45PC6) auf Basis Methacrylsäure, (ω-Methoxypolyethylenglycol)-Methacrylat-Ester und Methallylsulfonsäure entsprechend [1] verwendet. Das Verhältnis Methacrylsäure : Methacrylat-Ester betrug 6 : 1, die Seitenkette bestand aus 45 Ethylenoxideinheiten.

Als Hüttensande wurden gemahlene Proben aus drei verschiedenen Quellen eingesetzt. Sie unterscheiden sich hauptsächlich in ihrem CaO-Gehalt (**Tabelle 1**). HS I hat mit 42,8 Gew.-% den höchsten CaO-Gehalt, gefolgt von HS II und HS III mit jeweils 38,6 und 36,4 Gew.-% CaO. Weitere Unterschiede sind insbesondere im MgO-Gehalt, ihrer Mahlfeinheit sowie in den pH-Werten ihrer wässrigen Suspensionen festzustellen (**Tabelle 2)**.

Das Zeta-Potential der Hüttensand-Suspensionen wurde mittels elektroakustischer Meßmethode mit einem Gerät der Fa. Dispersion Technology (Model DT 1200) bestimmt. Mit dem Zeta-Potential kann näherungsweise die Oberflächenladung von Kolloidpartikeln in wässriger Suspension bestimmt und damit ein Adsorptionsvorgang verfolgt werden. 350 g Hüttensand wurden mit dest. Wasser oder synthetischer Porenlösung entsprechend dem jeweiligen w/f-Wert (Wasser : Feststoff-Verhältnis) intensiv vermischt und in die Meßzelle gegeben. Als Titrationsflüssigkeiten wurden 5 %ige Polycarboxylat- oder 1 %ige $CaCl_2$-Lösung verwendet.

Tabelle 1: Oxidgehalte (RFA) und spezifische Oberflächen der Hüttensandmehle

Probe	**HS I**	**HS II**	**HS III**
Quelle	Schwenk	Hansa Bremen	Salzgitter AG
CaO [Gew.-%]	42,8	38,6	36,4
SiO_2 [Gew.-%]	35,9	38,6	36,3
Al_2O_3 [Gew.-%]	11,4	12,4	11,5
Na_2O [Gew.-%]	0,27	0,45	0,34
K_2O [Gew.-%]	0,33	0,53	0,66
MgO [Gew.-%]	6,44	6,4	11,5
SO_3 [Gew.-%]	2,4	1,6	2,6
Oberfläche [cm²/g] (Blaine)	4000	4080	3480

Die Adsorption des Fließmittels auf den Hüttensandproben wurde mittels TOC bestimmt. Dazu wurden 0-1 Gew.-% Fließmittel in einer 0,147 %igen $CaCl_2 \bullet 2H_2O$-Lösung (enthält 0,4 g Ca^{2+} je Liter) gelöst und mit 16 g Hüttensand im jeweiligen w/f-Verhältnis zwei Minuten intensiv gemischt. Anschließend wurde die wässrige Phase von der Suspension mittels einer Zentrifuge bei 8500 min^{-1} getrennt, durch einen 0,2 µm Spritzenvorsatzfilter filtriert und um den Faktor 20 mit Salzsäure (0,8 Gew.-%) verdünnt. Das Anmachwasser ohne PCE wurde in gleicher Weise behandelt. Die adsorbierte Fließmittelmenge wurde anhand der Differenz zwischen dem TOC-Gehalt des Anmachwassers (Blindwert) und demjenigen des Filtrats berechnet.

Ergebnisse und Diskussion

a) Verhalten der Hüttensande in Wasser

In destilliertem Wasser dispergierte Hüttensande bilden eine Porenlösung, deren chemische Zusammensetzung **Tabelle 2** zu entnehmen ist. Es ist ersichtlich, dass insbesondere die Konzentrationen an Ca^{2+}- und K^{+}-Ionen in der Porenlösung stärker variieren kön-

nen. Erstaunlicherweise besteht kein direkter Zusammenhang zwischen den Oxidgehalten der Hüttensande und den Ionenkonzentrationen in der Porenlösung. Beispielsweise ist der Ca^{2+}-Gehalt der Porenlösung von Hüttensand II deutlich niedriger als der von Hüttensand III, obwohl der CaO-Gehalt von Hüttensand II um 2 Gew.- % höher liegt als der von Hüttensand III.

Tabelle 2: Chemische Analyse des Porenwassers und Zeta-Potential von Suspensionen der Hüttensande HS I, II und III in dest. Wasser

Probe	w/f	Ca^{2+} [mg//l]	Na^{+} [mg/l]	K^{+} [mg/l]	pH	Zeta-Potential
HS I	0,55	361	71	205	12,6	+ 20 mV
HS II	0,52	91	32	16	12,0	- 21 mV
HS III	0,46	214	39	56	12,5	~ 0 mV

Im Vergleich zu einer Zementporenlösung sind die Ionengehalte in der Porenlösung der Hüttensande jedoch eher gering [2-6]. Die Calciumionenkonzentration einer Zementporenlösung kann anfänglich bis zu 2 g/Liter betragen [7] und sinkt innerhalb der ersten Stunden auf Werte unter 400 mg/Liter ab. Weiterhin ist zu berücksichtigen, dass ein hydratisierender Zement verbrauchte Ca^{2+}-Ionen gemäß $C_3S + H_2O \rightarrow C_{\sim 1,7}SH + Ca(OH)_2$ nachliefern kann. Ähnliches gilt auch für den SO_4^{2-}-Gehalt einer Zementporenlösung.

Von besonderer Bedeutung sind die sehr unterschiedlichen Zeta-Potentiale der Hüttensande. Sie sind entweder stark positiv (+20 mV bei HS I), nahezu neutral (HS III) oder stark negativ (HS II). Eine Erklärung hierfür liefern die Ca^{2+}-Gehalte in den Hüttensand-Porenlösungen: Je höher die Ca^{2+}-Konzentration, umso stärker positiv ist das Zeta-Potential des Hüttensandes. Die Probe HS II mit der geringsten Ca^{2+}-Konzentration (91 mg/L) weist demnach ein stark negatives Zeta-Potential und die Probe HS I (Ca^{2+}-Konzentration 361 mg/L) eine besonders stark positive Oberflächenladung auf.

b) Beziehung zwischen Zeta-Potential von Hüttensand und der Ca^{2+}-Konzentration in der Porenlösung

Die Versuche in **Tabelle 2** zeigen, dass die in Zementleimen vorliegende, sehr hohe Ca^{2+}-Ionenkonzentration einen großen Einfluss auf die Oberflächenladung der Hüttensande ausüben kann. Im nächsten Schritt wurde deshalb die Oberflächenladung der Hüttensande in Abhängigkeit von der Ca^{2+}-Konzentration in der Porenlösung bestimmt. Zu diesem Zweck wurde 1 %ige $CaCl_2$-Lösung zu den Hüttensand-Suspensionen in dest. Wasser zutitriert und das Zeta-Potential gemessen. Die Ergebnisse sind in **Abbildung 1** dargestellt**.**

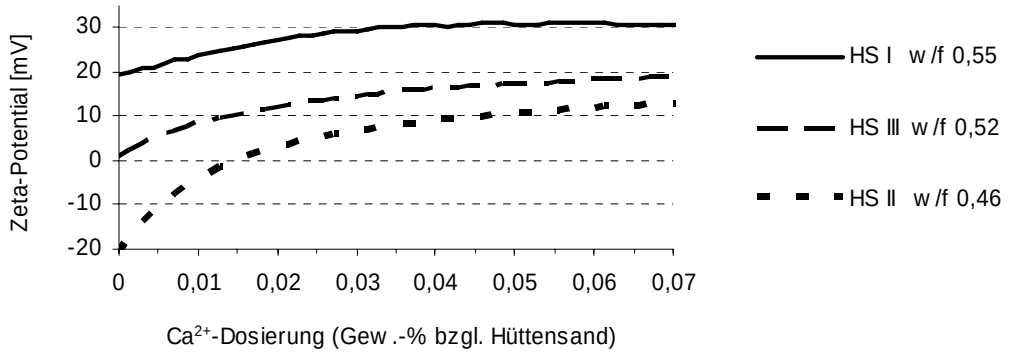

Abbildung 1: Zeta-Potentiale wässriger Hüttensand-Suspensionen in Abhängigkeit von der Ca^{2+}-Konzentration

Zugabe von Ca^{2+}-Ionen zu den Hüttensand-Suspensionen führt in allen Fällen zu deutlich stärker positiven Zeta-Potentialen. Ursache ist die Adsorption von Ca^{2+}-Ionen auf der Oberfläche der Hüttensande. Es werden Adsorptionsisothermen erhalten, deren Sättigungsbereiche bezüglich Ca^{2+}-Aufnahme durchwegs bei positiven Zeta-Potential-Werten liegen. Alle Hüttensande weisen somit in Zementporenlösung eine positiv geladene Oberfläche auf. Sie können demnach anionische Fließmittel adsorbieren und konkurrieren diesbezüglich mit den ebenfalls positiv geladenen Hydratphasen von Zement [8].

c) Adsorption des Polycarboxylat-Fließmittels auf Hüttensand

Im nächsten Schritt wurde die Adsorption des Polycarboxylat-Fließmittels 45PC6 auf den Hüttensand-Proben mittels Zeta-Potential- und Adsorptionsmessungen verfolgt. Zur Herstellung der Hüttensand-Suspensionen wurde eine 0,147 %ige $CaCl_2 \bullet 2H_2O$-Lösung verwendet. Sie weist einen Ca^{2+}-Gehalt von 0,4g/L auf und simuliert daher die Ca^{2+}-Konzentration in der Porenlösung eines Zementleims. Die Ausgangspotentiale der Hüttensandproben in der $CaCl_2$-Lösung liegen zwischen 0 und +25 mV (**Abbildung 2)**. Bei Zutitration des Fließmittels 45PC6 zu den Suspensionen vermindern sich die Zeta-Potentiale bei allen Proben und liegen schließlich um den isoelektrischen Punkt. Die Zeta-Potential-Kurven deuten an, dass HS I besonders viel Fließmittel adsorbiert, wohingegen von HS III eine mittlere Menge und von HS II nur wenig Polycarboxylat aufgenommen wird.

Dieses Verhalten wurde zusätzlich anhand von Adsorptionsmessungen mittels TOC bestätigt (**Abbildung 3)**. Die jeweils adsorbierten Fließmittelmengen werden maßgeb-

lich durch das Zeta-Potential eines Hüttensandes bestimmt. Je positiver sein Ausgangszetapotential, umso höher die adsorbierte Fließmittelmenge. Bemerkenswert ist, dass die adsorbierten Mengen des Polycarboxylats 45PC6 mit 0,5 bis 1,5 mg/g Hüttensand mit bei Zementen beobachteten Adsorptionswerten nahezu vergleichbar sind [9]. Die chemisch deutlich unterschiedlichen Oberflächen von Hüttensand und Zementhydratphasen spielen bei der Adsorption demnach eine untergeordnete Rolle. Entscheidend ist die positive Ladung der Oberfläche.

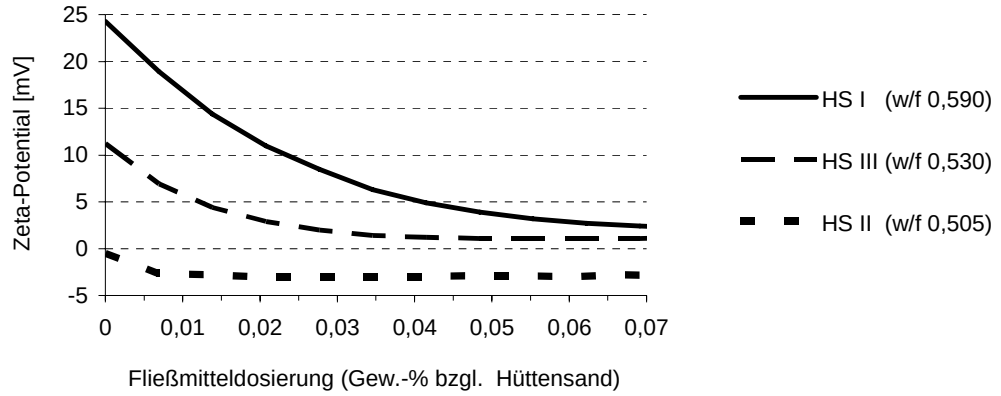

Abbildung 2: Zeta-Potentiale der Hüttensand-Suspensionen in $CaCl_2$-Lösung (0,4 g/L Ca^{2+}) in Abhängigkeit von der Dosierung an Polycarboxylat 45PC6

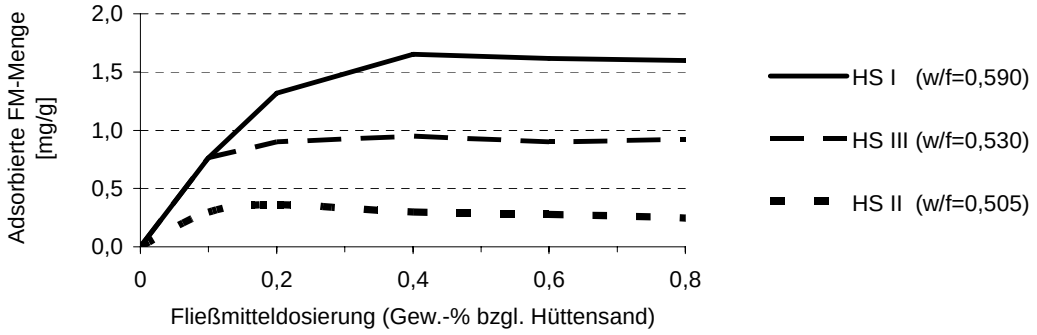

Abbildung 3: Adsorption des Fließmittels 45PC6 auf Hüttensandproben, suspendiert in $CaCl_2$-Lösung (0,4 g Ca^{2+}/Liter)

Zusammenfassung

Die Adsorption eines Polycarboxylat-Fließmittels auf Hüttensand wurde mittels Zeta-Potential- und Adsorptionsmessungen in synthetischer Ca^{2+}-Porenlösung untersucht. Es wurde gefunden, dass die Hüttensande Ca^{2+}-Ionen aus der Porenlösung bis zum Errei-

chen einer Sättigungsbelegung adsorbieren. Auf diese Weise entstehen positiv geladene Hüttensandpartikel, die auf ihren Oberflächen ähnlich hohe Fließmittelmengen wie Zement adsorbieren können. In Hüttensand enthaltenden CEM II- oder CEM III-Zementen konkurrieren somit Hüttensand und Zement um das Fließmittel, woraus ein erhöhter Fließmittelbedarf resultieren kann. Dies könnte einige der gelegentlich beobachteten Fließmittel-„Unverträglichkeiten“ mit diesen Zementen erklären. In weiteren Untersuchungen wird neben den Wechselwirkungen zwischen Polycarboxylaten und anderen Zementzumahlstoffen insbesondere auch der Einfluss von Sulfaten zu berücksichtigen sein.

References

[1] Plank, J.; Pöllmann, K.; Zouaoui, N.; Andres, P. R.; Schaefer, C., *"Synthesis and performance of methacrylic ester based polycarboxylate superplasticizers possessing hydroxy terminated poly(ethylene glycol) side chains."* Cem. Concr. Res. 38, (10) **2008,** 1210.

[2] Odler, I., *"Über die Zusammensetzung der Porenflüssigkeit hydratisierter Zementpasten."* TIZ- Fachberichte 106, (6) **1982,** 394-401.

[3] Rechenberg, W.; Sprung, S., *"Composition of the solution in the hydration of cement."* Cem. Concr. Res. 13, (1) **1983,** 119-126.

[4] Lothenbach, B.; Winnefeld, F.; Alder, C.; Wieland, E.; Lunk, P., *"Effect of temperature on the pore solution, microstructure and hydration products of Portland cement pastes."* Cem. Concr. Res. 37, **2007,** 483-491.

[5] Brouwers, H. J. H.; van Eijk, R. J., *"Alkali concentrations of pore solution in hydrating OPC."* Cem. Concr. Res. 33, (2) **2003,** 191-196.

[6] Bonen, D.; Sarkar, S. L., *"The superplasticizer adsorption capacity of cement pastes, pore solution composition, and parameters affecting flow loss."* Cem. Concr. Res. 25, (7) **1995,** 1423- 1434.

[7] Kelzenberg, A. L.; Tracy, S. L.; Christiansen, B. J.; Thomas, J. J.; Clarage, M. E.; Hodson, S.; Jennings, H. M., *"Chemistry of the Aqueous Phase of Ordinary Portland Cement Pastes at Early Reaction Times."* J. Am. Ceram. Soc. 81, (9) **1998,** 2349- 2359.

[8] Plank, J.; Hirsch, C., *"Impact of zeta potential of early cement hydration phases on superplasticizer adsorption."* Cem. Concr. Res. 37, (4) **2007,** 537-542.

[9] Schröfl, C. *"Untersuchungen zum Wirkmechanismus von Methacrylsäure-co(ω-Methoxypolyethylenglycol)methacrylat-Fließmitteln in Zementleimsuspensionen."* Diplomarbeit, Technische Universität München, Garching, **2005**.

Verfasser:

Prof. Dr. Johann Plank
M. Sc. Ahmed Habbaba
Dr. Roland Sieber

Technische Universität München
Lehrstuhl für Bauchemie
Lichtenbergstraße 4
85747 Garching